Valerio De Biagi

Complexity and robustness of structures against extreme events

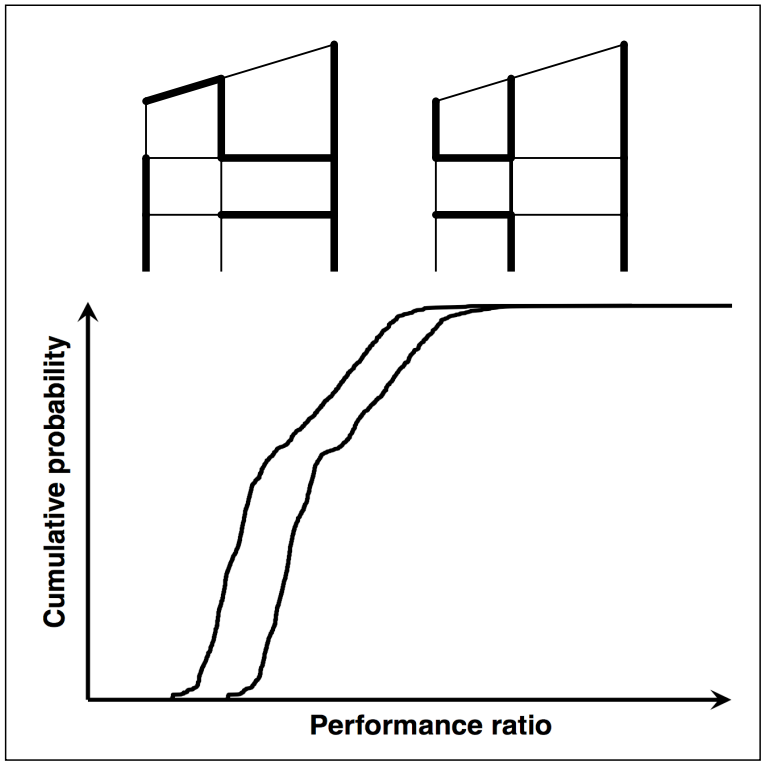

Dottorato di Ricerca in Ingegneria delle Strutture
Politecnico di Torino

Valerio De Biagi

Complexity and robustness of structures against extreme events

Tesi per il conseguimento del titolo di Dottore di Ricerca
XXVI Ciclo (A.A. 2011 - 2012 - 2013)

Dottorato di Ricerca in Ingegneria delle Strutture
Politecnico di Torino

Gennaio 2014

Dottorato di Ricerca in Ingegneria delle Strutture
Politecnico di Torino
10129 Torino, Italia
Tutore: Prof. Bernardino M. Chiaia
Coordinatore: Prof. Alberto Carpinteri
DOI: 10.6092/polito/porto/2540889

Summary

Civil structures are designed to support the loads acting on them. At present, the common practitioner considers both ordinary (winds, snow, accidental loads) and extreme events (earthquake, fire), combines the actions in such a way that, once the resistance of the elements is determined, the probability of failure is limited to a prescribed value. The set of events that may interest the structure is known and, therefore, a statistics of the actions is defined a priori. However, other events that are not forecastable may interest the construction. The sources of such events, called "Black Swans" after Taleb, are unknown, as well as their magnitude. For ensuring the integrity of the construction in such situations, which imply large damages, robust measures have to be taken (Chapter 3).

Structural engineering is not the only domain in which unexpected events occur. Nature is the realm of contrasts. By means of evolution, living species differentiates, differentiated, in order to survive and reproduce. Various strategies were implemented in order to guarantee a biological robustness. Such mechanisms evoke one fundamental property of systems, the complexity and the connectivity between the components. The interaction between the parts makes the whole system more robust and tolerant to errors and damages (Chapters 1 and 2).

Robustness in structures is implemented through classical strategies, which tend to limit the extent of damages through a design based on the consequences (Chapter 4). Being inspired by natural strategies, the idea of complexity in structural engineering is explored. Many issues arise, since a proper definition of this term has not been stated yet (Chapters 5 and 6). The effects of element removal on frame structures, which represent an example of highly connected structural scheme, are investigated. As a result of simple simulations, the trend observed in Nature, which wants the complex systems to be robust to random damages, are spotted in the loaded structural schemes (Chapter 7).

Sommario

Le strutture civili sono progettate per sostenere l'azione dei carichi agenti su queste. Allo stato attuale, i progettisti considerano, nell'analisi dei carichi, sia le azioni ordinarie (quali vento, neve, carichi accidentali) che quelle straordinarie (terremoto e incendio). Queste sono tra loro combinate in maniera tale per cui, una volta che la resistenza degli elementi strutturali è determinata, la probabilità di rottura è limitata ad un valore prefissato. Visto che l'insieme delle azioni agenti è noto a priori, l'elaborazione di una statistica è possibile. Tuttavia, altri fenomeni non prevedibili a priori possono interessare la costruzione. La fonte di tali eventi, definiti da Taleb "Cigni Neri", è sconosciuta, così com'è sconosciuta la loro intensità. Per garantire un'opportuna integrità strutturale (solitamente tali situazioni comportano danni estesi) devono essere adottate delle misure di robustezza strutturale (Capitolo 3).

L'ingegneria strutturale non è il solo campo in cui eventi inattesi possono accadere. La Natura è il regno dei contrasti. Grazie all'evoluzione, le specie viventi si differenziano, si sono differenziate, con il fine di sopravvivere e di riprodursi. La robustezza biologica è garantita attraverso differenti strategie. Questi meccanismi richiamano una proprietà fondamentale dei sistemi, ossia la complessità e la connettività tra le componenti dei sistema. L'interazione tra le parti garantisce, a livello globale, robustezza e tolleranza agli errori ed al danneggiamento (Capitoli 1 e 2).

Solitamente, la robustezza strutturale è garantita attraverso strategie classiche che tendono a limitare l'estensione del danneggiamento attraverso una progettazione basata sulle conseguenze e particolari accorgimenti (Capitolo 4). Lasciandosi ispirare dalla Natura, l'idea di una complessità strutturale è esplorata. Dal punto che una definizione vera e propria di complessità strutturale non è mai stata formulata, molte questioni nascono (Capitoli 5 e 6). Gli effetti della rimozione di elementi su strutture tipo telaio, le quali rappresentano un esempio di un sistema strutturale fortemente connesso, sono studiati. Come risultato di semplici simulazioni, i *trend* osservati in Natura, ossia che i sistemi complessi risultano essere robusti a danneggiamenti casuali, sono visibili anche a livello strutturale (Capitolo 7).

Contents

Part I

Unpredictable events and robustness

Chapter 1

Extreme events on Natural Systems

If one types "extreme event" on an Internet search engine, the first tens of results relate to meteorological or climate phenomena. These are the main research fields in which this term is employed; scrolling down, other results appear, related mostly to economy.

A proper definition of "extreme event" is difficult to state. In meteorology the term is usually referred to the initial meteorological phenomena (Easterling et al., 2000). In parallel, some authors include, in the definition, the consequential physical impact, like flooding (Young, 2002) or the entire spectrum of outcomes for humans and, in general, for the society.

If there are series of observations and measurements of a physical quantity and these are long enough, it is possible to develop a statistics and, then, to estimate the probability of having measurements above or below a given threshold. This represents the common way in designing and testing engineering objects. Climatologists defines the event as "extreme" if the thresholds to be used in the probability distribution are close to the upper (or lower) end of the range of the observed values of the variable.

It is important to point out the fact that the presence of observations and data is fundamental for the determination of the type and the shape of the statistical distribution. Taking as example weather observations, there are long-series of measurements for wind speeds and precipitations, but no soil moisture data with sufficient spatial resolution. Similarly, another problem is represented by the temporal resolution of the measurements. For example, seasonal observations are not sufficiently detailed for the set-up of a statistics for monthly extreme events in a changing climate, as illustrated by Frei and Schär (2001). This aspect would be detailed in Chapter 3 under the appellation of "lack of knowledge".

I define as *system* the set of animated and nonliving entities ascribable to common features, e.g. the human society, the natural physical environment, the ecosystem, which can be subjected and interested by events. The effects of the extreme events acting on the system are called *impacts* (Lavell et al., 2012). Furthermore, it is possible to define as *extreme impact* the one engendering highly significant consequences on the system. It is possible that extreme

events may have extreme impact on a particular system, and no impact (but even positive consequences) on another one. For example, very cold and long winters may increase the mortality of crops aphids, which translates into richer harvest the following summer (Butts and Schaalje, 1997).

As illustrated, extreme events do not necessarily presuppose extreme impacts. In addition, it is possible that extreme impacts are due to non-extreme events. The following cases are analysed in detail. In the former situation, an extreme event results in extreme impact for the system if there is a certain amount of exposure (and vulnerability) of the system to the event coupled with a high magnitude of the event. In the latter, if the system is highly exposed and vulnerable to a particular action, extreme impacts may be produced by non-extreme events.

Exposure is a necessary but not sufficient condition for impact: vulnerability is also required. Cutter and Emrich (2006), analysing the effects of Hurricane Katrina on Mississippi delta, have shown that some regions may be more susceptible to the impacts of hazards than other places based on the characteristics of the people residing within them.

The term *exposure* relates to the presence of elements of the system that could be affected by the physical event and can be potentially damaged, lost or simply harmed. Furthermore, the term *vulnerability* refers to the result of the interaction between the elements of the system and the physical event. In the most general terms, vulnerability is the propensity of an element of the system to be adversely affected. The vulnerability has a strong influence on the level of damage on the elements of the system. For example, low vulnerability results in high damages only in case of high magnitude events; on the contrary, a similar level of damages can be recorded in case of low magnitude events and high vulnerability (Wisner et al., 2012).

An extreme impact turns into a disaster if at least one of the following thresholds is surpassed (Alexander, 1993): (i) the spatial extension of the effects of the events is larger enough that the damages cannot be restored without the helps of neighbours similar systems; (ii) the required recovery time is long enough that further damages may occur; (iii) the impact of the event on the system is such to limit the possibilities of the elements of the system to repair themselves. Sometimes, the term disaster is directly linked to the number of killed (or injured) or to the reparation costs: *a disaster is a situation or event which overwhelms local capacity, necessitating a request to a national or international level for external assistance; an unforeseen and often sudden event that causes great damage, destruction and human suffering* (Below et al., 2009). Based on this statement, a detailed database of disasters was created and is constantly updated at the Centre for Research on the Epidemiology of Disasters (CRED, 2010).

It has been confirmed that extreme events does not presuppose a disaster, since the exposure of the components of the system to the event can be low. Is the inverse true, i.e. are disasters always generated by extreme events? The answer is negative, since, if particular conditions subsist, even probabilistically non-extreme events can engender a disaster. This is the case in which natural events have important social and economic impacts on local communities and governments, as highlighted by recent United Nations reports (International Strategy for Disaster Reduction, 2009, 2011). The same trend has been observed analysing University

of Louvaine EM-DAT database (CRED, 2010). Many disasters are not initiated by statistically extreme events, but rather exhibit extreme properties expressed as severe interruptions in the functioning of local social and economic systems (Lavell et al., 2012). In social systems, it has been shown that the range of disaster-inducing events can increase if social conditions deteriorate (Wisner et al., 2012).

Parallel to vulnerability concept, some authors have introduced the notion of *capacity*. This can be intended as the combination of all the strengths, attributes, and resources available to an element of the system to achieve established goals (Lavell et al., 2012), including the ability to cope with extreme events (Anderson and Woodrow, 1989). This idea serves as introduction to the concept of *resilience*, which is the ability of a system and its component parts to anticipate, absorb, accommodate, or recover from the effects of a potentially hazardous event in a timely and efficient manner, including through ensuring the preservation, restoration, or improvement of its essential basic structures and functions. The term takes its origins in engineering and is a useful concept in risk analysis (Aven and Renn, 2010).

In such environment, living entities live, develop and experience extreme situations; in other words, Nature is the domain of contrasts (Krakauer, 2006). On one side, it tends to transform, evolve and generate diversity (Ball, 2011a,b,c). On the other, the natural system tends to preserve itself keeping the species different the ones from the others. The first mechanism has been diffusely studied after the publication of Darwin (1859) evolutionary theories reported in *On the Origin of Species*. Based on the large amount of observations recorded, Darwin gave a unified view of the complexity of life by means of a unique process: the evolution. Despite the fact that the Eighteenth Century evolutionists considered, without details, the presence of mechanisms of inheritance of traits across different generations, another discipline more devoted to the biochemistry of the inheritance rose in the same period: genetics. The modes with which the traits are transferred from parents to children were defined and published by Mendel (1866) on an obscure Austrian journal. Since the scientists were not aware of the research work made by each other, no crossing between the two disciplines occurred. Only in the 20th century, the two fields of research merged together in order to give a solid experimental and theoretical basis for the study of the evolution.

The Evolution intended by Darwin was only concerned with the phenotype, which is the set of observable traits and characteristics of an individual. In this sense, traits have been shown to tend towards a mean, i.e. a small variation tends to be absorbed by the whole population in few generations (Galton, 1886). After the work of Huxley (1942), genotype, i.e. the genetic makeup of an organism, and phenotype were compared together and many interesting observations were highlighted and are still studied by population geneticists. Their purpose, more focused on statistics than on biology, is to determine the fate of a population whose individuals reproduce with variability and struggle for survival in an environment which discriminates their traits, favouring ones over others (Manrubia and Cuesta, 2010). Through the mutation of existing genes, new traits appear randomly and survive depending on how adaptable they are to the environment. Studies on population showed that there are geno-

types that are more robust against mutations depending on the topology of the genotype space (Van Nimwegen et al., 1999). Even if the selection pressure does not exist in an evolutionary system in which there is variation and heredity, i.e. the traits replicates at the same rate, there is a tendency for diversity and complexity to increase (McShea and Brandon, 2010).

The work of Kimura (1968), reporting that most mutations in the genome of mammals have no effect on their phenotype, represented a turning point in thinking about genotype and phenotype. In other words, although no genotype change occurs, i.e. the phenotype is identical, an hereditary variation of DNA takes place. This consideration, sustained by the concept of genetic drift, puts the bases of the concept of *robustness of biological systems*.

In Biology, different mechanisms are involved in the robustness, as detailed in the following.

- Suppose to conduce the following genetic experiment: (i) identify the functions of a gene in a given organism, (ii) make a reproduction of the organism by removing (or silencing) the gene, (iii) compare the phenotype of the two organisms related to the function. One may erroneously suppose that gene removal produces a variation in the organism. This effect emerges in a reduced percentage of cases: the phenotype of parent and child organisms is usually equal. The explanation of that is concerned with the **redundancy**, i.e. more than one gene contribute to the phenotype (Krakauer and Nowak, 1999). Redundancy as a principle, is more general, and describes any case in which the mechanism of robustness is only operative in case of perturbation (Krakauer, 2006).

- Nature has a series of structures working as **feedback controllers**. For example, considering species abundance as the system under control, death rate acts as controller. Biological robustness emerges after the happening of events (that may have different causes) since the system reacts through the action of the controllers. In general, more than one controller is present, resulting in a redundancy in the controlling mechanism.

- Each trait is the output of a set of genes. The pleiotropy, that is the influence of a single gene on multiple phenotypic traits, is reduced insomuch that any transmission error is bounded on a particular trait (Goldberg, 1995). In physiology, this **modularity** results in different levels of organisation (from genes, to cells) as highlighted by Winther (2001).

- Living systems perform a difficult task to implement in engineering: since redundancy mechanism lets the system to survive even if a part of it got lost, Nature is able to purify itself by an **anti-redundancy** mechanism (Krakauer and Plotkin, 2002). This phenomenon appears when the removal of a gene results in a larger variety of the phenotypic population. The mechanism is effective only when the replication rates are sufficiently large. For example, apoptosis, i.e. programmed cell death, is a common strategy for eliminating cells upon damage to their genomes or upon infection. The strategy is executed exclusively on these cell types that are capable of regeneration –

that is why nerve cells and germ cells produce factors that strongly inhibit apoptosis (Matsumoto et al., 1999).

- Natural systems are compartmentalised, i.e. they are made up from a finite number of macroscopic subsystems interacting the ones with the others through the exchange of material (Jacquez, 1985). Biochemically, the spatial **compartmentalisation** of reactions leads to robustness by minimising covariance among reaction components participating in functionally unrelated processes. Thus, spatial de-correlation through compartmentalisation substitutes for temporal correlation in biological functions. Robustness is achieved in at least two ways: (i) minimising interference - chemical, epistatic or physiological, and (ii) minimising mutual dependencies and thereby attenuating the propagation of error through a system.

Biological robustness is one of the key elements for survival in Nature. Through the mechanisms previously described, natural systems are able to maintain their functions if internal or external perturbations are applied to them; in parallel, living systems are able to be performant even if perturbations and uncertainty are present (Stelling et al., 2004). If both previous sentences can be considered as definitions of biological robustness, in such complex systems, in which there is a high degree of hierarchy, the ability of maintaining a function has to be distinguished with the ability to maintain a state. That is why Kitano (2007) defined as *homeostasis* the set of steady states that are kept by the system through the interaction between a complex set of physiological processes and that contribute to the robustness of the system. This stability has not to be confused as a state of constancy, but rather with a condition that varies during the time with small fluctuations, as outlined by (Cannon, 1932), and entails robust properties at cross-levels in living bodies. In this sense, an extraordinary example is represented by tardigrades and their uncontested ability to survive in extreme environments (Jönsson and Bertolani, 2001). They suspend metabolism almost completely, if not entirely, under extreme dehydration and enter the dormant state, surviving for years (Crowe and Crowe, 2000). This dormant state is attained by extensive production of trehalose and tardigrades become active again upon rehydration. Similar cases on other organisms have suggested Clegg (2001) to suppose a third form of life, the *cryptobiosis*, i.e. a suspension of metabolism. Such examples show that organisms can attain an impressive degree of robustness by switching from one steady state to the other, rather than trying to maintain a given state.

Biological entities are designed to be tolerant to various kinds of attacks. In this sense, the architecture of the system plays a fundamental role in its capacity of being robust. The metabolic network has been discovered being scale-free (Jeong et al., 2000). As detailed in Chapter 2, such architectures are robust to random attacks.

Living entities are able to dynamically change their internal architecture. This property, which is indirectly present in Darwin reports, lets the organism to modify itself through the reproduction in order to explore all the possible configurations and getting robust. Several evolutionary biologists calls as *evolveability* the capacity to generate heritable, selectable phe-

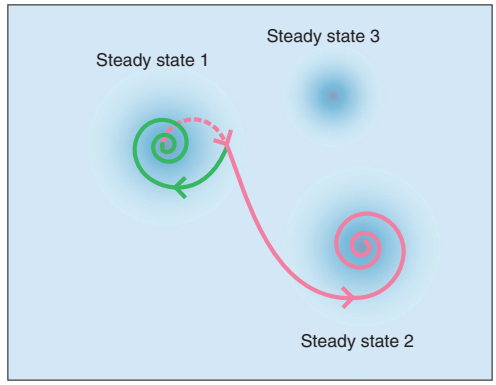

Figure 1.1: Stability, homeostasis, and robustness. Assume that the initial state of the system is at the centre of Steady state 1. A perturbation may drive the state of the system toward the boundary of the basin of attractor of Steady state 1. When the state of the system returns to its original state, it is called 'stability' and 'homeostasis'. When it transits to Steady state 2, stability is once lost and the system regains its stability in the new steady state. If the system's functions are still intact, such transition of state is considered a part of robust response. The system is considered to be robust if it maintains functions regardless of whether it is in Steady state 1 or 2. On extreme case, the system may continue to transit between multiple steady state points to cope with perturbations, after the original paper by Kitano (2007).

notypic variation (Kirschner and Gerhart, 1998). The capacity of natural systems to get the maximum benefit with the minimum effort in a specific situation or environment produces a large range of individuals, i.e. millions the species (8.7 millions). The architecture of the regulatory system of living entities, i.e. the biochemistry of the physiology, is the result of a continuous adding of control components (Kitano, 2004). It results a **complex system** able to sustain a large set of events acting on it. Unfortunately, a network composed by feedbacks loops is largely unstable when unexpected perturbations are encountered, leading to catastrophic failure. Examples of this behaviour exist in Nature, as suggested Carlson and Doyle (1999, 2002) to formulate the theory of *highly optimised tolerance* that argues that systems that have evolved to be robust against general perturbations are extremely fragile against certain types of rare perturbations. This trade-off between fragility and robustness shows that robustness is a conserved quantity, and this tendency has been recorded in biological systems (Csete and Doyle, 2002). In parallel, the scale-free architecture of the control system brings the attention to the preferential attachment procedure of creating complex networks, detailed in the following. As a result of that, Bak et al. (1987) argued that when a spatially extended system with many degrees of freedom is driven away from equilibrium by an external force, the stationary state is the one with power law spatial correlation. It spontaneously evolves to such a critical state and without any sort of tuning process. They gathered this property into the

self-organised criticality theory, which represents a different model of biological robustness.

Considering the ability of Nature to modify its internal structure in order to deal with external events, two examples are reported. The former relates to blood circulation in the brain, the latter to spider web. Both refer to systems that can be idealised as networks, in which the robustness is ensured by the presence of connections between the elements.

The circulatory system in the cortex can be seen as a large pipe network in which the blood flows. Despite the possibility of the vessels to change in diameter, and thus to oppose larger or smaller flow resistance, another strategy for ensuring the supply of nourishing to the cells is represented by the presence of additional links in the network. As said, other than increase the transfer to the brain mass, the presence of loops ensures the supply of blood in case of damage. First, from the perspective of static resource management, when a single surface vessel suffers a targeted occlusion, bloodstream in downstream vessels does not cease but rather is maintained in the surface network through reversal of flow direction in the nearest vessel, see Figure 1.2. This rerouting is also observed when a major tributary to the middle cerebral artery is occluded. The analysis the backbone of rats has highlighted the presence of loops. In detail, the ratio between the number of pipes and the number of connections is 3 to 2, showing a hexagonal lattice structure (similar to the honeycomb). Removing randomly the connections, i.e. supposing that a vessel is occluded, Blinder et al. (2010) found that 12.6 % of the backbone vessels can be removed before 5 % of the connections got isolated.

Another example that has to be mentioned relates to spider web. Spider webs are masterpieces of natural structural engineering (Alam et al., 2007); centuries of evolution shaped them in order to achieve a desired optimised functionality, i.e. the capture of prey by the minimum of silk (Hansell, 2005). The interest on this topic is mainly due to the fact that spider constructions are the result of an evolution process that started 450 millions years ago. The attention has to be put on two different structural characteristics: material and topology. Referring to material, the nature of the molecules constituting the silk and their hierarchical assembly into fibres are the secrets beyond the highly nonlinear behaviour. Four different stress-strain regimes can be identified, as shown in Figure 1.3. The distribution of stiffnesses and strengths across spider web, as well as its topology, are fundamental for an efficient hunting tool.

The stiff behaviour of silk under small deformation, before the yield point, is essential in maintaining the structural integrity of the web. A loading comparative study (radial *vs* spiral threads) demonstrated that the web structural performance is dominated by the properties of the stiffer and stronger radial dragline silk (with the force required to break radial threads within the web approximately 150% higher), suggesting that the spiral threads play non-structural roles (such as capturing prey).

The superior performance of silk in webs is therefore not due merely to its exceptional ultimate strength and strain, but arises from the nonlinear response of silk threads to strain as well as geometrical arrangement in a web.

Cranford et al. (2012) numerically compared the response of webs constructed from three

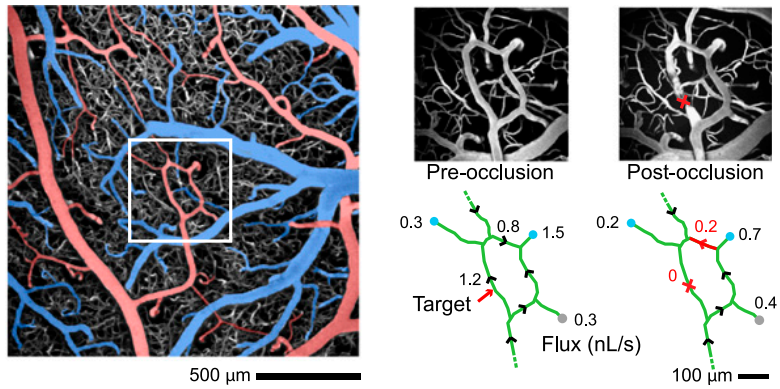

Figure 1.2: Preservation of flux through penetrating arterioles after single-point occlusion of a surface arteriole loop. On the left-hand side, maximal projection of a stack of images collected from the upper 300×10^{-6} m of rat cortical vasculature using in vivo TPLSM (Two-Photon Laser Scanning Microscopy). The pial arteriole network is pseudocolored in red and the venous network in blue. The inset highlights a small arteriole loop with three penetrating arteriole stubs. On the right-hand side, a localised clot is formed in one segment of the surface arteriole loop using targeted photothrombosis (x in loop). Pre- and post-occlusion measurements of the flux of erythrocytes in penetrating arterioles and surface arterioles were collected. Local penetrating arterioles were situated near the targeted surface arteriole, and distant penetrating arterioles were measured as controls, after the original paper by Blinder et al. (2010).

different types of fibres with distinct mechanical behaviour. Model A refers to the derived stress-strain behaviour of dragline silk, Models A' and A" are related to idealised engineered fibres that exhibit either linear elastic behaviour or elastic-perfectly plastic behaviour that involves severe softening (plastic yield), respectively. In all cases, one of the radial threads is loaded and the failure stress (about 1400 MPa) and strain (about 67%) of silk threads are assumed constant. In this configuration, any change in deformation behaviour and web damage would be a direct result of differences in the stress-strain behaviour of the fibres, see Figure 1.4. In the case of a web composed of natural dragline silk, all radial threads partially contribute to loading resistance. The fact that the material suddenly softens at the yield point, with immediate reduction of Young's Modulus (roughly 80% smaller than the initial value, say 1000 MPa), ensures that only the loaded radial thread enters into regime III and begin to stiffen. Finally the web collapses. Supposing linear elastic material behaviour, the loaded radial thread are subjected to the bulk of the load; but adjacent radial threads bear a higher fraction of the ultimate load, which results in a greater delocalisation of damage upon failure. With elastic-perfectly plastic behaviour, the softening of radial threads enhances load distribution throughout the web even more and, thereby, it greatly increases the damage zone once

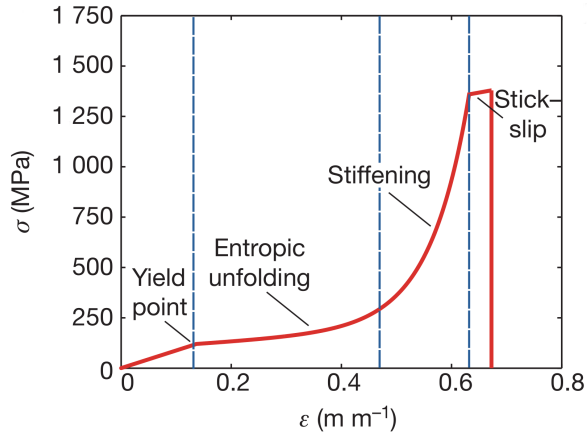

Figure 1.3: Derived stress-strain (σ-ϵ) behaviour of dragline silk from the species *Nephila clavipes*, parameterised from atomistic simulations and validated against experiments. There are four distinct regimes characteristic of silk. I, stiff initial response governed by homogeneous stretching; II, entropic unfolding of semi-amorphous protein domains; III, stiffening regime as molecules align and load is transferred to the β-sheet crystals; and IV, stick-slip deformation of β-sheet crystals until failure, after the original paper by Cranford et al. (2012).

failure occurred.

Numerical simulations performed by Alam et al. (2007) confirmed that transverse displacements in webs with initial tension are less than those without initial tension. When the initial tensions are taken into account, the total stiffness of the web increases due to the addition of geometrical stiffness, which is a function of initial tensile force. When stiffness is higher, the web is more stable and any broken element produces only a local effect. On the other hand, without initial tension, the web is less stable and any broken element affects the whole structure.

In the last years Taleb introduced the notion of antifragility (Taleb, 2011, 2012, Schmieder et al., 2012). Since fragility is related to how a system suffers from the variability of its environment beyond a certain preset threshold, anti-fragility refers to when it benefits from this variability. To understand his idea, he proposes a simple example: a coffee cup on a table suffers more from large deviations than from the cumulative effect of some shocks. Conditional on being unbroken, it has to suffer more from "tail" events than regular ones around the center of the distribution. This is the case of elements of nature that have survived: conditional on being in existence, then the class of events around the mean should matter considerably less than tail events, particularly when the probabilities decline faster than the inverse of the harm. In other words, exposure to tail events suffers from uncertainty.

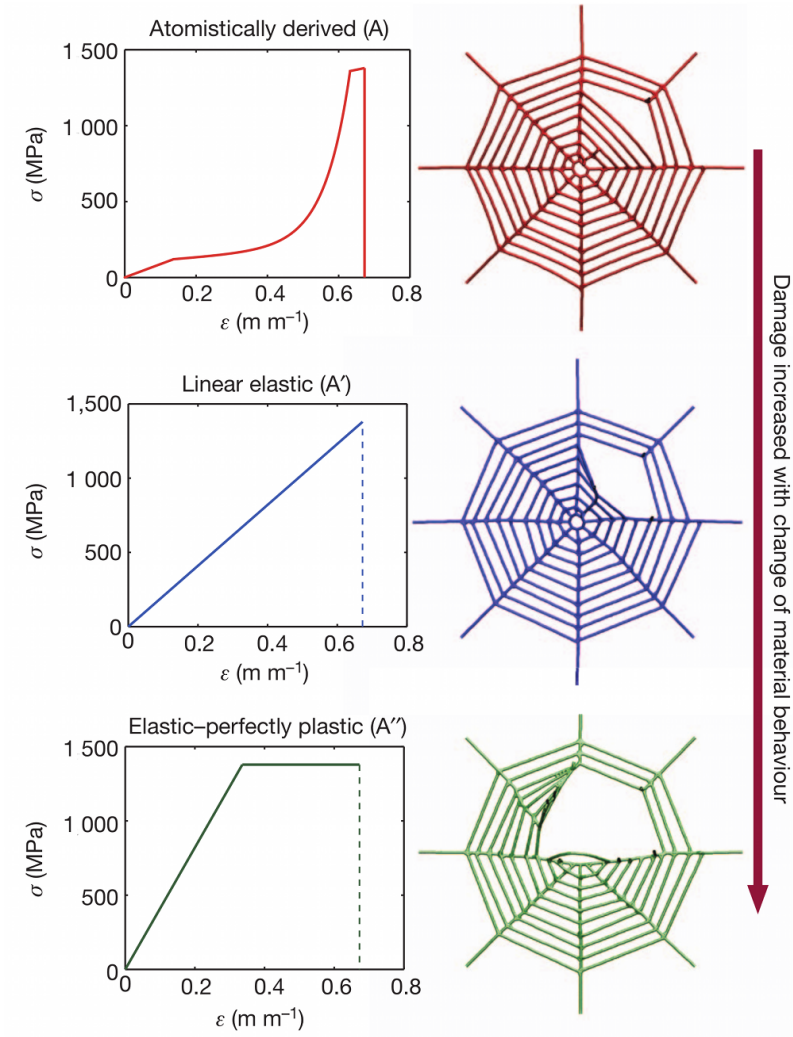

Figure 1.4: Web response for varied silk behaviour under targeted loading. Comparison of failure for derived dragline silk, linear elastic and elastic-perfectly plastic behaviours (models A, A' and A"). Comparison of failure confirms localised stresses and minimised damage for the natural nonlinear stiffening silk behaviour. When load is applied locally to a radial thread, other radial threads not subject to applied force reach a stress corresponding to the onset of yielding (that is, regime II in Figure 1.3). The elastic-perfectly plastic behaviour leads to an almost homogeneous distribution of stress, after the original paper by Cranford et al. (2012).

As shown in this chapter, Nature tends to be robust in order to let the species to progress through reproduction. In order to ensure such robustness in a highly hierarchal system, different strategies are used both intra-level and inter-level. One of the key elements in the robustness of such evolving system is represented, indeed, by evolution and adaptation. These are the driving forces and this mechanism is the terrain for the development of specific methods for ensuring the stability in the response of a system under unexpected events. This natural evolutionary mechanism takes "vital energy" from the volatile environment. That is why it may be considered anti-fragile (Taleb and Douady, 2013).

As mentioned in the second part of the chapter, robustness and fragility are characteristics that are contemporarily active in the system. If there is the capacity to maintain the vital functions when designed events act, the structure is highly vulnerable to unexpected events. This is the result of the complex number of the feedback controls that are implemented. It seems that different components linked together make the whole system robust, in the sense that the removal of one part, or the interruption of one link between the different functional components, is not deleterious for it. Complexity arises and represents the key element for the robustness of the biological world.

Chapter 2

A connected world

2.1 Graphs: a brief review

The city of Königsber (now called Kaliningrad) occupies both banks of the River Pregel and an island, Kneiphof, which lies in the river at a point where it branches into two parts. At the beginning of the Eighteenth century, seven bridges spanned the various section of the river and linked the different borough of the city[1]. The problem on traveling through the city was: could a person devise a path through Königsberg so that one could cross each of the seven bridges only once and return home? The answer is negative and the first mathematical proof of this was presented by Leonhard Euler in 1735 and later published in the Commentarii of the Petersburg Academy (Euler, 1741).

In his logical reasoning, the mathematician treated something more than the original problem; he begun a generalization to two islands and four rivers, as illustrated in the original drawings that are reproduced in Figure 2.1. Anyway, as Alexanderson (2006) notes, Euler gave only a necessary condition, and not a sufficient one, for solving the problem.

Without any doubt, the origins of graph theory are different from the ways other mathematical fields sprouted. Usually, disciplines are theorised after that fundamental problems in calculation, motion, and measurement have risen. This discipline on graphs takes its origins in puzzles and riddles. But, despite the apparent triviality of such puzzles, it captured the interest of mathematicians, with the result that graph theory has become a subject rich in theoretical results of a surprising variety and depth (Bigg et al., 1976).

The starting point is very simple and requires very few tools: a graph is a representation of a set of objects connected by links.

In the following, a review on graph theory (Diestel, 2010) and algebraic graph theory

[1] Unfortunately, after the bombing of the WWII, the map of the connections in the city changed and the original bridges were demolished or replaced by modern ones.

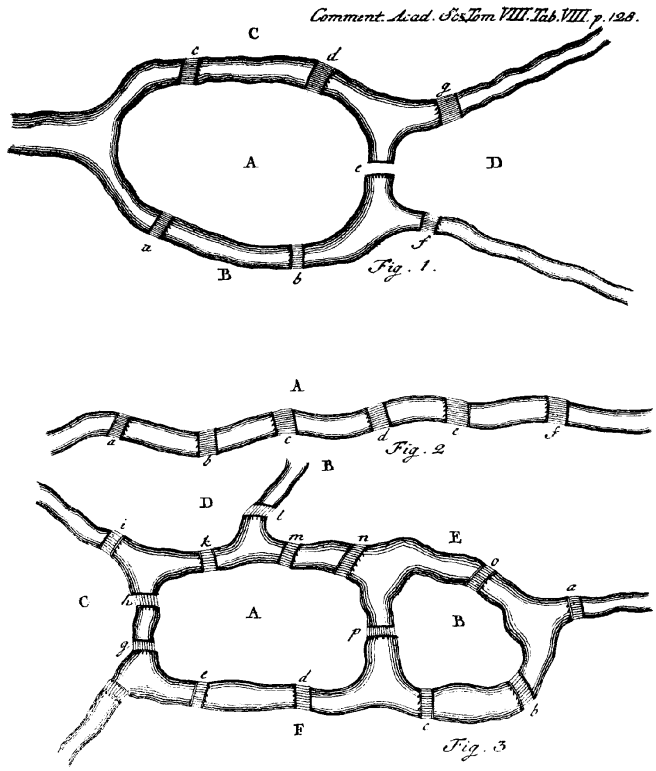

Figure 2.1: The engravings illustrating Euler's 1736 paper on the bridges of Königsberg.

(Godsil and Royle, 2001) is made in order to make the reader aware of the symbols used throughout the dissertation.

2.1.1 Basics on graph theory

A *graph* is a pair $G = (V, E)$ of sets such that $E \subseteq [V]^2$, that is, the elements of E are 2-element subsets of V, e.g. $e_m = (v_i, v_j)$. The elements of V are called either *vertices* or *nodes* or *points* of the graph G. The elements of E are called either *edges* or *lines*. Usually, drawing a dot for each vertex and joining two of these dots by a line if the corresponding two vertices form an edge pictures the graph. The position of the vertices on the drawing is irrelevant, since the interest is on which vertices form an edge and which do not, see Figure 2.2.

A graph with vertex set V is said to be a graph *on* V. The vertex and edge sets of a graph are referred to as $V(G)$ and $E(G)$, respectively. The number of vertices of a graph G is

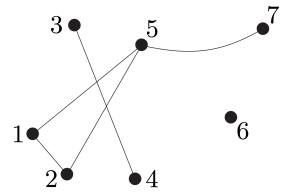

Figure 2.2: A pictorial representation of graph $G = (V, E)$. The vertices are $V = \{1, \ldots, 7\}$ and the edges are $E = \{\{1, 2\}, \{1, 5\}, \{2, 5\}, \{3, 4\}, \{5, 7\}\}$.

called *order* and is written as $|G|$, the number of vertices is denoted as $\|G\|$. In the present text the number of vertices is limited and, thus, the order is *finite*.

Ends and adjacency

A vertex $v \in V(G)$ is *incident* with an edge $e \in E(G)$ if $v \in e$. e is said to be an edge *at* v. The set of all the edges in E at a vertex v is denoted by $E(v)$. The two vertices incident with an edge are its *endvertices* or *ends* and, thus, an edge *joins* its ends. An edge $\{x, y\}$ is usually written as xy (or yx).

Two vertices x, y of G are *adjacents* or *neighbours* if xy is and edge of G, i.e. $xy \in E(G)$. The set of neighbours of a vertex v in G is denoted by $N_G(v)$, or briefly by $N(v)$. If all the vertices of G are pairwise adjacent, then G is *complete*. A triangle is a complete graph of order 3 and is indicated as K^3. In general, a complete graph on n vertices is a K^n.

If the edges have a direction associated with them, the resulting graph is called *directed* graph or *digraph*. In this case, the digraph is a pair $G = (V, A)$ of vertices, V, and ordered pairs of vertices, A, which can be named *directed edges* or *arrows*, since they can be sketched in this way.

Subgraphs

Let $G = (V, E)$ and $G' = (V', E')$ be two graphs. G and G' are *disjoint* if their intersection, that is $G \cap G' := (V \cap V', E \cap E')$, is an empty graph, i.e. $G \cap G' = \emptyset$. If $V' \subseteq V$ and $E' \subseteq E$, then $G' = (V', E')$ is a *subgraph* of G and it is written as $G' \subseteq G$.

If $G' \subseteq G$ and G' contains all the edges $xy \in E(G)$ with $x, y \in V(G')$, then G' is an *induced subgraph* of G, see Figure 2.3. It is said that V' *spans* G' in G. If the vertex set of the graph and of its subgraph are identical, i.e. $V' = V$, V' spans all of G, and then G' is said a *spanning* subgraph of G.

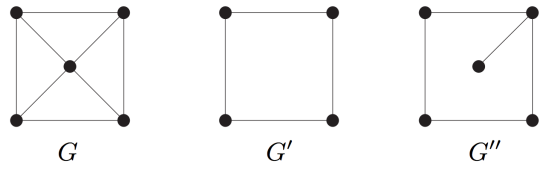

Figure 2.3: A graph G with subgraphs G' and G'': G' is an induces subgraph of G, but G'' is not. On the contrary, G'' is a spanning subgraph of G.

Degree and regularity

The *degree* of a vertex v, denoted as $d(v)$, is the number $|E(v)|$ of edges at v. A vertex with degree 0 is *isolated*. The number $\delta_G := \min\{d(v) \,|v \in V\}$ is the *minimum degree* of G, the number $\Delta_G := \max\{d(v) \,|v \in V\}$ its *maximum degree*.

If all the vertices of G have the same degree k, then G is *k-regular*, or *regular*. The number

$$d_G := \frac{1}{|V|} \sum_{v \in V} d(v)$$

is the *average degree* of G.

Paths and distances

A *path* is a non-empty graph $P = (V, E)$ of the form

$$V = \{x_0, x_1, ..., x_k\}$$

and

$$E = \{x_0, x_1x_2, ..., x_{k_1}, x_k\},$$

where the x_i are all distinct. The vertices x_0 and x_k are *linked* by P and are called its *end-vertices* or *ends*. The vertices $x_1, \dots, x_{k-1}$ are the *inner* vertices of P. The number of edges of a path is its *length*, and the path of length k is denoted by P^k, see Figure 2.4. The path is written as the sequence of its vertices, e.g. $P = x_0x_1x_2 \dots x_k$.

If $P = x_0x_1x_2 \dots x_{k-1}$ is a path and $k \leq 3$, then the graph $C := P + x_{k-1}x_0$ is called a *cycle*. The *length* of a cycle is its number of edges (or vertices); the cycle of length k is called a *k-cycle* and is denoted by C^k.

The length of the shortest path in G between two vertices x, y is called *distance*, $d_G(x, y)$. If no such path exists, the distance is set to infinite, i.e. $d_G(x, y) := \infty$. The greatest distance between any two vertices in G is the *diameter* of G, ϕ_G.

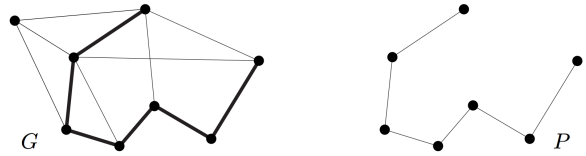

Figure 2.4: A path $P = P^6$ in G.

Connectivity

A graph G is called *connected* if any two of its vertices are linked by a path in G. If it is not, the graph is said *disconnected*. The maximal connected subgraph of G is a *component* of G. The components are clearly induced subgraphs, see Figure 2.5.

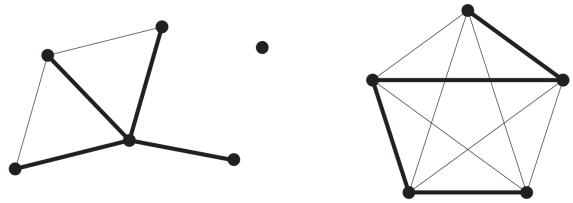

Figure 2.5: A graph with three components, and a minimal connected subgraph in each component.

Trees and forests

A graph without any cycles, i.e. and *acyclic* graph, is called a *forest*. A connected forest is called a *tree*, see Figure 2.6. In other words, a forest is a graph whose components are trees. Sometimes it is convenient to consider one vertex of a tree as special; such a vertex is then called the *root* of this tree. A tree T with a fixed root r is a *rooted tree*.

There is a theorem that can be useful for the identifying a tree in a graph. In particular it states that

The following four different assertions are equivalent for a graph T:

(i). T is a tree;

(ii). Any two vertices of T are linked by a unique path in T;

(iii). T is minimally connected, i.e. T is connected but $T - e$ is disconnected for every edge $e \in T$;

(iv). T is maximally acyclic, i.e. T contains no cycle but $T + xy$ does, for any two non-adjacent vertices $x, y \in T$.

The proof of the theorem is not quoted here, refer to Diestel (2010) for details.

For the understanding of the procedures implemented in Chapter 5, the following corollary is fundamental.

A connected graph with n vertices is a tree if and only if it has $n - 1$ edges.

The conceptual proof of the corollary derive from the possibility to enumerate the vertices of a connected graph, as extensively detailed in Diestel (2010).

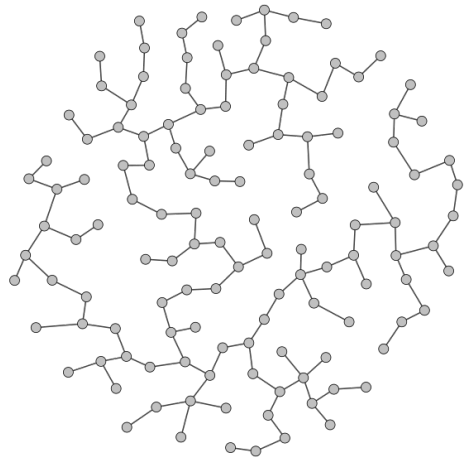

Figure 2.6: A tree.

2.1.2 Graphs and algebra

Algebraic graph theory is a branch of mathematics that aims to study graph problems with algebraic methods. Mainly, three different matrices can be associated to a graph: the adjacency matrix, the incidence matrix and the Laplacian. One of the main issues of algebraic graph theory is to determine precisely how, or whether, properties of graphs are reflected in the algebraic properties of such matrices (Godsil and Royle, 2001).

Adjacency matrix

The *adjacency matrix* $A(G)$ of a digraph G (directed graph) is the integer matrix with rows and columns indexed by the vertices of G, such that the uv-entry of $A(G)$ is equal to the number of arrows from u to v (which is usually 0 or 1), and not viceversa. If G is a graph, the each edge is a pair of arrows in opposite directions, and $A(G)$ is a symmetric 01-matrix. Since the graph has no loops, the diagonal entries of $A(G)$ are zero.

Incidence matrix

The *incidence matrix* $B(G)$ of a graph G is the 01-matrix with rows and columns indexed by the vertices and the edges of G, respectively, such that the uf-entry of $B(G)$ is equal to one if and only if vertex u is in edge f. If G has n vertices and e edges, then $A(G)$ has order $n \times e$.

In an directed graph, the incidence matrix $D(G)$ is the $\{0, \pm 1\}$-matrix with rows and columns indexed by the vertices and edges of G, respectively, such that the uf-entry is equal to 1 if vertex u is the head of edge f, -1 if u is the tail of f, and 0 otherwise.

If one considers the matrix $\Delta(G)$, which is the $n \times n$ matrix with rows and columns indexed by $V(G)$ with uu-entry equal to the degree of vertex u, the following lemma can be stated.

Let $\mathbf{B}$ *be the incidence matrix of the graph* G*. Then*

$$\mathbf{B}\mathbf{B}^T = \Delta(G) + A(G) \tag{2.1}$$

Let $\mathbf{D}$ *be the incidence matrix of the directed graph* G*. Then*

$$\mathbf{D}\mathbf{D}^T = \Delta(G) - A(G) \tag{2.2}$$

Laplacian matrix

Let G be a graph (directed or not) and let $\mathbf{B}$ its incidence matrix. The matrix $Q(G) = \mathbf{B}\mathbf{B}^T$ is called *Laplacian* of G. The Laplacian of a graph does not depend on its orientation.

The Laplacian gives information on different topological properties. For example,

Let G *be a graph with* n *vertices and* c *connected components. If* $\mathbf{Q}$ *is the Laplacian of* G*, then*

$$\operatorname{rank} \mathbf{Q} = n - c.$$

Remember that, since $\mathbf{Q}$ is a square symmetric matrix, it has real eigenvalues. In addition, $\mathbf{Q}$ is positive semidefinite and therefore its eigenvalues are all nonnegative. Denoting them by $\lambda_1(\mathbf{Q}), \ldots, \lambda_n(\mathbf{Q})$ with the assumption that

$$\lambda_1(\mathbf{Q}) \leq \lambda_2(\mathbf{Q}) \leq \cdots \leq \lambda_n(\mathbf{Q}),$$

the following conclusions can be drawn: $\lambda_1 = \lambda_1(\mathbf{Q}) = 0$ and

The multiplicity of zero as an eigenvalue of $\mathbf{Q}$ *is equal to the number of components of* G*.*

The number of spanning trees in a graph is determined by its Laplacian. Before stating the theorem, it is necessary to define the matrix $M[S]$ as the submatrix of M obtained by deleting the rows and the columns indexed by elements of S.

Let G *be a graph with Laplacian matrix* Q*. If* v *is an arbitrary vertex of* G*, then* $\det \mathbf{Q}[v]$ *is equal to the number of spanning trees.*

The proof of the theorem is not reported, refer to Godsil and Royle (2001) for details. Another important result is due to Kirchoff and states

Let G *be a graph on* n *vertices, and let* $\lambda_1, \ldots, \lambda_n$ *be the eigenvalues of the Laplacian of* G*. Then the number of spanning trees in* G *is*

$$\frac{1}{n}\prod_{i=2}^{n}\lambda_i.$$

Obviously, in the case that a graph is also a tree, the result of the previous expression is 1. On the contrary, if a graph has more than one component, since there is more than one eigenvalue that is equal to zero, the result of the previous expression is 0.

2.2 Connected and robust

"Summer 1996 was a sizzler [...] In the blistering heat of August 1996, everyone with an air-conditioner was running it full blast and every ice-cold Budweiser at every backyard barbecue was drawing its share of power from the grid" (Watts, 2004). On August 10, a transmission line in western Oregon sagged a little too far and struck a tree that had been left untrimmed a little too long, causing it to flash over. This was the spark that ignited the largest blackout ever in the western US. A cascading failure occurred since too many people were asking too much (power) from too little (capacity of the lines)[2]. This story may sound strange:

[2]The main event itself started at 15:47:36 Pacific time with a fault on the 230 kV Ross-Lexington line near Portland, Oregon. The protective relays opened the line along with the neighboring 230 kV line Lexington-Woodland,

the laws governing the power generation and transmission have been known since the 19th century and the modelling of systems is something straightforward to perform. Anyway, something difficult to imagine happened. The failure scenario was not a sequence of random independent events; on the contrary, subsequent failures occurred and, in consequence, other failures followed.

The American power network is a sum of lines and power stations connected together in a non-simple way in the sense that the whole results in something different from just a disassociated collection of components. A question rises: how does individual behaviour aggregate to collective behaviour? (Watts, 2004) This query is the fundamental key element in a world of connected objects. In order to discuss the robustness of connected systems, a brief insight into the ways the objects can be linked is presented in the following.

2.2.1 Random and scale-free graph models

At the end of the Fifties, different researches on graph and probability theory joined together into a new field of interests: random graphs (Gilbert, 1959, Erdös and Rényi, 1959). The efforts culminated in the monumental paper by Erdös and Rényi (1960), which represents a milestone for all the further studies. An *Erdös-Rényi random graph* is the mathematical object obtained adding, progressively and at random, successive edges between a set of isolated vertices. In a more mathematical language, let n a positive integer and $0 \leq p_{ER} \leq 1$. The random graph $G(n, p_{ER})$, which can be written $ER_n(p_{ER})$, is a probability space over the set of graphs on the vertex set $V = \{1, \ldots, n\}$ determined by

$$\Pr[\{i, j\} \in G] = p_{ER} \tag{2.3}$$

with these events mutually independent. Many properties of such a mathematical structure were highlighted. For example, Erdös-Rényi random graph exhibits a phase transition in the size of the maximal component when p_{ER} varies. Because of its simplicity, which is represented by the use of probabilistic rules, the random graph was initially used for describing real networks, which are large in size and difficult to model deterministically (Van Der Hofstad, 2009). The most important issue of random networks, which is relevant for the understanding of the following discussion, is that the distributions of vertex degrees follows a Poisson distribution (Erdös and Rényi, 1960, Bollobás, 2001). That is, the probability that a vertex has k edges is

$$\Pr(k) = e^{-\lambda} \frac{\lambda^k}{k!} \tag{2.4}$$

and the small generating unit at Swift was also tripped. Subsequently, when the reactive power output of the MacNary generation units was at about 480 MVAR to provide reactive support, the protective relays started tripping the McNary units one by one because of faulty relay operation. As the McNary units went out of service, the inter-area oscillations grew in magnitude, and the damping of the 0.25 COI inter-area mode appeared to change from positive damping values to negative damping values. At 15:48:51, within 75 seconds after the initial fault on the Ross-Lexington line, the COI lines were tripped which resulted in system separation and the blackout (Venkatasubramanian and Li, 2004).

where

$$\lambda = \binom{n-1}{k} p_{ER}^{k} \left(1 - p_{ER}^{k}\right)^{n-1-k}. \tag{2.5}$$

At the beginning, mathematicians were enthusiasts and thought to have found a good representation of the reality, but they were wrong. The ability of random networks to model the real world was put to the test few years later. de Solla Price (1965), analysing a catalogue of journal references, found that, for a scientific paper in a specific field of research, half of the references are to a research front of recent papers and the other half are to papers scattered uniformly through the literature. In particular, he plotted the percentage of papers containing a certain number of bibliographic references, see Figure 2.7, and noted that the average number of references per paper is about 15, but the distribution is far from being Gaussian. In particular, 50 percent of the references came from the 85 percent of the papers, which contain 25 or fewer references apiece. Within this category, the percentage of papers with 3 to 10 references was around 5 percent (per each class of number of references). On the contrary, considering the percentage of papers with many references each, de Solla Price observed that a 25 percent of the references came from the 5 percent of all papers containing 45 or more references, while 12 percent of the references came from one percent of papers (the ones having 84 or more references). Finally, he noted that the number of papers cited n times in a year followed an inverse power law (a Zipf Law) with the exponent in the range 2.5 – 3.0.

The heavy-tailed distribution found by de Solla Price is a symptom of scale-free trend. The explanation of this particular shape found in the network of references would come later under the denomination "Cumulative Advantage Distribution": the success of a publication fall equally on the heads of previous successes (de Solla Price, 1976). In other words, the most cited papers tend to be referenced more than the ones less mentioned.

In the Nineties, research interests in scale-free networks rose after the topological mapping of the World Wide Web by Barabási and colleagues (Albert et al., 1999, Barabási and Albert, 1999). They mapped the complete `nd.edu` domain (Notre Dame University, where they worked) containing $n = 325729$ documents and $e = 1469680$ links. In doing so, they determined the probabilities $p_{out}(k)$ and $p_{in}(k)$ that a document has k outgoing and incoming link, respectively and found that these follow a power law over several orders of magnitude, see Figure 2.8. In particular the tail of the distribution follows

$$\Pr(k) \sim k^{-\gamma}, \tag{2.6}$$

with $\gamma_{out} = 2.45$ and $\gamma_{in} = 2.1$. Similar behaviours were recorded for the network of actors playing together, in this case with Kevin Bacon, with $\gamma_{in} = 2.3$. Other examples can be found in Van Der Hofstad (2009). As a result, large networks self-organize into a scale-free state, a feature unpredicted by random network models. The way this is done, in the idea of Barabási and Albert, is that networks continuously grow by the addition of new vertices and new vertices connect preferentially to highly connected ones: this is the "preferential

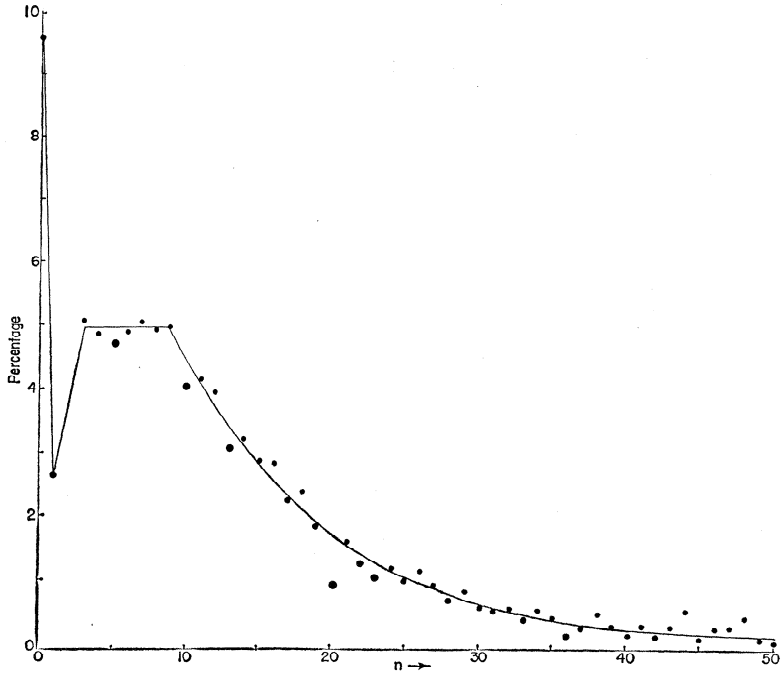

Figure 2.7: Percentage (relative to the total number of papers published in 1961) of papers published in 1961 which contain various number (n) of bibliographic references, after the original paper by de Solla Price (1965).

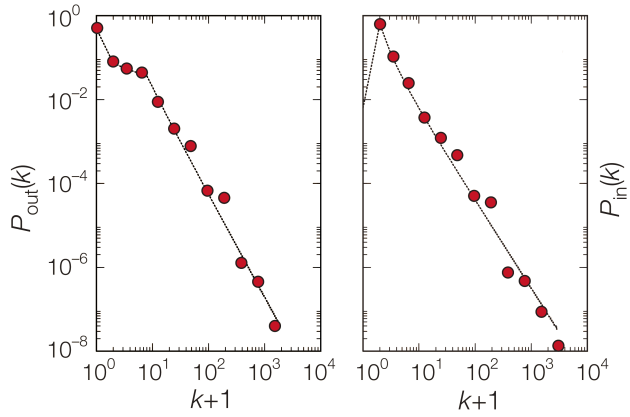

Figure 2.8: Distribution of links on the World-Wide Web obtained the complete map of the `nd.edu` domain. Left-hand side plot: Outgoing links (URLs found on an HTML document). Right-hand side plot: incoming links (URLs pointing to a certain HTML document). Dotted lines represent analytical fits used as input distributions in constructing the topological model of the web, after the original paper by Albert et al. (1999).

attachment", as de Solla Price (1976) imagined, finally modelled by Dorogovtsev et al. (2000), Krapivsky et al. (2000) and Bollobás (2001).

2.2.2 Attacks on networks: different behaviours

Since both models intend to describe the real world, their ability to resist to variation in their topology was assessed. The milestone in this field is reported in *Error and attack tolerance of complex networks* by Albert et al. (2000). In detail, they measured the effects of node removal by assessing the variation in the average length of the shortest path between any two nodes in the network, i.e. the diameter. Since the diameter characterises the ability of two nodes to communicate with each other: the smaller its value, the shorter is the expected path between them. It has been proved that networks with a very large number of nodes can have quite a small diameter. Imagine the entire population of the world, around 6 billion people: in 1967, Milgram (1967) proved that the length of the average path between two any person is around 6, which represents the famous *Six degrees of separation* invoked by Guare (1990).

The way the study on the impact of node removal was performed is simple. The diameter of the graphs is measured when a small fraction of the nodes, f, is removed. What is expected is that the absence of any node implies a general increase in the distance between the remaining nodes, as it can eliminate some paths that contribute to the system interconnectedness. That is, for Erdös-Rényi random networks, the diameter increases monotonically with

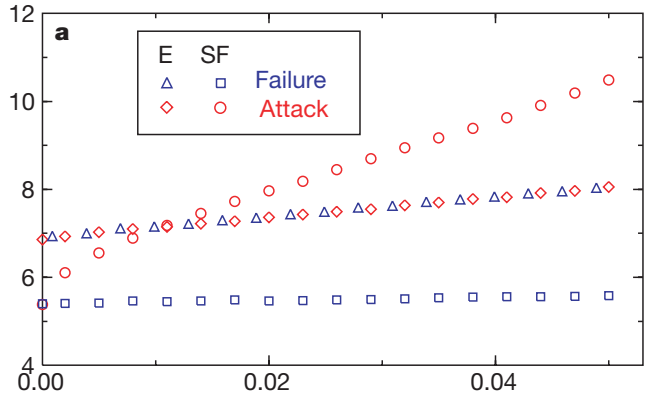

Figure 2.9: Comparison between the exponential, i.e. Erdös-Rényi, (E) and scale-free (SF) network models, each containing 10000 nodes and 20000 edges (that is, the average nodal degree is 4). The blue symbols correspond to the diameter of the exponential (triangles) and the scale-free (squares) networks when a fraction f of the nodes are removed randomly. Red symbols show the response of the exponential (diamonds) and the scale-free (circles) networks to attacks, when the most connected nodes are removed. Note that the diameter of the unperturbed ($f = 0$) scale-free network is smaller than that of the exponential network, indicating that scale-free networks use the links available to them more efficiently, generating a more interconnected web, after the original paper by Albert et al. (2000).

f. Thus, despite its redundant wiring, it is increasingly difficult for the remaining nodes to communicate with each other. This behaviour is rooted in the homogeneity of the network: for which the removal of each node causes the same amount of damage. A completely different trend emerges in case of scale-free networks. Here, the diameter remains unchanged even if more and more nodes are removed, at random. Because of the power-law distribution, the majority of nodes has only few links and, since there is no law that governs the choice in vertex removal, the ones with small connectivity will be selected with much higher probability. The removal of these weakly connected nodes does not alter the paths in the remaining part of the network and, thus, has no impact on the overall network topology (Albert et al., 2000). A robust nature emerges. This positive tendency is necessarily compensated by the fact that a targeted removal, i.e. an attack to the most connected nodes, in a scale-free is more deleterious than in random networks where, statistically, the nodes have the same degree (and no difference between random and targeted removal subsists). Figure 2.9 shows the change in diameter as much as nodes are removed. This general trend is recorded at different scales (Albert et al., 2000).

2.2.3 "Small-worlds"

Another question arises, especially in social networks. In networks in which the connections between the nodes are tightly knit and the density of ties is high, what does happen if the elements are removed? In other words, how much the clustering of the network changes as much as the nodes are removed?

The measure of clustering was defined by Watts and Strogatz (1998). For a given node, say v_i, the neighbourhood in graph G is defined as the set of vertices directly linked to the node, $N_G(v_i)$. If the number of vertices is k_i, the maximum number of connections among them is $k_i(k_i-1)$. The local clustering coefficient, C_i, is the ratio between the existing number of connections within the neighbourhood, $|N_G(v_i)|$, and its maximum, i.e.

$$C_i = \frac{|N_G(v_i)|}{k_i(k_i-1)}. \tag{2.7}$$

The global clustering coefficient, C, is the average of the local clustering coefficient across the entire network, i.e.

$$C = \frac{1}{n}\sum_{i=1}^{n} C_i, \tag{2.8}$$

where n is the number of nodes in the network.

Clustering in scale-free networks decreases as much as the node degree increases following a power law (Colomer-de Simon and Boguñá, 2012). Evidences of clustering are clearly visible in social networks in which people are nodes and acquaintance relationships between people are links. People form communities that are small groups in which everyone knows everyone. Within the community, there are people that know members of others communities, because of different interests, working exigencies,... At large scales, the links between communities are represented by the so called VIPs, e.g. celebrities, politicians, scientists, and so forth, that have relationships with people living far in distance. Watts and Strogatz (1998) performed the following experiment. They considered a regular ring lattice, i.e. a graph with n nodes each connected to d_G neighbours, $d_G/2$ on each side, as the one in the left-hand side of Figure 2.10 and, randomly, performed a rewiring of the connections at random with probability p. As much as the probability of rewiring increases, the regular graph ($p = 0$) turns into a random one ($p = 1$), as shown in the right-hand side of Figure 2.10.

They investigated the intermediate region, i.e. the case in which $0 < p < 1$, and they found a very interesting property: as much as the rewiring probability increases, the average path length, $L(p)$, rapidly reduces, but the clustering, $C(p)$, does not. At the end it drops rapidly, as plot in Figure 2.11. The network originated from this range of p, in which the previous behaviour is recorded, identifies to the so called "small-world", i.e. a situation in which clustering is present but, at the same time, the distance between the vertices is close to the situation of random networks. The drop of L is caused by the introduction of a few long-range edges, that connect vertices that would otherwise be much farther apart. For small p, each short cut has a highly nonlinear effect on the length, contracting the distance not just

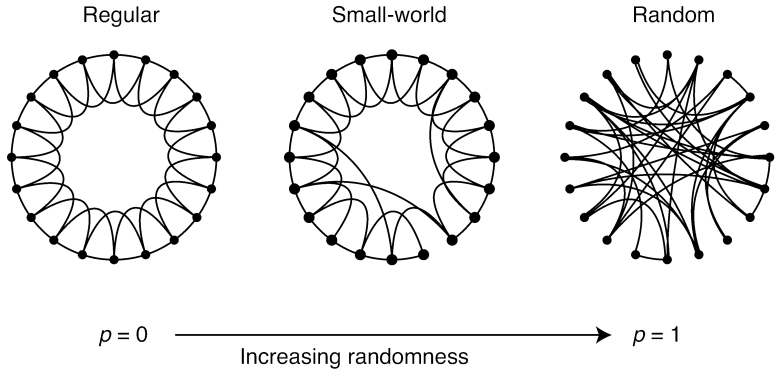

Figure 2.10: Regular to random graph depending on the probability of rewiring, p, after the original work by Watts and Strogatz (1998).

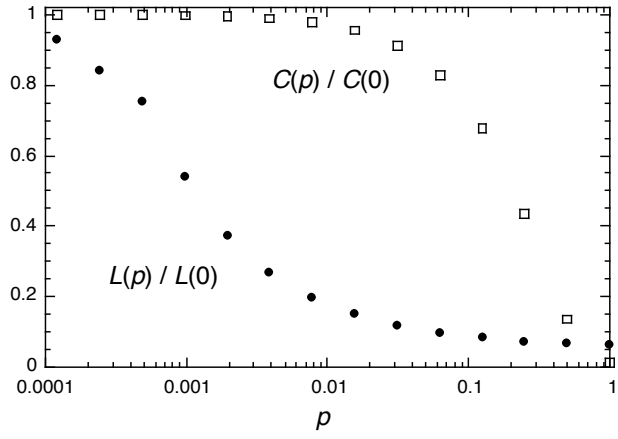

Figure 2.11: Regular to random graph depending on the probability of rewiring, p, after the original work by Watts and Strogatz (1998).

Situation	L	C
Regular graph ($p = 0$)	$\frac{n}{2d_G}$	$\frac{3}{4}$
Random graph ($p = 1$)	$\frac{\ln n}{\ln d_G}$	$\frac{d_G}{n}$

Table 2.1: Approximated lengths of a regular and a random graph with n nodes and k links within the neighbourhood. In order to guarantee a connected random graph, $n \gg d_G \gg \ln(n) \gg 1$ (Watts and Strogatz, 1998, Bollobás, 2001).

Situation	L_{obs}	L_{random}	C_{obs}	C_{random}
Film actors	3.65	2.99	0.79	0.00027
Power grid	18.7	12.4	0.080	0.005
C. elegans	2.65	2.25	0.28	0.05

Table 2.2: Observed characteristic path length L_{obs} and clustering coefficient C_{obs} for three real networks. The corresponding values for random networks with equal nodes and edges numbers are estimated using the formulae of Table 2.1, after (Watts and Strogatz, 1998).

between the pair of vertices that it connects, but between their immediate neighbourhoods, neighbourhoods of neighbourhoods and so on. By contrast, the effect on clustering is linear. For small p, C remains unchanged, and the transition from regular to small-world is practically undetectable (Watts and Strogatz, 1998).

Watts and Strogatz estimated the lengths and the clustering coefficients for regular and random network, see Table 2.1, and compared the observed values with their estimates for three real cases: the network of actors ($n = 225226$, $d_G = 61$) inserted in the database available at `www.imdb.com` as of April 1997, the power grid of the US ($n = 4941$, $d_G = 2.67$) and the neural connections of the *Caenorhabditis elegans* ($n = 282$, $d_G = 14$), which was mapped and transcribed by Achacoso and Yamamoto (1992). The observed average path length and clustering coefficient of the three real networks is reported in Table 2.2. In all cases, the observed path length is similar to the one on the corresponding random network, $L_{obs} \approx L_{random}$, while the clustering coefficient is at least one order of magnitude larger, $C_{obs} \gg C_{random}$.

2.3 Application: effect of the removal of routes

A simple application of the previous concepts is now illustrated. The scope of the present example is to show how graph analysis of networks can be useful for the estimation of the effects of element removal in systems.

Transportation systems can be considered as physical networks (Derrible and Kennedy, 2010). The concepts of network science can, thus, be applied to the transportation industry through graphs ideas and mathematical idealisation. In particular, the passage from abstract to real system can be done if the concept of weighted network is introduced. Various studies have highlighted the complex nature of transportation networks. Latora and Marchiori (2002) have shown that Boston underground system displays small-networks properties, Lu and Shi (2007) analysed the public transportation network of three different Chinese municipalities and suggested the ways for determining the most important and vulnerable parts of the system.

The concepts related to graphs have been applied in a simple model of the railways network of Piedmont, Aosta Valley and part of Liguria, see Figure 2.12. The system owned by Rete Ferroviaria Italiana (RFI) and is partially managed by Trenitalia and GTT (Gruppo Torinese Trasporti) is composed by 1888 kilometres of tracks and 284 railway stations. It is simplified in order to study its topological properties: the connections between different tracks are considered as nodes of the network, see Figure 2.13. Only 41 railroad stations, corresponding to the connections between the different lines, or the ends, are considered in the analysis. The whole railroad network is grouped into 68 edges.

The simple graph of the network is sketched in Figure 2.13. In Table 2.3, the correspondence between the idealized nodes (column #1) and the points in the real world (column #2) are listed. As can be read in column #3 of Table 2.3, the maximum nodal degree is equal to $\Delta_A = 7$ (Alessandria), while the average nodal degree is equal to $d_A = 3.366$. The connections between adjacent nodes are reported in Tables 2.4 and 2.5. As before, column #1 relates to the name of the edge in the graph, while columns #2 and #3 indicate the end vertices of each edge. Columns #4 and #5 are the cities linked by the edge. Since the traveling time through two cities play a fundamental role in the evaluation of the distance between two any points of the network, this parameter is a considered as weight for each edge of the graph. The time, in minutes, required for displacing is reported in column #6 of Tables 2.4 and 2.5 and found on Trenitalia website (`www.trenitalia.it`).

The topological properties of the graph are computed with a script on MATLAB. The central node of the network is represented by node 41 (Vercelli), while the peripheries are nodes 3 and 33 (Aosta and Savona, respectively). The weighted radius of the network is equal to 144 minutes and the weighted diameter, ϕ_A is equal to 259 minutes, i.e. the traveling time from Aosta to Savona, or viceversa.

The railroad network of Piedmont has been downsized in June 2012. In particular the regular service has been stopped on the eleven lines (460 km in total) listed below: (1) Santhià-Arona, (2) Pinerolo-Torre Pellice, (3) Cuneo-Saluzzo-Savigliano, (4) Cuneo-Mondovì, (5) Ceva-Ormea, (6) Asti-Castagnole-Alba, (7) Alessandria-Castagnole, (8) Asti-Casale-Mortara, (9) Asti-Chivasso, (10) Novi-Tortona and (11) Alessandria-Ovada. The graph of the network obtained after the suppression of the aforementioned roads is sketched in Figure 2.14.

The nodal degrees of the vertices of the graph reduce, see column #4 of Table 2.3, as the number of edges globally decreases. The maximum nodal degree, Δ_B, is equal to 6 (Torino) and the average nodal degree, d_B, is equal to 2.78. Some topological properties of the actual

Vertex #	Railroad station	Situation A nod.degree	Situation B nod.degree
1	Acqui Terme	4	4
2	Alessandria	7	5
3	Aosta	1	1
4	Arona	4	3
5	Arquata Scrivia	3	3
6	Asti	6	3
7	Bardonecchia	1	1
8	Biella	2	2
9	Borgomanero	5	3
10	Bra	4	2
11	Bussoleno	3	3
12	Carmagnola	3	3
13	Casale Monferrato	5	3
14	Cavallermaggiore	3	3
15	Ceva	2	2
16	Chieri	1	1
17	Chivasso	5	4
18	Cuneo	3	2
19	Domodossola	2	2
20	Fossano	3	3
21	Genova	3	3
22	Mondovì	3	2
23	Mortara	4	3
24	Nizza Monferrato	4	2
25	Novara	6	6
26	Novi Ligure	3	3
27	Oleggio	4	4
28	Ovada	3	2
29	Romagnano Sesia	4	2
30	Rovasenda	4	2
31	Santhià	4	3
32	Savigliano	2	2
33	Savona	4	4
34	Susa	1	1
35	Torino	6	6
36	Torre Pellice/Pinerolo	1	1
37	Tortona	3	3
38	Valenza	3	3
39	Varallo	1	1
40	Verbania	4	4
41	Vercelli	4	4
d_G		3.366	2.780

Table 2.3: Nodes/Railroad stations of the graph related to the north-western part of the Italian railways system. The nodal degrees refer to the Situation before (Situation A) and after (Situation B) June 17, 2012.

Tr#	i	j	S_i	S_j	T
1	19	40	Domodossola	Verbania	19
2	19	40	Domodossola	Verbania	36
3	40	4	Verbania	Arona	18
4	40	9	Verbania	Borgomanero	100
5	4	27	Arona	Oleggio	57
6	4	27	Arona	Oleggio	21
7	4	9	Arona	Borgomanero	18
8	27	25	Oleggio	Novara	20
9	9	25	Borgomanero	Novara	32
10	9	29	Borgomanero	Romagnano Sesia	17
11	29	25	Romagnano Sesia	Novara	35
12	39	29	Varallo	Romagnano Sesia	33
13	29	30	Romagnano Sesia	Rovasenda	20
14	30	8	Rovasenda	Biella	23
15	8	31	Biella	Santhià	18
16	30	31	Rovasenda	Santhià	31
17	30	25	Rovasenda	Novara	32
18	25	41	Novara	Vercelli	15
19	25	23	Novara	Mortara	16
20	31	41	Santhià	Vercelli	10
21	31	17	Santhià	Chivasso	19
22	41	13	Vercelli	Casale Monferrato	18
23	41	23	Vercelli	Mortara	27
24	17	13	Chivasso	Casale Monferrato	57
25	17	35	Chivasso	Torino	18
26	17	3	Chivasso	Aosta	106
27	17	6	Chivasso	Asti	63
28	6	13	Asti	Casale Monferrato	44
29	13	38	Casale Monferrato	Valenza	17
30	13	23	Casale Monferrato	Mortara	35
31	23	38	Mortara	Valenza	19
32	38	2	Valenza	Alessandria	9
33	2	37	Alessandria	Tortona	17
34	6	2	Asti	Alessandria	31
35	6	10	Asti	Bra	37

Table 2.4: Edges of the graph related to the north-western part of the Italian railways system - Part 1.

Tr#	i	j	$\mathcal{S}_i$	$\mathcal{S}_j$	T
36	6	24	Asti	Nizza Monferrato	34
37	24	2	Nizza Monferrato	Alessandria	32
38	7	11	Bardonecchia	Bussoleno	41
39	34	11	Susa	Bussoleno	9
40	11	35	Bussoleno	Torino	56
41	35	16	Torino	Chieri	21
42	36	35	Torre Pellice/Pinerolo	Torino	42
43	12	35	Carmagnola	Torino	23
44	12	10	Carmagnola	Bra	23
45	12	14	Carmagnola	Cavallermaggiore	12
46	14	10	Cavallermaggiore	Bra	13
47	10	24	Bra	Nizza Monferrato	70
48	24	1	Nizza Monferrato	Acqui Terme	26
49	14	32	Cavallermaggiore	Savigliano	5
50	18	20	Cuneo	Fossano	23
51	32	20	Savigliano	Fossano	7
52	20	22	Fossano	Mondovì	17
53	22	18	Mondovì	Cuneo	46
54	18	33	Cuneo	Savona	227
55	15	22	Ceva	Mondovì	19
56	15	33	Ceva	Savona	52
57	33	1	Savona	Acqui Terme	77
58	1	2	Acqui Terme	Alessandria	42
59	1	28	Acqui Terme	Ovada	23
60	33	21	Savona	Genova	42
61	21	28	Genova	Ovada	53
62	21	5	Genova	Arquata Scrivia	28
63	5	26	Arquata Scrivia	Novi Ligure	12
64	26	2	Novi Ligure	Alessandria	16
65	28	2	Ovada	Alessandria	40
66	26	37	Novi Ligure	Tortona	21
67	37	5	Tortona	Arquata Scrivia	17
68	35	6	Torino	Asti	36

Table 2.5: Edges of the graph related to the north-western part of the Italian railways system - Part 2.

Figure 2.12: Except from the maps of the railroad network owned by Rete Ferroviaria Italiana, source www.rfi.it

railroad network (after the downsizing) are equal to the ones of the situation before June 2012, i.e. the radius is still 144 minutes and the diameter, ϕ_B, 259 minutes.

A "line interruption scenario" is applied to both railways systems. Tables 2.7 and 2.8 show the effects of the removal of one edge, ϕ_i, on the value of the diameter of the network. In particular, remembering the diameter of the original network (259 minutes in both cases A and B), the increments in Situations A and B are computed through the following expressions

$$\left(\frac{\phi_j - 259}{259}\right)_i \tag{2.9}$$

where $j = 1 \dots 68$ and $j = A, B$, depending on the considered situation. The difference

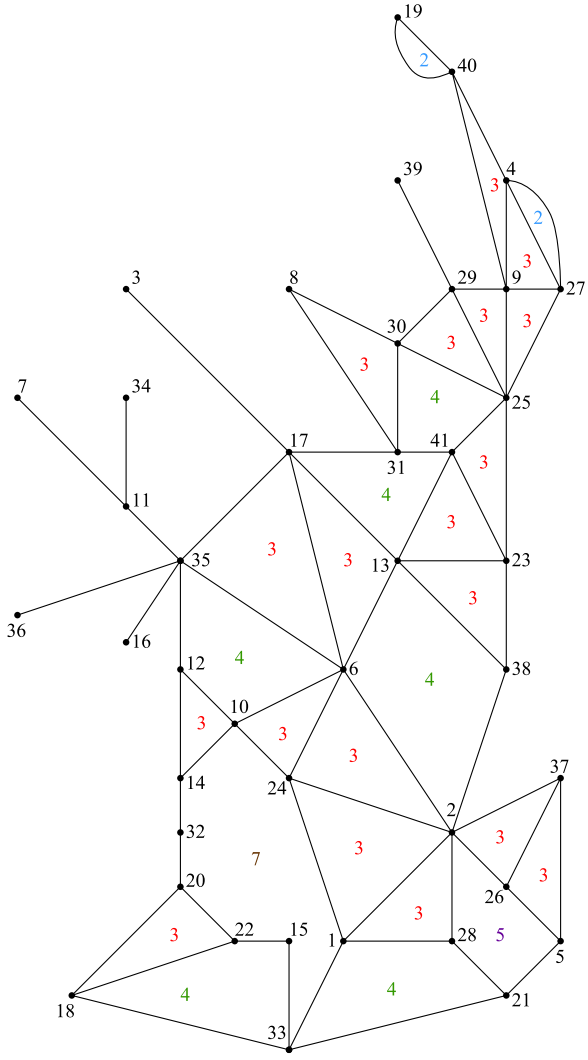

Figure 2.13: Graph of the railroad network of Piedmont, Aosta Valley and part of Liguria before June 17, 2012.

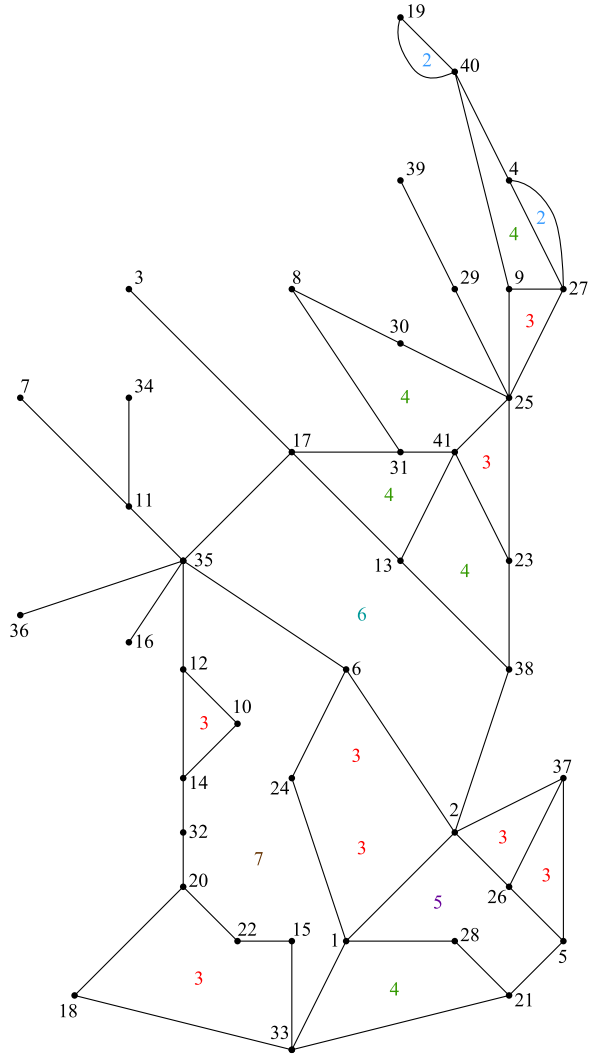

Figure 2.14: Graph of the railroad network of Piedmont, Aosta Valley and part of Liguria after June 17, 2012.

Number of edges	Situation A	Situation B
2	2	2
3	19	7
4	6	5
5	1	1
6	0	1
7	1	1
Average nodal degree	3.794	3.088

Table 2.6: Number of cycles in the network with a given and average nodal degree, provided that the branches are removed.

between the effects of edge removal in Situation A and Situation B are evaluated as

$$\left(\frac{\phi_B - \phi_A}{\phi_A}\right)_i . \tag{2.10}$$

Different considerations can be made.

1. The downsize of June 17, 2012 interested the lines which removal (in Situation A) leaves the diameter unchanged. That is why the topological parameters remain constant.

2. In some cases, edge removal creates a graph which is made of two components and, thus, its diameter is infinite. This happens both in Situation A and B if one of the following edges is removed: 12, 26, 38-42. In Situation B, the removal of edge 11 (Romagnano Sesia – Novara) isolates nodes 29 and 39 and edge 12. This is because edges 11 + 12 form a branch and then, the removal of 11 or 12, isolates at least a node.

3. In Situation B the network can be apparently divided into two parts connected by two main paths: Torino – Chivasso (35-17) and Alessandria – Valenza (2-38), see Figure 2.14. The interruption of one of the previous edges implies a general increase of traveling times through the railroad network. In case of suppression of both edges two components form and the diameter becomes infinite.

4. The removal of edges 49 or 51 increases the traveling times on the network since Cuneo area can be only reached through Liguria railroads.

5. In Situation B, the removal of edge 43 implies a large increment in traveling times towards Cuneo area since no intermediate connections between nodes 10, 6 and 24 are present.

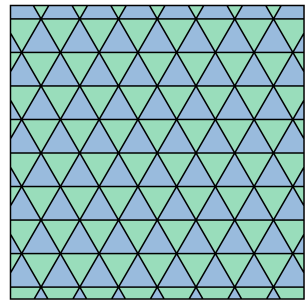

Figure 2.15: Tiles forming a triangular pattern.

6. The worst effect of the downsize of June 2012 can be seen if edge 50 (Cuneo – Fossano) is removed. Despite a small increase in diameter can be seen in Situation A, the diameter of the network rises to 486 minutes (+87.64%) in Situation B. This behaviour is expected since the only way to reach Cuneo (node 18) is represented by Savona – Cuneo edge that is time consuming (227 minutes).

7. As expected, Situation B is more vulnerable, in the sense that the diameter (therefore the traveling times) is generally larger after edge removal, if compared with analogous damages on Situation A.

8. The number of closed cycles decreased from 29 to 17, as can be seen in Figures 2.13 and 2.14.

Suppressing the branches of the network, i.e. nodes 3, 7, 11, 16, 34, 36, 39 and the adjacent edges, the resulting graph is composed by cycles and the average nodal degree is $d_A = 3.794$ and $d_B = 3.088$ for Situation A and B, respectively. The number of cycles with given number of edges is reported in Table 2.6.

Since the mode of the distribution of number of edges is 3, independently from the situation, one can suppose that the arrangement of the nodes and connections in the graph would be comparable to the one of triangular tiles, see Figure 2.15. In case of perfect triangular pattern, the nodal degree would be equal to 6. In the two situations presented herein, the nodal degree of the graph is between 3 and 4. The limited extension of the network and the presence of various cycles with elevate number of edges are the responsible of this inconsistency.

Removed edge	Situation A		Situation B		$\frac{\phi_B - \phi_A}{\phi_A}$
	ϕ_A	$\frac{\phi_A - 259}{259}$	ϕ_B	$\frac{\phi_B - 259}{259}$	
none	259		259		
1	259	0.00%	259	0.00%	0.00%
2	259	0.00%	259	0.00%	0.00%
3	327	26.25%	327	26.25%	0.00%
4	259	0.00%	259	0.00%	0.00%
5	259	0.00%	259	0.00%	0.00%
6	263	1.54%	290	11.97%	10.42%
7	259	0.00%	———	———	———
8	263	1.54%	330	27.41%	25.87%
9	259	0.00%	318	22.78%	22.78%
10	259	0.00%	———	———	———
11	259	0.00%	∞	∞	——
12	∞	∞	∞	∞	——
13	259	0.00%	———	———	———
14	259	0.00%	259	0.00%	0.00%
15	259	0.00%	259	0.00%	0.00%
16	259	0.00%	———	———	———
17	259	0.00%	259	0.00%	0.00%
18	274	5.79%	282	8.88%	3.09%
19	259	0.00%	259	0.00%	0.00%
20	274	5.79%	300	15.83%	10.04%
21	300	15.83%	300	15.83%	0.00%
22	259	0.00%	259	0.00%	0.00%
23	259	0.00%	259	0.00%	0.00%
24	259	0.00%	259	0.00%	0.00%
25	303	16.99%	343	32.43%	15.44%
26	∞	∞	∞	∞	——
27	259	0.00%	———	———	———
28	259	0.00%	———	———	———
29	259	0.00%	259	0.00%	0.00%
30	259	0.00%	———	———	———
31	259	0.00%	259	0.00%	0.00%
32	292	12.74%	292	12.74%	0.00%
33	259	0.00%	259	0.00%	0.00%
34	259	0.00%	259	0.00%	0.00%
35	259	0.00%	———	———	———

Table 2.7: Effects of the removal of one edge: for each removed edge, the diameter of the damaged network is computed both in cases A and B. The increments with respect to the original Situation are reported in columns #3 and #5, the difference between the response of the network in Situation A and the response of the network in Situation B is computed in column#6 - Part 1.

Removed edge	Situation A ϕ_A	Situation A $\frac{\phi_A - 259}{259}$	Situation B ϕ_B	Situation B $\frac{\phi_B - 259}{259}$	$\frac{\phi_B - \phi_A}{\phi_A}$
36	259	0.00%	259	0.00%	0.00%
37	259	0.00%			
38	∞	∞	∞	∞	—
39	∞	∞	∞	∞	—
40	∞	∞	∞	∞	—
41	∞	∞	∞	∞	—
42	∞	∞	∞	∞	—
43	277	6.95%	390	50.58%	43.63%
44	259	0.00%	259	0.00%	0.00%
45	277	6.95%	277	6.95%	0.00%
46	259	0.00%	259	0.00%	0.00%
47	259	0.00%			
48	259	0.00%	259	0.00%	0.00%
49	388	49.81%	388	49.81%	0.00%
50	267	3.09%	486	87.64%	84.56%
51	388	49.81%	388	49.81%	0.00%
52	289	11.58%	348	34.36%	22.78%
53	259	0.00%			
54	259	0.00%	259	0.00%	0.00%
55	329	27.03%	329	27.03%	0.00%
56	277	6.95%	277	6.95%	0.00%
57	259	0.00%	259	0.00%	0.00%
58	259	0.00%	259	0.00%	0.00%
59	259	0.00%	288	11.20%	11.20%
60	259	0.00%	259	0.00%	0.00%
61	259	0.00%	259	0.00%	0.00%
62	272	5.02%	296	14.29%	9.27%
63	259	0.00%	259	0.00%	0.00%
64	259	0.00%	259	0.00%	0.00%
65	259	0.00%			
66	259	0.00%	259	0.00%	0.00%
67	259	0.00%	259	0.00%	0.00%
68	259	0.00%	259	0.00%	0.00%

Table 2.8: Effects of the removal of one edge: for each removed edge, the diameter of the damaged network is computed both in cases A and B. The increments with respect to the original Situation are reported in columns #3 and #5, the difference between the response of the network in Situation A and the response of the network in Situation B is computed in column#6 - Part 2.

Chapter 3

Extreme events on structures

There are events that make surprise. After Willem Janszoon's discover in 1606, a similar belief had been certainly experienced by the first ornithologists across Australia in observing the *Cygnus Atratus*, alias a black swan. In the Old Europe, it was convinced that all swans were white coloured; an unassailable belief as it seemed completely confirmed by empirical evidence. Although this discovery did not changed natural history and had no impact on the theories on evolution, it simply shows the limitations of the learning based on observations. Just one observation can invalidate a general statement derived from millennia of confirmatory sightings of millions of white swans. Note that the vision of a black swan is something unusual for Europeans, but not for aborigines. The outcomes of this comment would be clearer in the following.

The use of locution "black swan" for indicating quasi-impossible events dates back to the Romans. Giovenale wrote in his sixth book of "Satire", *Rara avis in terris nigroque simillima cycno* as indicating something that is far from being usual in the everyday life.

The idea behind the feathered black swan is the main characteristics of Taleb's Black Swan. In 2007, after the subprime mortgage crisis, in the bookshops of the US a new book forecasting the future effects of the finance appeared. In *The Black Swan: The Impact of the Highly Improbable*, Taleb (2007a) states that the economy (and in more general, the World intended as a whole) is dominated by extreme events, which are unknown and not forecastable. The key point, which led to the crisis, is the fact that economists base their decisions on what they observe and know, while the world works completely different. Ergo, the predictions are wrong.

The book by Taleb does not concern economy, first. It is more a critical text on the use of statistics as an engine for solving and interpreting whichever natural phenomenon. Statistics is an extremely useful tool for all the situations in which the sensitivity to errors in the probability distribution can be neglected. A practical example is represented by such disciplines like measurement estimations, gambling theory, thermodynamics, and quantum mechanics.

In many other situations, the output of a mathematical model of the real world is not a linear combination of random parameters. Where nonlinearity is present, the sensitivity to estimation errors of the higher moments of probability distributions increases dramatically. That is why Taleb criticises three common beliefs: (i) the unrigorous use of statistics, and reliance on probability in domains where the current methods can lead us to make consequential mistakes (the "high impact") where, on logical grounds, we need to force ourselves to be suspicious of inference about low probabilities; (ii) the psychological effects of statistical numbers in lowering risk consciousness and the suspension of healthy scepticism – in spite of the unreliability of the numbers produced about low-probability events, and (iii) the use of commoditised metrics such as "standard deviation", "shape ratio", "mean-variance", and so on in fat-tailed domains where these terms have little practical meaning, and where reliance by the untrained has been significant, unchecked and, alas, consequential. In other words, the central idea behind Taleb's work is the confusion that most people make between *absence of evidence* and *evidence of absence*.

Since Taleb's essay focuses on general topics, the faced problem can be reached out to structural engineering. Before going further in the discussion, it is important to spend few words on the fundamental characteristics that turn a common event into a Black Swan.

3.1 Black Swans in structural engineering

Three main features characterise a Black Swan Event. First, (i) it has to be singular, in the sense that, in the past, no possibilities of forecasting it existed, neither to imagine that such situation would be experienced by the structure. In this sense, 9/11 Attack represents a good example. Twin Towers airplane crash, with airplane reservoirs fully charged, is an *unicum* in the possible situations that a tall building can experience. Then, (ii) the effects of Black Swan on the system are extremely large, i.e. the towers collapsed. At the end, the third characteristic (iii) that turns an event/situation into a Black Swan is the fact that, thinking about the event after its occurrence, a possible solution to limit the impact of it on the system could have been implemented without much effort.

Without any doubt, terroristic attacks are structural Black Swans. Remembering Murrah Federal Building Attack, the explosion of the bomb in the car in front of the construction caused the collapse of half of the building and 168 deaths. There is a disproportion between the cause and the effect: unfortunately, this is due to the ability of the structure to propagate the damage through the scheme. If adequate strategies limiting this undesired property were implemented, the damages would had been reduced.

Although terroristic attacks are the common events on structures that one can easily refer to black swans, the list of possible Black Swans Events is larger. For example, consider earthquakes with very high magnitude combined with particular site conditions: the effects are sometimes unforecastable. On September 19, 1985 Mexico experienced one to the most dramatic earthquakes of 20th century. The M8.0 earthquake (known as "Mexico City Earth-

quake 1985") epicentre was set in the proximity of the Pacific Coast, 350 km far from Mexico City. The areas around the source of the shaking suffered only mild to moderate damage, the worst situation was in the capital. Mexico city is vulnerable to earthquakes. The reason is represented by the geology of the area: the city mostly lies on silt and volcanic clay sediments of the bed of the historic Lake Texcoco, which are between seven and thirty-seven meters deep and have a high water content. Above this there is a layer of sand and, above, a layer of sand and rock. This particular stratification amplifies ground shaking and fosters soil liquefaction. In addition, the old lakebed resonates with certain seismic waves and low frequency signals. This local effect caused the amplification of the seismic wave which provoked extended damages in the urban area (Lomnitz, 1988).

Similar exaggerated situation can occur after "chain events". On March 11, 2011 a violent trembler shake the Pacific Coast of Sendai, the main island of Japan. The M9.0 megathrust earthquake (known as "2011 Tohoku earthquake") had epicentre 70 km off the coast and hypocentre at an underwater depth of approximately 30 km. The generated tsunami struck the coast of Honshu with 13 to 15 m tall sea waves. This natural event is well remembered because of the disaster occurred at Fukushima-Daiichi Nuclear Power Plant, which is summarised briefly. When the acceleration threshold was reached, i.e the earthquake struck the nuclear power plant, the sliding control rods got down into the three running reactor cores. The fission of the enriched uranium fuel that allows a nuclear reactor to produce the steam that spins a turbine to make electricity was instantly stopped. Anyway, even if fission is stopped, nuclear fuel rods must be kept cool, as by-products of the nuclear reaction continue to break down and produce heat for years. The key to cooling the rods is simple: a flow of fresh water. But, because of the earthquake, no electricity could be delivered to the nuclear power plant to run the cooling pumps. The back-up diesel generators that should have kicked in when power was lost did not survive the tsunami (13 m high sea waves), which easily overtopped the seawall protecting the plant (10 m tall). Only batteries were available to run all the systems. At the same time, the tsunami flooded the critical electrical equipment. After eight hours, the batteries went dead, meaning the nuclear power plant had no electricity, and no way to cool itself. In essence, the now-still water inside the reactors began to boil off, exposing the fuel rods and threatening a meltdown of the uranium fuel pellets inside the core (Biello, 2011). What resulted were the explosion of four nuclear reactors and an extended contamination of air and water, which still continues.

Disastrous combinations of events are extremely rare but entail large, say, enormous costs (damage + social), see Figure 3.1. In 2008, a road bridge over an important railway at Studenka (Czech Republic) was under essential repair. The composite concrete-steel bridge was partly pulled out to one side of the tracks and repaired. During the first steps of backward traction, the bridge suddenly slipped down from temporary supports and went on the railway. Incidentally, at the same time, the passing intercity train crashed at high speed the collapsed bridge. Eight people were killed and 63 were injured. The overloading of a part of the temporary support entailed the collapse of the deck, because of combination of events, caused the train accident (Agarwal et al., 2012, Holickỳ et al., 2013).

MEDIOCRISTAN	EXTREMISTAN
crowd that moves on a bridge	crowd that moves after an unexpected event (like gunshot)
behaviour of a structure subjected to extreme actions that is designed properly at ULS	behaviour of a structure subjected to extreme actions that has design errors at ULS
natural hazards with limited return period	natural hazards with large return period
ordinary impacts (as EC 1)	terroristic attacks on structures

Table 3.1: Mediocristan and Extremistan in structural engineering.

As said, Taleb (2007a) attacks the common practice in evaluating data and making prediction. The central limit theorem, in its simplest form, states that the arithmetic mean of a sufficiently large number of iterates of independent random variables, each with a well-defined expected value and well-defined variance, is approximately normally distributed. In this sense, the normal distribution seems to be the best tool for converting the real world into mathematical equations. This idea is true and provides good predictions in many situations, but sometimes it fails and underestimates the real behaviour. Taleb, in his book, classifies the economical tools into two categories: economical practices and financial strategies that can be related to a normal distribution belong to "mediocristan", the others, being influenced by fat tails and unexpected situations, belong to "extremistan".

This classification can be performed in the light of structural engineering. Table 3.1 shows examples of mediocristan and extremistan in structural engineering

Before going into a classification of situations that can potentially be told as Black Swans, it is suitable to summarize the philosophy that lies at the base of structural design: once there is sufficient awareness about the approach usually used in design, one can understand its limitation in dealing with such blemish events.

The main idea behind the design of a structure starts analysing the potential actions acting on it, combining them into design situations and, then, assigning size, material and resistance to the single elements of the construction in order to fulfil the capacity demand. The approach has a probabilistic basis: for any element, one can compute the statistics of the action, $\mathcal{A}$, acting on it and the corresponding capacity, $\mathcal{C}$. The reliability of the structural element, $\mathcal{R}$, is computed as the difference between capacity and action, i.e.

$$\mathcal{R} = \mathcal{C} - \mathcal{A}. \tag{3.1}$$

The element is "safe" if the capacity is larger than the action, that is $\mathcal{R} > 0$. Since action and resistance vary, the $\mathcal{R}$ can also be negative and, consequently, the corresponding situation is "unsafe". The purpose of the probabilistic method is to limit the probability of having unsafe situations to a target value, p_r, which depends on many aspects, as detailed in Chapter 4,

$$\Pr\left(\mathcal{R} < 0\right) < p_r. \tag{3.2}$$

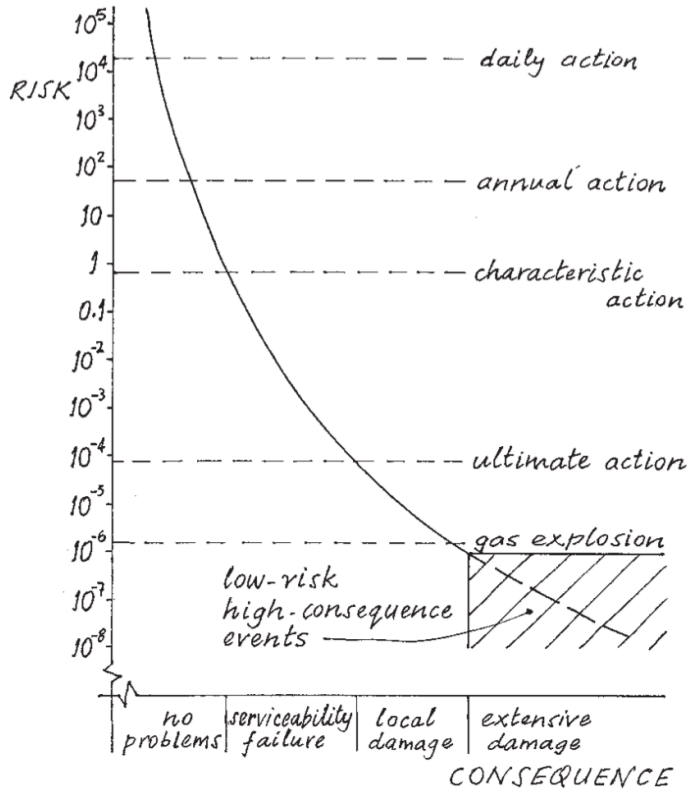

Figure 3.1: Risk *vs* consequence in a plot reported in Alexander (2004).

The main prerequisite for this design approach, called "Reliability Based Method", is represented by the necessity of having the statistics of the actions acting on the construction. Events with severe consequences occur extremely rarely. This can be illustrated as in the graph of Figure 3.1, which shows likely consequences against frequency of occurrence; this is shown on a log scale of frequency (or probability) in a 50-year life. Starting at the top, no significant risk is laid by problems occurring frequently, but the consequences become more severe beyond the threshold of ultimate design (0.7×10^{-4}). Below about 10^{-6} (one in a million), the risk is so small that the logical conclusion is to ignore it; this is the zone of low-risk high-consequence events, as is shown by the shaded area.

The necessity of statistics is totally incompatible with the idea behind the Black Swan, since the nature of the events, and thus their magnitude, is not known *a priori*.

3.1.1 Black Swans situations: classification

Actions or, alternatively, situations can be identified as Black Swans events. The action refers to the final set of forces acting on the construction, or on one of its parts, while the situation relates to a set of events. These can be grouped into three main classes.

Exceptional natural events The first class of actions relates to natural events with exceptional magnitude. The simple fact of using the term "exceptional" for something that will occur, give the idea of the quantities behind such phenomena: the return period. In the field of measurements of natural phenomena, the first systematic meteorological observations date back to the beginning of 19th century, just 200 years ago. The idea of having a statistics on events with a return period larger than, say, 200 years is far from being possible with certitude, since the observation period is too short. The same problem turns into the forecasting of future events. Supposing that the trend recorded in the past observations is, in some sense, similar to the one expected in the future, the magnitude of the event is inversely proportional to its probability of occurrence.

For example, a flooding with return period equal to 10 years is more frequent than one with return period 100 years. The magnitude of the first event is smaller than the one of the second. Hence, the impact on the society, thought as the destructive capacity of the natural event, would be reduced. What can we state about 300yrs return period flooding if the measurements series are one century and half long? Mathematical strategies have to be implemented in order to get the magnitude for such event. Extreme value theory is a branch of statistics dealing with the extreme deviations from the median of probability distributions, and is particularly devoted to the study of natural phenomena (Sornette, 2004). A probability distribution is a mathematical tool that assigns to each outcome a value representing the possibility of its occurrence. The probability distribution of a natural event is estimated from data on measurements. If we are interested on the maximum annual discharge rate of a river through a section, all the possible annual maxima measurable as much as water flows through the control point represent the *population* of events. In the real world, we have only access to a *sample* of the population. The analysis of the sample can offer three different distributions of maxima (or minima, if necessary):

- if the population has unlimited right-hand side exponential tail, i.e. the discharge rate can reach infinite values, the distribution follows Gumbel Law, which is called Type 1 distribution. Its cumulative expression is

$$F(z) = e^{-e^{-\frac{z-b}{a}}}, \tag{3.3}$$

  where a and b are parameters;

- if the population has light tail with finite upper bound, i.e. the maximum possible discharge rate is finite, the distribution follows Weibull Law, which is called Type

3 distribution. Its cumulative expression is

$$F(z) = \begin{cases} e^{-\left(-\frac{z-b}{a}\right)^{\alpha}} & z < b \\ 1 & z \geq b \end{cases}, \tag{3.4}$$

where a, b and α are parameters;

- if the population has a heavy tail with polynomial decay, i.e. the large events are more frequent than the ones of Gumbel's case, the distribution follows Fréchet Law, which is called Type 2 distribution. Its cumulative expression is

$$F(z) = \begin{cases} 0 & z \leq b \\ e^{-\left(\frac{z-b}{a}\right)^{-\alpha}} & z > b \end{cases}, \tag{3.5}$$

where a, b and α are parameters.

The previous three expressions are grouped into the Generalized Extreme Value (GEV) distribution, or Fisher-Tippett distribution, i.e.

$$F(z) = \exp\left\{-\left[1 + c\left(\frac{z-b}{a}\right)\right]^{-1/c}\right\} \tag{3.6}$$

where a, b and c are parameters. The idea of "tuning" an extreme value distribution with data related to a narrow temporal window crashes with the importance that the tails have in the prediction of events with large return period. This fundamental problem has been defined by Mandelbrot (1963) with the locution "fat tails". GEV distribution presents scale invariance in the tails. In other words, for z sufficiently large, i.e. in the tails, the ratio

$$\frac{\Pr(z > m\xi)}{\Pr(z > \xi)} \tag{3.7}$$

depends on m rather than on ξ. The self-similarity at all scales produces fractal-like probability distribution, i.e. Eqn. (3.6), which is commonly employed for the analysis of historical data series. Taleb (2007b) notices that, as much as the probability of occurrence diminishes, it is necessary to increment the size of the sample in order to reduce the error in the estimation distribution parameters. In parallel, as much as the probability of occurrence reduces, the effects of an error in the estimation of the magnitude of the event increase dramatically (Taleb, 2009).

Unexpected combination of events The reliability analysis implemented in the modern design methods considers a set of situations that a structure can experience during its design life. Black Swans can be the result of an unfavourable combination of events, i.e. an unexpected situation that was not considered in the design stage. The knowledge

of the spectrum of possible actions and the "surrounding", intended as the natural environment, the society, the geographical area, are tips for limiting the possibility of Black Swans.

The so-called chain events are binned in the same category of events. Fukushima-Daiichi Nuclear Power Plant accident, previously described in detail, represents a suitable example. Other than the common actions acting on constructions, e.g. wind, snow, crowd, vehicles load on bridges, chain events are partially considered in the common practice. For exceptional actions, no specific combinations are considered *a priori*. Anyway, the designer has the possibility to make hypotheses on more burdensome load combinations.

Anthropic actions The most devastating effects on structures are due to anthropic actions. The main peculiarity of these actions is the fact that they are not governed by random processes. Since no statistics on the occurrence and the operating methods is available, they cannot be forecasted, and no possibilities of implementation in the reliability-based design approach are possible. Terroristic attacks are a clear example of that: the human will drive the position of the actions and their magnitude in order to maximise the losses on the construction and its occupants.

In Donald Rumsfeld's idea, these are *unknown unknowns*, i.e. things we do not know since both the type of event and its likelihood are unknown. Black swans (unknown event, unknown likelihood) are unpredictable by probabilistic means (Nafday, 2011).

3.2 How to deal with Black swans?

Is there the possibility to deal with structural Black Swans? Luckily, the answer is positive. The basic approach is to shift the attention from the spectrum of actions to the gamut of damages on the structural scheme. That is, the consequences on the construction are the main interests of the designer. The philosophy is to prevent the propagation of damage to other structural components, which is in the field of interests of robustness concepts. That is, having a robust structure is a fundamental requisite for dealing with Black Swans situations.

As recalled previously, the design approach has to be based on the consequences. The inadequacy of the current design practices for particular situation has been already highlighted by Starossek and Wolff (2005) when considering progressive collapse. Two deficiencies are identified: first, the global effects are lost in the design. In detail, all actions and resistances are statistically determined on the basis of empirical data. After the evaluation of an allowable probability of failure, the design values for actions and resistances can be calculated using probabilistic methods, but the resistance is usually considered only on a local level (cross section, structural element) while the global resistance remains disregarded. Then, the authors criticise the assumption that low probability events and unforeseeable incidents (accidental

circumstances) need not be taken into consideration in the design, while they are the most dangerous for the construction.

The idea of implementing a design based on the consequences rather than on reliability takes its origins at the beginning of the new millennium. In a conference hold at the University of Notre-Dame, IN, Abrams et al. (2002) proposed a new engineering approach for reducing the loss due to seismic hazard. The statement of the idea is summarised in their words: "consequence-based engineering is a new paradigm for seismic risk reduction across regions or systems that incorporates identification of uncertainty in all components of seismic risk modelling and quantifies the risk to societal systems and subsystems enabling policy-makers and decision-makers to ultimately develop risk reduction strategies and implement mitigation actions". The steps in the decisional process consider the definition of the system, intended as the sum of geophysical, transport and socio-economical assets, on which the earthquake potentially would acts. Then, before any engineering calculation, there is the estimation of the possible consequences. This is the relevant point in the methodology. The impacts on the system relate to different properties of it, say not only structural/construction considerations. Then, a four-step decision tree is used to determine if: (a) estimated consequences are acceptable, (b) if acceptable consequences should be redefined, (c) if modelling parameters should be refined and (d) if further system interventions should be considered. If anticipated consequences exceed tolerable ones, and no further redefinition of acceptability is feasible, parameters defining the hazard and built environment can be refined to reduce anticipated losses (assuming that the preliminary analysis were conservative), and/or system interventions can be prescribed for the same purpose. Iteratively, consequences can be estimated for a number of different system intervention strategies with various input parameters describing the hazard or the built environment (Abrams, 2002).

The theoretical foundations being poured, Wen et al. (2004) set up a framework for vulnerability assessment of building structures under seismic excitation. This topic was detailed by Kinali and Ellingwood (2007), who applied the previous concepts for the analysis of steel frames with different lateral load carrying systems and different connection strengths under ground motion.

Bos (2007) introduced consequence-based design in the evaluation of the reliability of structural glass members, see Table 3.2. He proposed the concept of member consequence class, which permits to differentiate members requirements based on their role within a structure and, in addition, to consider the function and accessibility of the structure, see Figure 3.3. The idea behind the approach is to control the consequences of a failure, taken as a given, in order to minimise the risk associated with structural failure. The consequences of failure of a structural member are limited by requiring the member to retain a certain amount of strength for a certain period of time after the failure has set in, i.e. the concept of a residual strength. This is possible since the structural glass member is composed by many layers of material working in parallel (Bos and Veer, 2007).

Porter (2003) provided a probabilistic description of the system-level performance of bridges and buildings in terms of greatest meaning to owners and other stakeholders, namely,

Function of member within structure	Accessibility/Building Type	MCC
Key member	High - Public	6
Key member	Medium - Semi-public/office	6
Key member	Low - Private	5
Primary member	High - Public	4
Primary member	Medium - Semi-public/office	3
Primary member	Low - Private	2
Secondary member	High - Public	3
Secondary member	Medium - Semi-public/office	2
Secondary member	Low - Private	1

Table 3.2: Member Consequence Classes for combinations of building type and member function, after the original paper by Bos (2007).

MMC	Number ϱ of broken layers							
	$\varrho < 1$		$\varrho = 1$		$\varrho = m$		$\varrho = n$	
	Str.	time	Str.	time	Str.	time	Str.	time
1	S_{uls}	t_{ref}	S_{uls} S_{sls}	2:00 h 24:00 h	S_{mom}	>30s	0	0
2	S_{uls}	t_{ref}	S_{uls} S_{sls}	24:00 h 72:00 h	S_{uls} S_{sls}	2:00 h 24:00 h	S_{mom}	>30s
3	S_{uls}	t_{ref}	S_{sls}	72:00 h	S_{uls} S_{sls}	24:00 h 72:00 h	S_{mom}	2:00 h
4	S_{uls}	t_{ref}	S_{uls}	t_{ref}	S_{uls} S_{sls}	72:00 h t_{ref}	S_{sls} S_{mom}	24:00 h 72:00 h
5	S_{uls}	t_{ref}	S_{uls}	t_{ref}	S_{uls}	t_{ref}	S_{uls} S_{sls}	24:00 h 72:00 h
6	S_{uls}	t_{ref}	S_{rep}	t_{ref}	S_{rep}	t_{ref}	S_{rep}	t_{ref}

Table 3.3: Numerical formulation of the post-failure requirements for each of the six Member Consequence Classes. The table shows the required strength and period of time for certain amount of damage (which is represented by the number, ϱ, of broken layers). The case $\varrho < 1$ refers to pre-failure, $\varrho = 1$ is the case in which the outer layer, only, breaks, $\varrho = m$ is the case in which all the outer layers break. The case in which all layers break is represented by $\varrho = n$. The reference life time is indicated as t_{ref}. Referring to material strength, different classes are identified: S_{sw} is the strength equal to the self weight of the member, S_{mom} is the strength equal to the momentary load, S_{sls} is the strength equal to the serviceability limit state action, S_{uls} is the strength equal to the ultimate limit state action and S_{rep} is the strength equal to the representative strength of the member, after the original paper by Bos (2007).

uncertain future repair costs, casualties, and post-earthquake operability (dollars, deaths, and downtime). His research explores geotechnical and structural modelling, damageability of structural and non-structural components and contents, and the human and socioeconomic consequences of physical damage. Four distinct stages are considered: hazard analysis, structural analysis, damage and loss analysis, to produce a probabilistic estimate of various system-level performance metrics.

The idea of dealing with singular events in structural engineering by means of consequence-based approach was introduced by Nafday (2011). In a probabilistic framework, this complete lack of events, likelihood and data makes the design of structures for specific abnormal loads impossible and, therefore, there is little systematic code-based or regulatory guidance for limiting adverse system consequences due to unforeseen events. The fundamental aspect lies in the fact that the approach does not need a triggering event (or its likelihood), making it apt for Black Swan events. Capacity-based design strategies optimise robustness and general structural integrity by controlling adverse system consequences resulting from unexpected loads. In this sense, the idea of uniform reliability for all the structural members has to be rethought as an explicit variable reliability member design, to account for the differing system consequences of individual member failures. The design for Black Swan events is a secondary design. In the primary stage, structure is designed as usual using the current probabilistic member-based code provisions for normal loads, providing appropriate minimum joint resistance, continuity and inter-member ties. Thereafter, members are selectively redesigned for ensuring adequate structural system integrity, based on their role and importance in contributing to adverse consequences. These consequences can either be structural system collapse or any other pre-defined structural performance criterion. Unlike specific resistance method, where "key" members are empirically chosen for hardening based on threat-specific knowledge, Nafday's proposed design method applies a logical quantitative approach to upgrade structural members based on their individual role and importance in contributing to pre-defined adverse structural consequences (Nafday, 2008).

This design setup requires a metric to measure structural system consequences due to member failures. The basic idea is that, in general, the increase of the degree of static indeterminacy is not related to any measure of system safety performance. Gorman (1984) reported examples where reliability of structural systems was found to decrease with increase in the degree of static indeterminacy. Similar results were confirmed by Frangopol and Curley (1987): a large number of interconnected "weak" members does not add any "true" redundancy to the structure. Nafday (2008) formulated a metric based on data available in the structural stiffness matrix, which is able to give information about configuration, member sizes, material properties, connection types,... The singularity of the matrix represents the extreme case of loss of structural integrity. Given a stiffness matrix, say $\mathbf{K}$, the shortest distance between the set of singular matrices and the $(n \times n)$ stiffness matrix $\mathbf{K}$ is

$$\delta_S = \frac{1}{\kappa\left(\mathbf{K}\right)}, \tag{3.8}$$

i.e. the distance metric δ_S is the reciprocal of the condition number of the matrix. The condi-

tion number varies between 1 for orthogonal matrix to infinity for singular matrix. Therefore, the distance metric δ_S conveniently ranges between 0 and 1 (higher value indicating more stable system) and indicates how stable (with respect to overall collapse) a given structure is independently from the loading conditions. The system integrity, which is measured in terms of distance metric δ_S, is applicable both to intact and damaged structures, using appropriate stiffness matrices for evaluation.

The idea of consequence based design enters in the design procedure through a member consequence factors, Γ_f. This parameter measures the changes in the stiffness matrix due to element removal. Let $\mathbf{K}_N^i$ be the normalised stiffness matrix after removal of the i-th member in the system. In general, the determinant of the normalised stiffness matrix gives the volume of the geometrical parallelepiped defined by the column vectors of the stiffness matrix, which is obtained from stiffness matrix $\mathbf{K}$ by dividing the i-th row by $\left(\sum_{j=1}^{n} k_{ij}^2\right)^{1/2}$, i.e. the matrix is normalised. Then, the consequence factor Γ_f^i for the i-th member is defined as

$$\Gamma_f^i = \frac{|\mathbf{K}_N^i|}{|\mathbf{K}_N|}. \tag{3.9}$$

Note that $|\mathbf{K}_N|$ is the volume of the geometrical shape which is spanned by the vectors of matrix $\mathbf{K}_N$ for "intact condition" and $|\mathbf{K}_N^i|$ is the similar volume under "damaged condition", i.e. after the removal of the i-th member. Member consequence factor is used in common design procedure as an additional partial safety factor on the resistance side of the equations. The resulting design equation for system oriented design will consequently be

$$\Phi^i \Gamma_f^i \mathcal{C}_n^i \geq \sum \gamma_j \mathcal{A}_j^i, \tag{3.10}$$

where $\sum \gamma_j \mathcal{A}_j^i$ is the the factored load combination from design codes, Φ^i the resistance factor for the material of i-th member, and $\mathcal{C}_n^i$ the nominal strength of i-th member. Since member consequence factor ranges between 0 and 1, member resistance is reduced. This approach in dealing with Black Swans is still probability-based and all requirements in the current codes shall apply, even in cases of dynamic and non-linear targeted design.

Despite the goodness of the results given by the procedure implemented by Nafday for hinged structures, say truss structures, problems emerge when one considers frame structures. Different strategies for ensuring residual capacity after element removal, i.e. after a local failure occurrence, can be implemented: "alternate load paths" and "isolation by compartmentalisation" are two methods that can be pursued to make the structure robust and limit a beginning collapse to an acceptable extent (Starossek and Wolff, 2005). That is why robustness is the topic of the following Chapter 4.

Chapter 4

A robust structure

As shown in Chapter 1, natural systems tend to survive to extreme events through various strategies. As illustrated, there are various mechanisms for which a natural system, once subjected to unexpected situations, limits damage occurrence and propagation. Such a system is said to be *robust*; in other words, it is able to survive unforeseen or unusual circumstances.

Survival capacity of natural systems is a result of the evolution and selection, as outlined previously. Human-made systems do not have such property: they are designed to resist to a set of precisely identified scenarios (Knoll and Vogel, 2009). In case of structures or, in general, constructions, the scenarios account for physical conditions, anthropogenic loads, and so forth.

What does happen to the structure if the design conditions turned out to be of greater magnitude than foreseen? Is the system able to survive? Are there strategies that may reduce the losses on it in case of extreme actions? Strategies and techniques on this topic are the subjects of the investigation field of structural robustness. The research conduced on this topic is both theoretical and practical: on one side there are solutions devoted to close the theoretical gap that is still present, e.g. the discussions in the scientific community for a unique definition of structural robustness, or on the various metrics for measuring it; on the other, there are more practical issues that can be useful in the everyday structural design (Canisius et al., 2011).

Before going further, for sake of completeness, it is natural to precise that researches in the field of the robustness of structures began in the Seventies after the tragic event of May 16, 1968 in London. That is, in the early morning hours of May 16, 1968, the occupant of apartment 90 on the 18th floor of the 22-stories Ronan Point apartment tower, in London, lit a match to brew her morning cup of tea (Pearson and Delatte, 2005). A small gas explosion occurred and the resulting pressure increase blew out the walls of her apartment, and initiated a partial collapse of the structure that killed four people and injured 17. As can be read in the report of the investigation team that was designated for the analysis of the event, the trigger event in the collapse was attributed to the gas explosion displacing walls and initiating

a progressive collapse upward and then downward through the corner of the building (Griffiths et al., 1968). Ronan Point was 22-stories tall. There were a total of 110 apartment units in the building, grouped five to a floor and was constructed using the Larsen-Neilsen system that is "composed of factory-built, precast concrete components designed to minimize on-site construction work. Walls, floors and stairways are all precast. All units, installed one-story high, are load bearing" (Pearson and Delatte, 2005).

Previously to this event, progressive collapses during construction phase had occurred and had usually been attributed to construction errors. For preventing this kind of events, the Building Research Station published special recommendation for preformed structural system, in particular for their erection (BRS, 1963).

Since it was found that there was neither a violation of applicable building standards nor any defect in workmanship in the design (based on the state of the art) and the construction of Ronan Point (Griffiths et al., 1968), the problems involved in the robustness of such structure were questioned. The first provisions arrived rapidly (Canisius et al., 2011): "key elements have to be designed for an overpressure of 34 kPa". This disposition is still present in the modern codes of practice and reflects the idea of internal gas explosion present in the UK requirements. Other aspects that can be found in the modern directives relates to (i) the need of considering "accidental" or "abnormal" loading cases and to (ii) the idea of special design for buildings with high consequences in case of collapse (or, in general, failure). According to CIRIA (1977), an acceptable risk target based on a building consequence classes was defined and further implemented in Table A1 of Eurocode 1-7 (CEN, 2006).

Researches in the field of structural robustness continued throughout the decades. After Murray Building Attack in Oklahoma City, in 1995, researches on the causes and consequences of malicious attack and on the possibility of preventing such events through hazard mitigation were conduced (Corley et al., 1996). A significant interest in the topic was regenerated by the World Trade Attack on September 11, 2001 (Canisius et al., 2011).

4.1 Is there a definition for robustness?

The idea of robustness is present in many technical applications. The broad range of interpretations made on the term is listed in Table 4.1, which collects definitions from engineering as well as similar concepts from control theory, statistics, linguistics.

Specifically, in the field of structural engineering, the design codes implemented the concept and formulated a proper definition. Many of these codes specify that structures should be robust in the sense that the consequences of structural failure should not be disproportional to the effect causing the failure, as can be seen in Table 4.2.

"The ability. . . to react appropriately to abnormal circumstances (i.e. circumstances 'outside of specifications'). [A system] may be correct without being robust", after Meyer (1988)
"The ability of a system to maintain function even with changes in internal structure or external environment", after Callaway et al. (2000)
"A design principle of natural, engineering, or social systems that have been designed or selected for stability", as reported in Santa Fe Institute (2001)
"The degree to which a system is insensitive to effects that are not considered in the design", after Slotine and Li (1991)
"A robust solution in an optimization problem is one that has the best performance under its worst case (max-min rule)", after Kouvelis and Yu (1997)
"Instead of a nominal system, we study a family of systems and we say that a certain property (e.g. performance or stability) is robustly satisfied if it is satisfied for all members of the family", after Tempo and Blanchini (1996)
"The robustness of language. . . is a measure of the ability of human speakers to communicate despite incomplete information, ambiguity, and the constant element of surprise", after Briscoe (1997)

Table 4.1: Different definitions of robustness in technical sciences, as highlighted in Santa Fe Institute (2001).

4.2 Implementation in the design codes

As said, the idea of robustness is implemented in the design codes. According to Eurocode EN 1991-1-7:2006 (CEN, 2006), *a localised failure due to accidental actions may be acceptable, provided it will not endanger the stability of the whole structure, and that the overall load-bearing capacity of the structure is maintained and allows necessary emergency measures to be taken.*

As a basic requirement, the Eurocode for structural design, EN 1990:2002 (CEN, 2002) states that *a structure shall be designed and executed in such a way that it will not be damaged by events such as:*

- *explosion,*
- *impact, and*
- *consequences of human errors,*

to an extent disproportionate to the original cause. Potential damage shall be avoided or limited by appropriate choice of one or more of the following:

"The ability of a structure not to be damaged by events like fire, explosions, impact or consequences of human errors, to an extent disproportionate to the original cause", after ISO (1998)
"The ability of a structure to withstand events like fire, explosions, impact or the consequences of human error without being damaged to an extent disproportionate to the original cause", after CEN (2006).
"Ability of a structure or structural components to resist damage without premature and/or brittle failure due to events like explosions, impacts, fire or consequences of human error, due to its vigorous strength and toughness", after ARA (2003).
"The robustness of a system is defined as the ratio between the direct risks and the total risks (total risks is equal to the sum of direct and indirect risks), for a specified time frame and considering all relevant exposure events and all relevant damage states for the constituents of the system", after JCSS (2011).
"Robustness is [...] the ability of a structure to avoid disproportionate consequences in relation to the initial damage", after Agarwal and England (2008).
'Structural robustness can be viewed as the ability of the system to suffer an amount of damage not disproportionate with respect to the causes of the damage itself", after Biondini et al. (2008).
"The robustness of a structure, intended as its ability not to suffer disproportionate damages as a result of limited initial failure, is an intrinsic requirement, inherent to the structural system organization", after Bontempi et al. (2007).
"[...] ability of a structure to absorb [...] the effect of an accidental event [...] without suffering damage disproportionate to the event that caused it" "[...] ability of the structure to withstand local damage without disproportionate collapse [...]", after Val et al. (2006).
"The notion of robustness is that a structure should not be too sensitive to local damage, whatever the source of damage [...]", after Vrouwenvelder (2008)

Table 4.2: Different definitions of structural robustness, as highlighted in Starossek and Haberland (2010).

- *avoiding, eliminating or reducing the hazards to which the structure can be subjected;*
- *selecting a structural form which has low sensitivity to the hazards considered;*
- *selecting a structural form and design that can survive adequately the accidental removal of an individual member or a limited part of the structure, or the occurrence of acceptable localised damage;*
- *avoiding as far as possible structural systems that can collapse without warning;*
- *tying the structural members together.*

The approaches to structural robustness can be either deterministic or semi-probabilistic. Although accidental actions are considered in the design codes, robustness is also the property of systems that enables them to withstand unforeseen or unusual circumstances without unacceptable levels of consequences or intolerable risks (Gulvanessian, 2002). In this sense, the failure of the system can occur in case of:

- extreme **but foreseen** adverse combinations of actions (like explosion, impact of vehicles) and material properties (e.g. degradation);
- **unforeseen** events that may be hardly identified or whose intensity cannot be known in advance (e.g such as bomb explosions, malicious impacts or the effects of unknown errors.

Thus, structural robustness aims at limiting the consequences of local failure and prevents the formation of a disproportionate collapse. As reported by Canisius et al. (2011), *a disproportionate collapse need not be progressive, but suffers damage that is disproportionate to the original cause of failure. An example is the collapse of a statically determinate structure from the failure of a single member. In the case of a progressive collapse, different members of a statically indeterminate structure fail one after the other as they get overloaded with an accompanying redistribution of load.*

Eurocode 1 proposes two alternative strategies for ensuring enough safety (CEN, 2006):

- by identifying the extreme events (limiting the exposure to the event, reducing its intensity with protective measures, designing the construction for the expected action intensity);
- by limiting the extent of failure (enhanced redundancy, key elements, ductility,...).

The key point in the design of a robust structure is represented by time. In fact, in the case a failure would occur a little time past the activation of the hazard, the code prescription concerns the minimum period of time that the structure must withstand after the event (Canisius et al., 2011). For example, this is a requirement for fire resisting structures.

US regulations reported in ASCE 7-10 propose different approaches to structural robustness in case of progressive collapse (ASCE/SEI, 2010a):

- the resistance to progressive collapse can be considered explicitly during the design process itself. In this case, a direct design is implemented. Examples of direct designs are the alternative load path strategy or the specific load resistance strategy. Direct methods require the definition of hazard scenarios (ASCE/SEI, 2010b);
- the indirect method provides a sufficient resistance to progressive collapse during the design process through minimum levels of strength, continuity and ductility. This is done without consideration of hazard scenarios and without demonstrating that performance objectives are met (ASCE/SEI, 2010b)

4.3 Hazards and risk

A fundamental approach to structural robustness is represented by the so-called risk analysis. Simple steps make the flowchart of this approach: identification of the hazard scenarios, evaluation of risk, analysis of countermeasures for reducing the impact of the scenario.

A hazard scenario is a situation in which the resistance of the structure has been overcome, leaving it in an impaired, damaged or altered state. Various examples compete to that: yielding, element removal, instability, reduction of material properties, and so forth. There are various families of hazard scenarios. On one side there are those situations in which the origin of the scenario belongs to the structural system. In this case, material resistance, mechanical properties, durability, stiffnesses are not as expected in the design step. That is, the previous properties are variable quantities and, obviously, they can be described through a statistic. As highlighted by Knoll and Vogel (2009), the key question is that, in reality, large variations from nominal or mean values are more frequent than the theoretical (Gaussian, etc.) distributions would permit. This is due to the fact that there is a large human intervention in the realisation process: errors due to lack of attention or communication cannot be avoided.

The other family of hazards is represented by the external causes, i.e. the set of actions that have bad effects on the structure when the resistance is overcome. Scenarios belonging to this class are represented by exceptional natural events (in areas in which such events have never been recorded, or no traces are present) or by human-driven actions. As stated, terroristic plans and, more generally, anthropogenic actions are difficult to predict since they largely depend on future technology, economy and the interaction of nature with human behaviour. In this case, the scenario can be evaluated through the definition of a maximum credible event, which, in turn, can be estimated on the basis on known physical limits, or expressed as forces/deformations that the structure will experience. In case of unknown events of unknown magnitude none is known, i.e. a Black Swans, the hazard scenario should be represented both by element(s) loss and by localised reduced resistance. This concept is recalled at the end of Chapter 3 in the strategies for dealing with Black Swans, exactly.

Risk is notoriously composed by three components: hazard, consequences and context. Hazard and consequences are the well-known parameters usually evaluated in risk analysis. On the contrary, the context represents the way the consequences of the hazard are perceived

by the society. In this sense, there is a common belief that expect the built environment to be essentially risk free (Ellingwood, 2011, Aven and Renn, 2010). The personal ability in estimating risk is very difficult and non univocal: Starr (1969) showed that voluntary risks are accepted by individuals roughly 1000 times greater than involuntary risks. Clearly, it appears that the public awareness of the benefits of an activity changes the perception of risk on doing the activity. That is, Corotis (2003) and Vrijling et al. (1998) illustrated that the perception of risk plays a fundamental role in its acceptance (e.g. deaths from alcohol consumption, smoking, car accidents and so forth). The notion of measuring risk in structural design through probabilities or expected losses has been adopted in general building codes only relatively recently (Ellingwood, 1994, Reid, 2000). Anyway, although design codes provides requirements for structural robustness, they do not provide acceptable values for the risk related to the global failure of the structure (Diamantidis and Vogel, 2011). Only target reliability values are given for structural components, e.g. JCSS (2011), and cannot be used for larger failures. Targeted values have been proposed in specific cases: Moan (2009) estimated values for the failure of industrial plants for oil production and transport, Hamburger et al. (2003) discussed on failure of buildings due to earthquakes, Tanner (2008) analysed steel buildings in Spain in order to evaluate the level of risk in those constructions with high concentration of people.

In many practical analyses, it may result useful to relate the number of fatalities with the annual frequency of occurrence. This is what is plot in F-N graphs, see Figure 4.1 from Trbojevic (2005). Otherwise, risk matrices have been formulated (Harding and Carpenter, 2009).

Risk analysis represents the fundamental and preliminary step in the evaluation of the effects on structures. Any possible strategy for structural robustness confronts with a probabilistic analysis stating the "amount" of effectiveness the solution offers. Although dangers cannot be quantified at all, risk R can be expressed by the following product (Gulvanessian and Vrouwenvelder, 2006):

$$R = \sum_{i=1}^{N_H} p\left(H_i\right) \sum_{j=1}^{N_D} \sum_{k=1}^{N_S} p\left(D_j|H_i\right) p\left(S_k|D_j\right) C\left(S_k\right), \tag{4.1}$$

where N_H is the number of hazards H_i, N_D the number of direct (local) damages D_j, N_S the number of types of indirect behaviour S_k, $p\left(H_i\right)$ the probability of occurrence of hazard H_i (first term), $p\left(D_j|H_i\right)$ the probability of the occurrence of direct damage D_j due to hazard H_i (second term), $p\left(S_k|D_j\right)$ the probability of the occurrence of structural behaviour S_k due to direct damage D_j (third term) and $C\left(S_k\right)$ the (monetarised) consequences of structural behaviour S_k (fourth term).

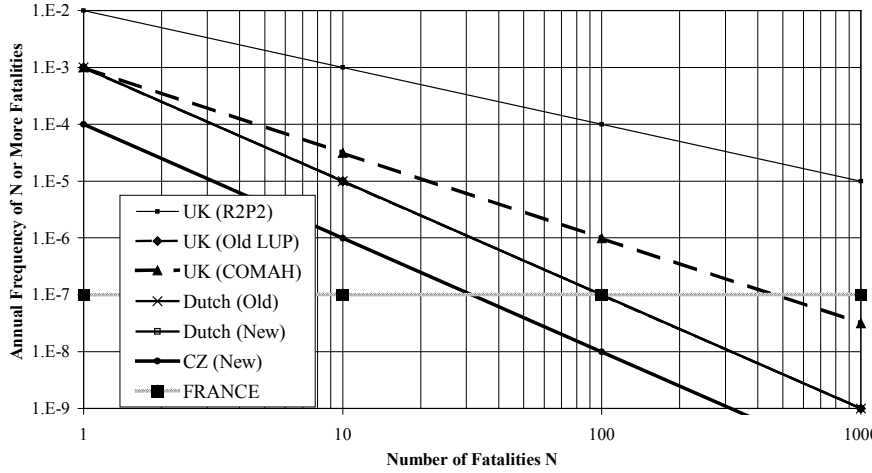

Figure 4.1: F-N curves relating expected fatalities (N) form an accidental event and the annual frequency of occurrence (F) of events with not less than N fatalities, after Trbojevic (2005).

4.4 Strategies for structural robustness

Whichever solution adopted for increasing structural robustness has to be associated with a prescribed performance objective, as stated in the previous section. In this sense, the idea proposed by Lind (1996) of "damage tolerance", intended as the capacity of the system to be able to sustain some damage without failure, fits well the general approach to structural integrity. Following that, different strategies are possible.

Event Control Event control refers to avoiding or protecting the construction against an incident that might lead to its disproportionate failure. This approach does not increase the inherent resistance of a structure, as reported by Starossek and Haberland (2010), but limits the possibility of occurrence of the event. Examples of event control measures are: (i) planning of the geographical location of the building, provision (ii) of stand-off perimeter, (iii) for surveillance systems such as alarm and security, (iv) prohibiting the storage of explosives, (v) placing fenders around the columns to prevent vehicle impact, (vi) placing barriers around the ground area, (vii) gas detectors and automatic cut-off devices for gas, (viii) control or limiting of fire ignition sources, (ix) limiting fire loads, (x) fire suppression systems, (xi) installation of smoke detectors and alarms, (xii) use of Structural Health and Monitoring Systems, (xiii) quality control during construction, maintenance and repair activities. Some of these measures require a specific design and have to be maintained throughout the whole life of the construction (Diamantidis and Vogel, 2011).

Specific Load Resistance If sufficient strength is provided to structural elements, they would be able to resist overloads. This is the principle at the base of the Specific Load Resistance strategy for robustness. The members have to be classified with respect to their importance for the survival of the structure and the key elements have to be identified in such a way that a failure of one of them does not exceed the performance objectives. Examples of key elements can be found in Starossek and Haberland (2012): piers in continuous bridges, cables in suspended bridges, and so forth. Sorensen and Christensen (2006) proposed to increase the capacity of key elements in order to account for the overload required in case of damage of the structure. Anyway, increasing the capacity of the elements is more expensive than preventing the initiation of the damage. That is why the strategy can be applied in those cases in which the key elements are few in number and easy to identify.

Alternate Load Path The strategy consists in providing alternatives for a load to be transferred from the point of application to a point of resistance, namely the foundations. Provided that the alternative paths are sufficiently strong, this enables redistribution of forces originally carried by failed components to prevent a failure from spreading. In order to achieve this requirement, the remaining structural elements must be strong enough, collectively, to resist the loads corresponding to the situation after the event. The resistance of the elements must be associated with a proper capacity in deformation without loss of resistance. In any case, it is necessary that, after the failure, the overall stability is guaranteed. An important issue has to be addressed in these cases in which the redundancy of the structural scheme is increased in order to achieve robustness requirements: multiple load-paths may sometimes involve brittle situations or limit deformations with negative consequences. These situations must be avoided (Knoll and Vogel, 2009).

Alternate Load Path strategy is effective in case of both hazard-specific and non-hazard-specific situations because the notional damage to be considered in the application of the alternative-paths method is non-threat-specific (Diamantidis and Vogel, 2011). Because of that, the approach is useful in dealing with Black Swan situations.

In order to implement the strategy, a set of structural components that have to be alternatively removed, or that are able to loose their load bearing capacity, have to be considered. The remaining part of the structure has to be able to support the loads with a given reliability for the time, t, required for the reparation or the evacuation of the people (JCSS, 2011). That is

$$\Pr\left(\mathcal{C} < \mathcal{A} \text{ in time t} \mid \text{one/more element(s) removed}\right) < p_t, \tag{4.2}$$

where $\mathcal{C}$ represent the strength of the residual part of the structure, $\mathcal{A}$ are the external forces acting during the period of time t. The target reliability, p_t, depends essentially on the safety requirements for the building and the length of the period for reparation/evacuation.

The probability that an element is removed by some cause depends on the sophistication of the design procedure and on the type of structure. In the case of non-hazard-specific design, the Alternate Load Paths strategy starts with the assumption of reasonable scenarios of initial damage. The structure is then designed such that the spread of this local initial damage remains limited to an acceptable extent (Starossek and Haberland, 2012).

Consequence reducing measures In order to ensure the safety of the occupants of a constructions, alternative measures can be implemented. These are not necessarily linked to structural aspects of the construction. In many cases, technological equipment (like sprinkler for fire, alarms, ...) can be installed in order to prevent the damages on the construction. Emergency planning, as well, represents a way for ensuring the safety of the occupants. Structurally speaking, an effective way for reducing the consequences of events are the isolation of parts of the structure in order to prevent the spreading of the damages (Starossek, 2007a). Structural segmentation has been demonstrated to be effective in various cases. For example, consider the collapse of part of the New Terminal 2E at Paris – Charles De Gaulle Airport on May 23, 2004. The design of the roof of the terminal was unusual with a shell consisting of curved concrete sections. The causes of failure are pretty unknown. Someone supposes that there was a sum of circumstances that lead to the event: the high flexibility of the structures under dead load, the external actions increased by cracking, a lack of robustness and redundancy able to transfer loads away from local failure, the high local punching stresses where the struts were seated in the concrete shell, and weakness of the longitudinal support beam and its horizontal ties to the columns (Wood, 2005). Only six modules were interested by the failure, due to the compartmentalisation of the structural scheme (Starossek, 2007a).

Obviously, in the design phase, one may choose one or more strategies for robustness. For example, consider the terroristic attacks of 9/11 in which the Pentagon Building in Washington, D.C. was stroke by an airplane. The extension of the damages created by the airplane and its burning fuel, i.e. 50 damaged columns at the first level, was relatively reduced if compared with the source. As extensively outlined by Mlakar et al. (2003), this fact is mainly due of the contemporarily occurrence of various structural situation: (i) redundant and alternative load paths of the beam and girder framing system, (ii) short spans between columns, (iii) substantial continuity of beam and girder bottom reinforcement through the supports, (iv) design for overloads, (v) significant residual load capacity of damaged spirally reinforced columns and (iv) ability of the exterior walls to act as transfer girders.

Considering the analytical expression of the risk, Eqn. (4.1), the following considerations can be made:

- event control strategies act on the events and on the possibility the hazard interests the construction. In other terms, such strategies involve a reduction of term $p\left(H_i\right)$ of Eqn. (4.1);
- specific load resistance strategies tend to limit the generation of damage once the event

takes place. In this sense, the more efficient the precautions, the less probable the possibility of local damage. This strategy acts directly on the term $p\left(D_j|H_i\right)$ of Eqn. (4.1).

- alternate load path strategies work as stopper for the propagation of the damage from a local to a global extent. That is why the act on term $p\left(S_k|D_j\right)$ of Eqn. (4.1).

- consequence reducing measures are strategies that tend to limit the social/physical costs involved by the event on the structure. Therefore, the strategy is linked with term $C\left(S_k\right)$ of Eqn. (4.1).

4.5 Metrics for robustness

The absence of a unique definition of robustness is reflected by the absence of a unique metric for quantifying it. As underlined by Starossek and Haberland (2011), a quantitative description by means of a measure is useful. Although various approaches for the quantification of robustness or related characteristics have been published, so far, none of these has emerged as distinctly superior and preferable. In the following, a selection of simple formulations of stiffness-, damage- or energy- based measures of robustness developed by various authors are presented and discussed.

First, it is suitable to clarify the ambiguous use of the word "robust". The terms robustness and redundancy and static indeterminacy are often used as synonymous. However, they denote different properties of the structural system. In fact, structural robustness can be viewed as the ability of the system to suffer an amount of damage not disproportionate with respect to the causes of the damage itself. Structural redundancy can instead be defined as the ability of the system to redistribute among its members the load that cannot longer be sustained by some other damaged members. Redundancy is usually associated with the degree of static indeterminacy. However, it has been demonstrated that the degree of static indeterminacy is not a consistent measure for structural redundancy (Frangopol and Curley, 1987). In fact, structures with lower degrees of static indeterminacy can have a greater redundancy than structures with higher degrees of static indeterminacy. It has been shown, that structural redundancy depends on many factors, such as structural topology, member sizes, material properties, applied loads and load sequence, among others (Frangopol and Curley, 1987).

Biondini and Restelli (2008) noted that performance indicators of the serviceability conditions under linear behaviour, like elastic stiffness and first yielding, may become of major importance in life-cycle robustness evaluations associated with ageing of structures. Looking at the properties of the structural system, they considered different performance indicators

based on stiffness matrix, $\mathbf{K}$, and on mass matrix, $\mathbf{M}$, i.e.

$$\zeta = \det(\mathbf{K}) \tag{4.3}$$

$$\tau = \sum_i \lambda_i(\mathbf{K}) \tag{4.4}$$

$$\kappa = \frac{\max_i \lambda_i(\mathbf{K})}{\min_i \lambda_i(\mathbf{K})} \tag{4.5}$$

$$T = 2\pi\sqrt{\max_i \lambda_i(\mathbf{K}^{-1}\mathbf{M})} \tag{4.6}$$

where ζ, τ, and κ are, respectively, the determinant, the trace, and the conditioning number of the stiffness matrix $\mathbf{K}$, T is the first vibration period associated with the mass matrix $\mathbf{M}$, and $\lambda_i(\mathbf{K})$ denotes the i-th eigenvalue of the matrix $\mathbf{K}$. These indicators are quite general, since they are related to the properties of the structural system only. However, a structural system may have different performance under different loads. For this reason, they considered, in addition, the following indicators:

$$s = \|\mathbf{s}\| = \|\mathbf{K}^{-1}\mathbf{f}\| \tag{4.7}$$

$$\Phi = \frac{1}{2}\mathbf{s}^T\mathbf{K}\mathbf{s} = \frac{1}{2}\mathbf{s}^T\mathbf{f} \tag{4.8}$$

where $\mathbf{s}$ is the displacement vector, $\mathbf{f}$ is the applied load vector, Φ is the stored energy, and $\|\cdot\|$ denotes the Euclidean scalar norm. These indicators depend on both system properties and loading condition, and they may refer either to the system in the original state, in which the structure is fully intact, or to the system in a perturbed state, in which a prescribed damage scenario is applied.

Since the definition of robustness reflects the ability of the structure to respond to damage, the comparison between the structural performance of the system in the original state, in which the structure is fully intact, and in a perturbed state, in which a prescribed damage scenario is applied (Frangopol and Curley, 1987, Biondini et al., 2008). A direct measure of structural robustness within the range [0, 1] is then obtained through functions of such variables, i.e.

$$\rho_\zeta = \frac{\zeta_1}{\zeta_0} \tag{4.9}$$

$$\rho_\tau = \frac{\tau_1}{\tau_0} \tag{4.10}$$

$$\rho_\kappa = \frac{\iota_1}{\iota_0} \tag{4.11}$$

$$\rho_T = \frac{T_1}{T_0} \tag{4.12}$$

$$\rho_s = \frac{\mathbf{s}_1}{\mathbf{s}_0} \tag{4.13}$$

$$\rho_\Phi = \frac{\Phi_1}{\Phi_0} \tag{4.14}$$

where subscripts $_0$ and $_1$ refer to the intact state and the damaged state of the structure, respectively. The indices ρ_ζ, ρ_τ, ρ_κ, and ρ_T, are related to the properties of the structural system only, while the indices ρ_s and ρ_Φ take into account loading condition. As a result of a comparative analysis, Biondini and Restelli (2008) found that indices ρ_ζ, ρ_τ and ρ_κ seem to be not suitable to fully describe the effects of damage on the structural performance. On the contrary, indices ρ_T, ρ_s and ρ_Φ can provide a very effective measure of structural robustness. Biondini et al. (2008), using ρ_s as robustness indicator, analysed progressive collapse in frame structures through a fault-tree analysis.

Other approaches based on stiffness matrix were proposed by Starossek and Haberland (2011). They evaluate the robustness of the scheme, R_s, as

$$R_s = \min_j \frac{\det \mathbf{K}_j}{\det \mathbf{K}_0}, \tag{4.15}$$

where $\mathbf{K}_0$ and $\mathbf{K}_j$ are the active system stiffness matrix of the intact structure and of the structure after removing a structural element or a connection j, respectively. Haberland (2007) highlighted the necessity of a sort of calibration or at least a normalisation to obtain a practical and plausible measure with a range of values between zero, in case of a total lack of robustness, and one. The reduction in load capacity due to the removal of structural elements does not correlate very well with the corresponding values of R_s, reason for which the measure is a quantification of the connectivity of the system rather than of the robustness of the structure.

Baker et al. (2008) proposed a definition of a robustness index based on risk measures. The approach considers "direct" consequences associated with local component damage (that might be considered proportional to the initiating damage) and "indirect" consequences associated with subsequent system failure (that might be considered disproportional to the initiating damage). An index is formulated by comparing the two risks. The index of robustness, I_{rob}, is defined as:

$$I_{rob} = \frac{R_{dir}}{R_{dir} + R_{ind}} \tag{4.16}$$

where R_{dir} and R_{ind} are the direct and indirect risks associated with the first and the second term in Eqn. (4.1). The index takes values between zero and one, with larger values indicating larger robustness. A difficult step in the risk assessment is modelling and quantifying the probability of exposure. Therefore, it can be very convenient and helpful to use a conditional index of robustness obtained using risks $R_{dir|exposure}$ and $R_{ind|exposure}$ conditioned of a given exposure:

$$I_{rob|exposure} = \frac{R_{dir|exposure}}{R_{dir|exposure} + R_{ind|exposure}} \tag{4.17}$$

Frangopol and colleagues (Frangopol and Curley, 1987, Fu and Frangopol, 1990) proposed some probabilistic measures related to structural redundancy – which also indicates the level of robustness. A redundancy index (RI) is defined by

$$RI = \frac{p_f\,(d \neq 0) - p_f\,(d = 0)}{p_f\,(d = 0)} \tag{4.18}$$

where $p_f\,(d \neq 0)$ is the probability of failure related to a damaged structural system and $p_f\,(d = 0)$ is the probability of failure of an intact one. The redundancy index provides a measure on the robustness/redundancy of the structural system. The index takes values between zero and infinity, with smaller values indicating larger robustness.

Lind (1995) formulated a robustness metrics based on a probabilistic framework. First, he defined vulnerability: let $p_f\,(r, \mathcal{A})$ denote the probability of failure of the system in a state r for prospective loading $\mathcal{A}$, i.e.

$$p_f\,(r, \mathcal{A}) = \Pr\left(\mathcal{C} < \mathcal{A} \mid \text{system state} = r\right) \tag{4.19}$$

Denote a pristine system state by r_0 and a particular damaged state by r_d. Then the vulnerability V of the system in state r_d for prospective loading $\mathcal{A}$ is the ratio

$$V = V\,(r_d, \mathcal{A}) = \frac{p_f\,(r_d, \mathcal{A})}{p_f\,(r_0, \mathcal{A})}. \tag{4.20}$$

The vulnerability is unity if the probability of failure is the same in both the damaged and undamaged states. If transition from r_0 to r_d increases the probability of failure by a factor f, then the associated vulnerability is equal to f. The damage tolerance of a system, T_d, is defined as the reciprocal of the vulnerability:

$$T_d = \frac{p_f\,(r_0, \mathcal{A})}{p_f\,(r_d, \mathcal{A})}. \tag{4.21}$$

For T_d equal to one, the structure is tolerant to the damage, while for T_d tending to zero, no tolerance exists.

The idea of quantifying the damage progression resulting from initial damage emerges in the damage-based metric, R_d, proposed by Starossek and Haberland (2011). The formulation is based on the complement of the dimensionless total damage:

$$R_d = 1 - \frac{\xi_{d_{in}}}{d_{acc}}, \tag{4.22}$$

where $\xi_{d_{in}}$ is the maximum total damage resulting from the assumable initial damage d_{in}, and d_{acc} is the acceptable total damage. Note that $\xi_{d_{in}}$ and d_{acc} refer to damage occurring additionally to the initial damage d_{in}. The quantification of damage required here can be performed by reference to the affected masses, volumes, floor areas (in buildings) or even the resulting costs. They proposed, in parallel, an integral measure, $R_{d,int}$, that uses the complement of the integral of the dimensionless damage progression caused by various extents of initial damage i:

$$R_{d,int} = 1 - 2\int_0^1 \left[\xi\,(d_{in}) - d_{in}\right] dd \tag{4.23}$$

where $\xi\,(d_{in})$ is the maximum total damage resulting from and including the initial damage of extent d_{in}. As before, both $\xi\,(d_{in})$ and d_{in} are dimensionless variables obtained by dividing

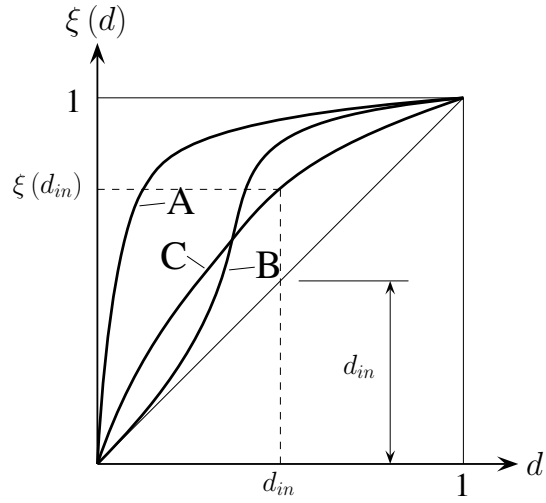

Figure 4.2: Damage evolution $\xi\,(d_{in})$, after the original paper by Starossek and Haberland (2011).

the respective reference value (mass, volume, floor area or cost) by the corresponding value of the intact structure. The effectiveness of the integral measure has been proved. Figure 4.2 shows three different scenarios of the damage evolution $\xi\,(d_{in})$, each referring to a different structure of different robustness. Curve A describes a non-robust structure; even small initial damage results in large total damage. Curve B illustrates a comparatively robust structure; major additional damage only occurs after large initial damage. Now consider curve C. Compared to curve B, it indicates a larger sensitivity to small initial damage. Since $R_{d,int}$ is defined by the area surrounded by the lines $\xi\,(d_{in})$ and d_{in}, the measures of robustness resulting from curves B and C are of the same order of magnitude. Thus, $R_{d,int}$ does not adequately reflect the relatively larger importance of the effect of small initial damage. This weakness can be remedied by weighting the initial damage so as to increase the importance of small initial damage in conjunction with re-normalising the measure to a range of values between zero and one (Starossek and Haberland, 2011).

Analogies between progressive collapse of simple structures and energy criterion borrowed from fracture mechanics are present in literature (Chiaia and Masoero, 2008, Masoero et al., 2010). In order to explain 9/11 Twin Towers implosion, Bazant and Zhou (2002) considered energy equilibrium in the damaged towers. As well, measures of robustness based on energy parameters, have been formulated.

In its simplest form, as proposed by Starossek and Haberland (2011), the comparison of the energy released during an initial failure and the energy required for failure to progress can

be considered as a robustness indicator, i.e.

$$R_e = 1 - \max_j \frac{E_{r,j}}{E_{f,k}}, \tag{4.24}$$

where R_e is the energy-based measure of robustness, $E_{r,j}$ is the energy released during the initial failure of a structural element j and contributing to damaging a subsequently affected structural element k, and $E_{f,k}$ is the energy required for the failure of the subsequently affected structural element k. Despite the simplicity of the expression, the attention focuses on the way the energy is computed. In structures susceptible to pancake-type or domino-type collapse (Starossek, 2007b), the gravitational potential energy of separating or overturning elements, which is transformed into kinetic energy makes a major and possibly dominant contribution to the total released energy. In structures susceptible to other types of collapse, the value can only be determined through a complete structural analysis.

England et al. (2008) considered hazard potential as measure of the potential for the progression of damage through a particular failure scenario under a stated set of loads. The measure depends on the flow of potential energy of the loads into internal strain energy caused by the damage event and the consequent change in well-formedness. The quality of well-formedness is a measure of the shape of a structural cluster (which can be a ring, a round, a cluster or the whole structure) and it describes the ability to resist loading from any arbitrary direction. It is calculated as the determinant of the stiffness sub-matrices of the joints associated with all the members contained in the structural cluster, i.e.

$$\mathcal{W}(Z) = \sum_{i=1}^{N(Z)} \frac{\det(\mathbf{K}_{ii})}{N(Z)} \tag{4.25}$$

where $\mathcal{W}(Z)$ is the well-formedness of structural cluster Z, $N(Z)$ is the total number of joints in cluster Z and $\mathbf{K}_{ii}$ is the stiffness sub-matrix of the i-th joint contained in cluster R. The hazard potential of a structure before a particular damage event is defined as the ratio of the change in strain energy to the change in well-formedness due to that event, i.e.

$$H_i = \frac{U_i/U_0}{\mathcal{W}_i/\mathcal{W}_0} \tag{4.26}$$

where U_i and $\mathcal{W}_i$ represent strain energy and well-formedness after the i-th event and U_0 and $\mathcal{W}_0$ correspond to the undamaged state. As damage progresses, the hazard potential increases until it reaches a maximum. This is a critical state: further damage would cause the structure to collapse totally or progressively.

Part II

Structural complexity: a possible definition and its applications

In the first part of this dissertation, I presented some strategies that let natural system or, more in general, the Nature, intended as a unique vital and evolving object, to be robust against events. Different tactics are implemented, the most relevant being represented by differentiation and redundancy in the vital tasks. The system itself shows features that can be ascribed to the idea of anti-fragility.

Obviously, we evaluate the naturally adopted schemes and the effectiveness of the countermeasures only by the observation of the real world. Anyway, what we photograph nowadays, or what we observe analysing fossils, is an instantaneous frame of what is optimal in the precise instant we take the picture. Environmental conditions, food supply, and so forth, were different 100 million years ago, and would be different in the next 100 million years. That is why living entities are different. The Nature adapts itself in order to accomplish the maximum survival.

The key concept resides in the term "evolution". Following the darwinian idea, each species, each biological mechanism, each biochemical process conform itself moved by an idea of adaptation, which is governed by the subtle force that wants the Nature to survive. There is a perfect tuning between the time required to the evolution to modify the phenotype bequeathed from one generation to the other, and the time across which the external condition varies. Keeping in mind that the strategies set up by any living body are tailored by the external conditions – in which Black Swans live – through the cloud of randomness that impregnates any process in the Universe and are intended to preserve the system at the least cost, the picture of the real world we take disguises all the possible strategies for robustness.

In technology, the unbalanced ratio between the time required to evolve towards robust objects and the time required to design and build these objects, leads to strategies that tends to optimise a characteristic in detriment to another one.

Engineering strategies for a robust construction were illustrated in Chapter 4. Among them, as found in literature, no attention was devoted to the complexity, which is a way largely implemented in Nature for ensuring its survival. That is why the following chapters are devoted to the implementation of this concept in structural engineering.

Chapter 5

Complexity of structures

5.1 What is complexity?

What is complexity? This question is the title of some interesting research papers one can find on scientific databases. The problem dates back to the days when the term was first used. In 1927, Heisenberg (1927) formulated the principle that bear its name; the world, which was driven by Newtonian laws, was shown to be intrinsically unpredictable. The reductionism approach proposed by Descartes based on understanding any complex phenomenon and taking it apart, i.e. reducing it to its individual components, displayed its lacks of completeness in the "very small" scale. In parallel, the vision of a world known with analysis, isolation and gathering of complete information about a phenomenon was overturned by Smuts' idea of *holism* (Smuts, 1926). Holism is the tendency of a whole to be greater than the sum of its parts. Nowadays, the current language would say that the whole has emergent properties, i.e. properties that cannot be reduced to the properties of the parts. Examples are easy to formulate: a musical piece has the properties of rhythm, melody and harmony, which are absent in the individual notes that constitute the piece. A car has the property of being able to drive. Its individual components, such as motor, steering wheel, tires or frame, lack this property (Heylighen et al., 2006).

In the second half of 20th century, the studies on a new science, cybernetics, demonstrated that certain types of circular coupling between systems could give rise to a negative feedback loop, which suppresses deviations from an equilibrium state. This means that the system will actively compensate perturbations originating in its environment in order to maintain or reach its "preferred" state of affairs (Ashby, 1955).

In this growing terrain, in the Eighties, a new approach emerged. Holland (1996) and Mitchell (1992) labelled it as *complexity science*. Despite the idea at the base of the term is clear, no precise and univocal definition has been formulated. In this sense Edmonds (1995b,a) found more than forty-eight ideas of complexity (e.g. algorithmic information complexity, en-

tropy, minimum size). Later, collecting the outcomes on different research topics in which an idea of what is complex has been given, e.g. biology, game theory, communication, computer science, Lloyd (2001) found more than forty different definitions, which can be substantially grouped into two categories. On one side, there are the measures that capture the randomness, the information content or the description of a process, e.g. periodical systems are less complex than random ones. On the other side, complexity depends upon the size of the process: the larger the system the greater the complexity.

In such framework, the idea of measuring the length of shortest message conveying certain information as a measure of complexity becomes established. In this sense, when Turing formulated the theory on computing machines, there was the exigency to measure the amount of work necessary to produce an output of a computer program. In very simple terms, the amount of characters that form the algorithm is taken as a measure of complexity of the output of the program. This approach is due to Kolmogorov (1963), who proposed it in the Sixties. In its more formal definition, Kolmogorov complexity, $\mathcal{K}(\tilde{s})$, is

$$\mathcal{K}(\tilde{s}) = |\varkappa(\tilde{s})| \tag{5.1}$$

where $\tilde{s}$ is the output and $\varkappa(\tilde{s})$ is the algorithm to produce the output. It is not hard to see that the minimal description of a string cannot be larger than the string itself, i.e. there is a constant $\tilde{c}$ such that

$$\forall \tilde{s} \qquad \mathcal{K}(\tilde{s}) \leq |\tilde{s}| + \tilde{c} \tag{5.2}$$

It has been seen that Kolmogorov complexity of a long bit string can readily be shown to be less than or equal to some value. But for any such value there is no way of excluding the possibility that the complexity could be lower. A bit string that is incompressible has no such regularities and is defined as "random". A measure corresponding much better to what is usually meant by complexity in ordinary conversation, as well as in scientific discourse, refers to the length of a concise description of a set of the entity's regularities rather than to the length of the most concise description of an entity (which is roughly what Kolmogorov complexity is). This is what Gell-Mann (1995) defines as *effective complexity*. Thus something almost entirely random, with practically no regularities, would have effective complexity near zero. So would something completely regular, such as a bit string consisting entirely of zeroes. Effective complexity can be high only in a region intermediate between total order and complete disorder.

5.1.1 Information Theory

Despite the mathematical digressions and approaches to the definition and estimation of complexity, which is concerned to the measure of the amount of regularity within something, in more practical terms, the complexity of a sequence, independently from what the sequence refers (e.g. genome, language, data, words in a book, speech...), can be identified as the amount of information that is stored in that sequence. For example, Adami and Cerf (1996)

used the so called physical complexity to analyse the amount of information that an organism stores in its genome from the environment where it evolves.

The approach is based on the concept of entropy introduced by Shannon (1948) that captures the amount of information within a sequence. Shannon was interested in one of the fundamental problems of communication: reproducing at one point either exactly or approximately a message selected at another point.

His approach considers the fact that messages have meaning since they refer to something that is known and defined by both speakers. Because of that, the actual message is one selected from a set of possible messages. If the number of messages in the set is finite then this number or any monotonic function of this number can be regarded as a measure of the information produced when one message is chosen from the set, all choices being equally likely.

Information content and entropy can be found in other approaches to complexity (Grassberger, 1986, Dehmer and Mowshowitz, 2011). In the classical thermodynamic definition, the entropy is defined as the natural force that carries a system from an improbable to a probable condition (Calinescu, 2002). In statistical mechanics, entropy is essentially a measure of the number of ways in which a system may be arranged, often taken to be a measure of disorder: the higher the entropy, the higher the disorder. The entropy is proportional to the logarithm of the number of possible microscopic configurations of the individual atoms and molecules of the system (microstates), which could give rise to the observed macroscopic state (macrostate) of the system through Boltzmann's constant of proportionality.

According to the information perspective, entropy is defined as the amount of information required to describe the state of the system (Shannon, 1948, Beer, 1994, Cover and Thomas, 2006). Entropy increases with an increase in the variety and uncertainty in the system. Correspondingly, a highly complex system requires a larger amount of information to describe its state. An increase of the complexity of a system, through increased disorder, variety and uncertainty, would be represented by an increase of its entropy, which, as stated, quantifies the amount of information required to describe the state of the system (Calinescu, 2002).

In 1948, Shannon (1948) was the first who introduced the concept of measuring the quantity of information by means of entropy within the frame of a general theory of communication. Supposing to have a set of possible n outcomes to which a set of probabilities $(p_1, p_2, ..., p_n)$ is assigned, i.e. $\sum_{i=1}^{n} p_i = 1$, a measure of how much uncertain is the choice (or how much choice is involved in the event) can be expressed as:

$$\mathcal{H} = -S \sum_{i=1}^{n} p_i \log p_i \tag{5.3}$$

where S is a positive constant that merely depends upon the unit of measure. This quantity $\mathcal{H}$ is called information-entropy and is the only function that satisfies the following axioms:

1. $\mathcal{H} = 0$ if and only if all the p_i are zero, except one having unit value. Thus only when we are certain of the outcome, will the entropy be null.

2. If all p_i are equal, i.e. $p_i = \frac{1}{n}$, then $\mathcal{H}$ is a monotonically increasing function of n. This means that with equally likely events there is more choice, or uncertainty, when there are more possible events.

3. $\mathcal{H}$ achieves its maximum, $\log n$ (for $S = 1$), when all the events have equal probability

$$p_1 = p_2 = ... = p_n = \frac{1}{n}.$$

This situation corresponds to the maximum uncertainty.

The quantification of how much complex a system is has been handled, for example, in computer science, by using graph theory. A program, i.e. an algorithm, can be imagined as a graph between an initial and a final node: in the case in which there are cycles or cases, the flow from the beginning to the end is not unique. In that sense, McCabe (1976) suggested to analyse the number of possible paths through a program between the initial and the final node and to relate to that quantity the value of the complexity.

Other approaches to measure the complexity of a graph have been introduced, e.g. the connectivity of each node or graph diameter. The structural complexity of a graph has been extensively used in different fields of chemistry, biology and social sciences. In these applications, entropy is interpreted as the structural information content and serves as a complexity measure (Dehmer and Mowshowitz, 2011).

Due to the wide field of application, graph entropy has been defined in various ways. Körner (1973) first studied the problem in order to define the amount of information that can be transferred through a communication in which pairs of symbol may be confused. The structural information content of a graph has been studied by Bosák (1990), Wheater and McCue (1992) and Colbourn and Ling (2003) who have proposed to decompose a graph into special subgraph to solve math and computer science problems. Dehmer (2008b) formulated a method for determining the information content of graphs based on a tree decomposition, which supposes to derive a tree from any node of the graph. He defined also an entropy measure based on an arbitrary information functional (Dehmer, 2008a) in such a way that, for a given vertex $\tilde{v}_i$ belonging to the set of vertices $\tilde{V}$, and for an information functional f, he computes the quantity

$$p\left(\tilde{v}_i\right) = \frac{f\left(\tilde{v}_i\right)}{\sum_{j=1}^{|\tilde{V}|} f\left(\tilde{v}_j\right)}, \tag{5.4}$$

where $|\tilde{v}|$ is the number of vertices. The previous quantity can be defined as vertex probability because the equation holds:

$$p\left(\tilde{v}_1\right) + p\left(\tilde{v}_2\right) + ... + p\left(\tilde{v}_{|\tilde{V}|}\right) = 1. \tag{5.5}$$

The entropy $\mathcal{H}_f$ of the graph is then computed as follows:

$$\mathcal{H}_f = -\sum_{i=1}^{|\tilde{V}|} \frac{f\left(\tilde{v}_i\right)}{\sum_{j=1}^{|\tilde{V}|} f\left(\tilde{v}_j\right)} \log\left(\frac{f\left(\tilde{v}_i\right)}{\sum_{j=1}^{|\tilde{V}|} f\left(\tilde{v}_j\right)}\right). \tag{5.6}$$

The wide range of applications of graph theory in contexts different from pure mathematics makes graphs particularly well-suited objects for a mathematical study of complexity (Mowshowitz, 1968). In structural engineering, as detailed in Section 5.7.1, graphs have served as means for solving computational optimisation questions. The entropy approach to structural topological properties of graphs associated to structures requires a simple framework able to be applicable to real engineering cases.

5.2 Complexity in structures[1]

In civil engineering practice, the term "complex" is extensively employed even if a proper definition has not been formulated yet. The general definition of complexity given by Simon (1962) can be translated to structural engineering. Thus, a complex structure can be defined as the one made up by a large number of parts that interact in a non-simple way. In such systems, the different contributions of each part contribute to the whole system (Ay et al., 2006), i.e. each element has different resisting mechanisms that interact with each other in such a way that the performance of the overall structure is not simply the sum of the single mechanisms.

Transposing the above concepts to structural analysis, let us consider the following example. In Figure 5.2 two similar 6-stories frames are shown. Beam lengths, mechanical and material properties are identical in both schemes except for certain columns and beams of the structure on the bottom that are larger, as illustrated. Which scheme is more complex? If no load is applied to the structure, the mutual interaction that exists between the elements due to the indeterminacy, i.e. the redundancy of resisting mechanisms, cannot be activated. Thus, the two schemes are quite similar. On the contrary, when external loads are applied, both structures deform. The overall performance can be evaluated: structure (b), as shown later in the present work, is more efficient than (a) in the sense that its structural performance is greater. In other words, under the same loads, the displacements are smaller. A prevailing resisting scheme can be found in the right-hand side structure. The vertical loads are carried by the deep beams on the top and are preferentially transferred to the foundation through the large column. The horizontal loads are transmitted directly to the central column.

The simple considerations highlighted in the previous example can lead to an idea of structural complexity. For instance, the complexity of a system should be independent of the entity and the position of the external forces. Hence, a complex structure can be defined as the one made up by a *large number of parts that interact in a non-simple way under an arbitrary loading scheme*.

A large number of resisting mechanisms that ensure the transfer of the applied loads from the top nodes to the foundation through the structure implies, in a certain sense, a complex response of the system. Hence, I propose a measure of structural complexity that quantifies the amount of interaction through different force paths, i.e. different resisting mechanisms.

[1] The present section and the following ones are part of the paper published on International Journal of Solids and Structures (De Biagi and Chiaia, 2013a).

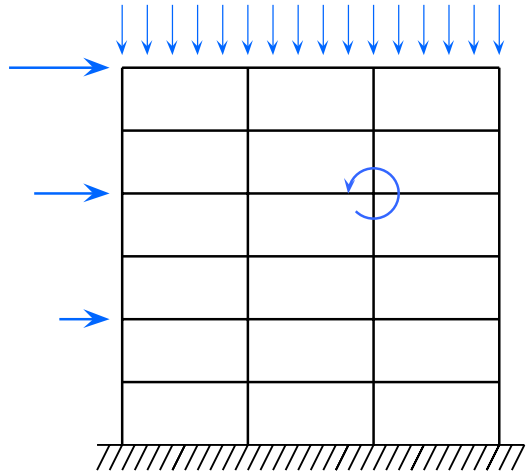

(a)

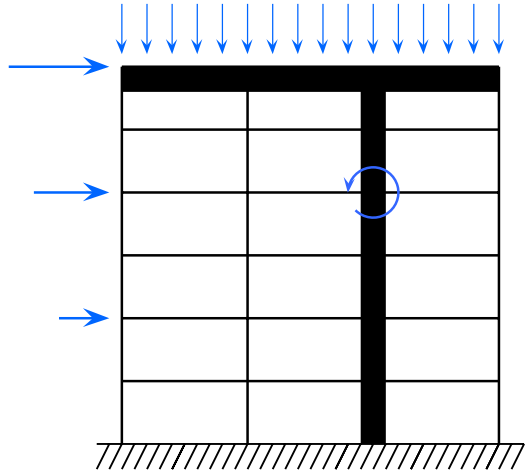

(b)

Figure 5.1: Two similarly connected and loaded structures. The one on the left-hand side (a) is composed by elements that have comparable stiffnesses, while the other (b) is composed by certain elements with higher stiffness.

Examples of this metric are presented in order to understand its influence on the structural behaviour. In particular, the examples refer to frame structures, which are the most common schemes in the current practice of steel and reinforced concrete structures.

By analysing a structural scheme, the expert structural engineer is able to identify the paths through which the load is transferred from the elevation to the foundation. As rule of thumb, the stiffer parts of the structure carry the load, while the weaker are less stressed. The former should then be accurately designed because of their importance in the structural scheme. Anyway, it may be interesting to identify these paths in order to understand the functioning of the structure and to direct forces through desired elements rather than other ones.

5.3 Corollary of Menabrea's Theorem

All the discussion presented in this work is based on the static conditions of the structural scheme; it is therefore necessary to restate correctly few definitions.

- An externally statically indeterminate structure is the one for which removal of a number of external constrain makes the scheme statically determinate.
- An internally statically indeterminate structure is the one for which removal of the external constrain still leaves the scheme statically indeterminate. In that case, the structure can be turned into a statically determinate one by properly removing internal constrain, i.e. making cuts or inserting hinges.

Figures 5.2(a) and 5.2(b) show, respectively, an external and an internal statically indeterminate structure.

Let us now consider the structural scheme in Figure 5.2(b). Following the previous definitions, it can be classified as an internal statically indeterminate structure, as the removal of neither of the fixed ends makes the structure statically determinate. Two cuts can be made, see Figure 5.3, and the structure turns into the sum of two statically determined different schemes. In order to guarantee the compatibility of displacements at the two sides of the cuts, a system of forces X must be applied at the interfaces of the cuts C_1 and C_2, see Figure 5.4. Once a reference system for displacements is introduced, six compatibility equations can be written:

$$\begin{cases} u^I_{k_i} = u^{II}_{k_i} \\ v^I_{k_i} = v^{II}_{k_i} \\ \varphi^I_{k_i} = \varphi^{II}_{k_i} \end{cases} \qquad i = 1, 2, \tag{5.7}$$

i.e. for horizontal and vertical displacements and for rotations. This approach has the same operative bases as the solution of statically indeterminate schemes by means of the Virtual Work Theorem in order to get the flexibility of the structure under a unitary redundant (internal or external) reaction (Carpinteri, 2002).

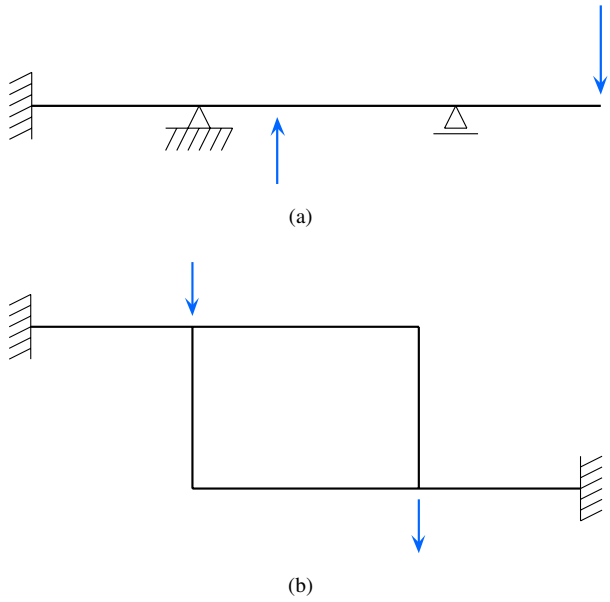

Figure 5.2: External (a) and internal (b) statically indeterminate structures. Usually, the presence of closed loops in the structural scheme implies internal statical indeterminacy.

As a result of the previous discussion, we define *fundamental structure* (F.S.) the statically determinate structure subjected to the loads and extracted from a statically indeterminate scheme, like the one of Figure 5.3. An explanation of what a fundamental structure is is given in Section 6.4.

5.4 An extension of Menabrea's Theorem

The Principle of the Minimum of Complementary Potential, which is known as Menabrea's Theorem, can be used for the analysis of the fundamental structures of a scheme. It is one among the four principles of minimum stated in elasticity theory (Hlaváček, 1967): the Principle of *Minimum of Potential Energy* by Lagrange-Dirichlet, the Principle of *Minimum of Complementary Potential* by Menabrea-Castigliano, the *Hu Hai-Chang and Washìzu's* Principle (Hai-Chang, 1954) and the *Hellinger-Prange-Reissner's* Principle (Reissner, 1961).

Menabrea's principle was formulated in 1858 in order to generate the required compatibility equations for the solution of statically indeterminate structures (Menabrea, 1858). Castigliano (1875), few years later, proposed a proof of the principle that is known as Menabrea's Theorem. Frankel and Cotterill obtained, independently, similar results (Grave and Ben-

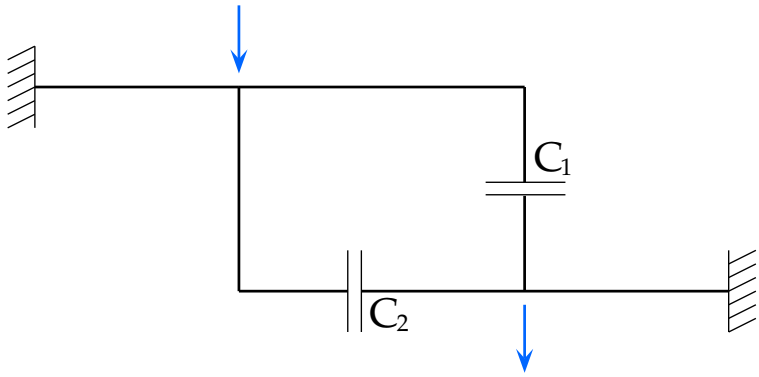

Figure 5.3: Cuts in C_1 and C_2 to turn the statically indeterminate structure shown in Figure 5.2(b) into a statically determinate one.

venuto, 1995). Menabrea's Theorem states that, in a n-times statically indeterminate structure, the n unknown external reactions are the ones for which the complementary energy reaches a minimum.

Let us consider a structural scheme, loaded with a force system F, with a degree of static indeterminacy equal to Γ. The previous structure can be split into two parts. The former, **A**, is the one on which all the loads are applied, the second one, **B**, is the remaining part of the original structure. At the interfaces of the cuts between **A** and **B**, Γ forces corresponding to the internal reactions do act. This system of forces is equilibrated between the two sides of each cut, therefore the original structure can be considered as the sum of system **A** and system **B**. This statement is correct if and only if compatibility equations are satisfied for each cut.

The work of deformation for the statically indeterminate structure, W_{in}, is equal to

$$W_{in} = W_{F,A} + \sum_{j=1}^{\Gamma} W_{j,A} + \sum_{j=1}^{\Gamma} W_{j,B}, \tag{5.8}$$

i.e. the sum of the work of deformation due to the external forces acting on structure **A**, $W_{F,A}$, and the contribution due to the Γ internal unknown that rise at the interfaces of the cuts on the scheme **A**, $W_{j,A}$, and on scheme **B**, $W_{j,A}$, with $j = 1 \dots \Gamma$.

As anticipated, the displacement field, δ, should respect compatibility equations:

$$\delta_{j,A} = -\delta_{j,B} \qquad \forall j. \tag{5.9}$$

The minus on the right-hand side of Eqn. (5.9) reflects the fact that the redundant force vectors have equal modulus but opposite direction on the two faces of the cut.

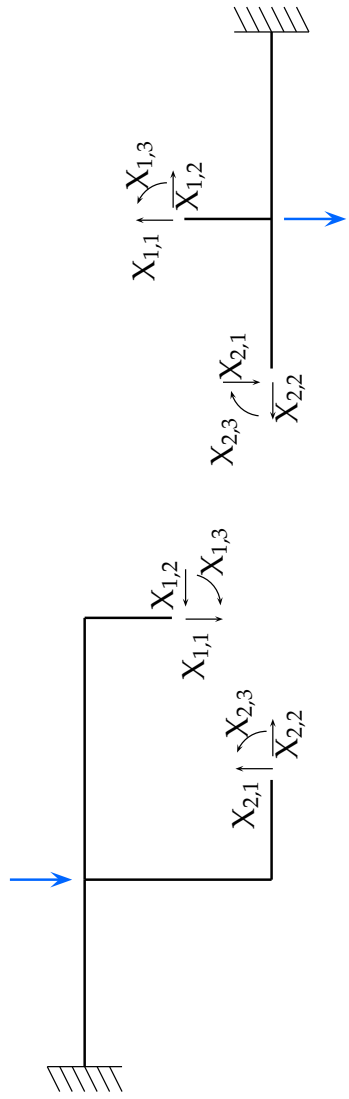

Figure 5.4: Redundant forces $X_{i,m}$, with $i = 1, 2$ and $m = 1, 2, 3$, at the cuts C_1 and C_2.

The work of deformation made by system **A** is equal to

$$W_A = W_{F,A} + \sum_{j=1}^{\Gamma} W_{j,A}. \tag{5.10}$$

where each $W_{j,A}$ depends only upon the j-th redundant force X_j acting on scheme **A**, i.e.

$$W_{j,A} = W_{j,A}\left(X_j\right). \tag{5.11}$$

The work of deformation made by system **B** is equal to

$$W_B = \sum_{j=1}^{\Gamma} W_{j,B}. \tag{5.12}$$

where each $W_{j,B}$ depends only upon the j-th redundant force X_j acting on scheme **B**, i.e.

$$W_{j,B} = W_{j,B}\left(X_j\right). \tag{5.13}$$

Applying the First Castigliano's Theorem (Castigliano, 1875), Eqn. (5.9) becomes

$$\frac{\partial W_A}{\partial X_i} = -\frac{\partial W_B}{\partial X_i} \qquad \forall i. \tag{5.14}$$

Rewriting the previous expression, we get

$$\frac{\partial W_{F,A}}{\partial X_i} + \sum_{j=1}^{\Gamma} \frac{\partial W_{j,A}}{\partial X_i} = -\sum_{j=1}^{\Gamma} \frac{\partial W_{j,B}}{\partial X_i} \qquad \forall i. \tag{5.15}$$

Remembering Eqns. (5.11) and (5.13, all the partial derivations are equal to zero except in the case of the partial derivation of the work of deformation performed by the i-th redundant force with respect to itself, i.e.

$$\frac{\partial W_{j,A}}{\partial X_i} = 0 \qquad i \neq j \tag{5.16}$$

$$\frac{\partial W_{j,B}}{\partial X_i} = 0 \qquad i \neq j \tag{5.17}$$

$$\frac{\partial W_{F,A}}{\partial X_i} = 0 \qquad \forall i. \tag{5.18}$$

Eqn. (5.9) can thus be rewritten as:

$$\frac{\partial W_{j,A}}{\partial X_i} = -\frac{\partial W_{j,B}}{\partial X_i} \;\Rightarrow\; \frac{\partial W_{j,A}}{\partial X_i} + \frac{\partial W_{j,B}}{\partial X_i} = 0 \tag{5.19}$$

Considering Eqn. (5.8), the partial derivative of the deformation of the original statically indeterminate structure with respect to the i-th redundant force is equal to

$$\frac{\partial W_{in}}{\partial X_i} = \frac{\partial W_{F,A}}{\partial X_i} + \sum_{j=1}^{\Gamma} \frac{\partial W_{j,A}}{\partial X_i} + \sum_{j=1}^{\Gamma} \frac{\partial W_{j,B}}{\partial X_i} =$$

$$= \sum_{j=1}^{\Gamma} \left[\frac{\partial W_{j,A}}{\partial X_i} + \frac{\partial W_{j,B}}{\partial X_i} \right]. \tag{5.20}$$

Substituting Eqn. (5.19) into the previous Expr.(5.20), we get

$$\frac{\partial W_{in}}{\partial X_i} = 0. \tag{5.21}$$

The obtained result is valid for all the Γ redundant forces and, thus,

$$\frac{\partial}{\partial X_i} W_{in} \left(F, X_1, ..., X_\Gamma \right) = 0 \tag{5.22}$$

for the X_i redundant forces for which the compatibility equations are satisfied.

In the $(\Gamma + 1)$-dimensional space, the point

$$\left(X_1, X_2, ..., X_\Gamma, W_{in} \right)$$

is a stationary point. The work of deformation is a positive defined functional and, therefore, that point is also a minimum.

Thus, it is possible to state that

For an internally statically indeterminate structure, the values of the internal redundant forces are those that minimise the work of deformation of the structure.

5.5 Performance factor

Let us consider, again, a scheme for which the indeterminacy is due to the internal connections, i.e. an internally static indeterminate structure. Does the complementary energy behave in the same manner when the redundant forces are internal? As proved in Section 5.4, the same conclusion can be drawn for internal statically indeterminate structures, as detailed below.

Referring to Figure 5.4, which represent the fundamental structures extracted from the scheme of Figure 5.2(b), consider the work of deformation W. It can be expressed as a function of both the external forces F and the internal redundant forces $X_{i,m}$ ($i = 1, 2$ and $m = 1, 2, 3$), i.e.

$$W = W \left(F, X_{1,1}, X_{1,2}, X_{1,3}, X_{2,1}, X_{2,2}, X_{2,3} \right).$$

For any arbitrary value of the external loads $F^\star$, the value of the work of deformation W can be plotted in a 7-dimensions space as a function of the $X_{i,m}$ (index i spans over the cuts, index m spans over the internal force components, i.e. $i = 1, 2$ and $m = 1, 2, 3$). As a corollary of Menabrea's Theorem presented in 5.4, the function

$$W^* = W\left(F^\star, X^*_{1,1}, X^*_{1,2}, X^*_{1,3}, X^*_{2,1}, X^*_{2,2}, X^*_{2,3}\right)$$

reaches a minimum in correspondence of the $X^*_{i,m}$ values satisfying Eqns. (5.7). W^* represents the work of deformation W_{in} of the original statically indeterminate structure, which is independent of the cuts made, i.e. of the chosen fundamental structure.

For better understanding, consider that all the internal forces are supposed fixed to their values $X^*_{1,2}, ..., X^*_{2,3}$, except $X_{1,1}$. Figure 5.5 plots W versus $X_{1,1}$. As demonstrated, the minimum of W is attained when $X_{1,1} = X^*_{1,1}$. At $X_{1,1} = 0$ no horizontal force acts on the structure at cut C_1. That represents an internal disconnection. The same reasoning can be extended to the other internal forces in such a way that, for $X_{i,m} = 0$, for $i = 1, 2$ and $m = 1, 2, 3$, the cut structure is subjected only to external forces. In the last case the statically determinate structure is the fundamental structure previously defined.

The work of deformation, $W_{\mathcal{S}}$, can now be computed in the fundamental structure and one of the following situations may appear.

- $W_{\mathcal{S}} > W_{in}$, i.e. the work of deformation in the fundamental structure is greater than the work of deformation in the original statically indeterminate structure: the forces at the interfaces of the cuts, i.e. the redundant internal forces, give a contribution for the performance of the structure. The application of these forces reduces the overall work performed by the structure;

- $W_{\mathcal{S}} = W_{in}$, i.e. the work of deformation in the cut structure is equal to the work of deformation in the original statically indeterminate structure: no extra contribution is given to the performance of the structure by the application of the internal redundant forces.

Although it is not possible to equal the work of deformation of the fundamental structure, $W_{\mathcal{S}}$, and of the original one, W_{in}, because each element has, even if small, a proper stiffness, the proposed approach permit to highlight the presence of mechanisms that give significant contribution to the response of the global structure under the external actions. In other words, the presence of a fundamental structure for which the work of deformation $W_{\mathcal{S}}$ approximates the W_{in} implies that there is a preferential path through which the loads are carried. An example of that is represented in Figure 5.6; beam CD has larger cross-section. Two possible fundamental structures can be imagined: e.g. one represented by the horizontal beams ADB, the other one by the vertical beam CD. For the applied external load, the former exhibits larger work of deformation than the latter. As much as this discrepancy increases, i.e. as the flexural and shear stiffness of beam AD and DB reduce, force path through the scheme moves totally towards the vertical beam CD. In the hypothesis of flexural and shear stiffnesses of

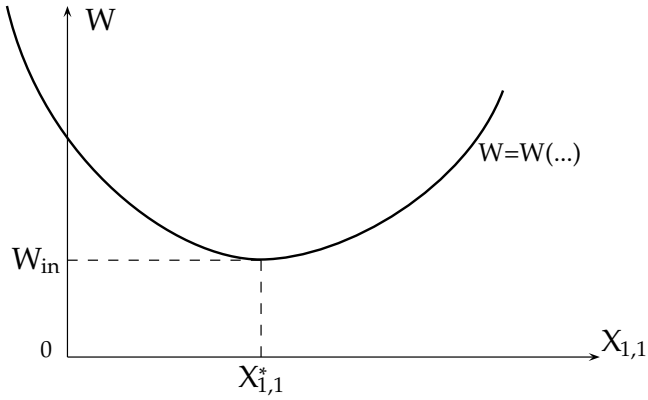

Figure 5.5: Values of $W = W\left(F, X_{1,1}, X_{1,2}, X_{1,3}, X_{2,1}, X_{2,2}, X_{2,3}\right)$ versus $X_{1,1}$. At $X^*_{i,m}$, the function reaches a minimum, that is the work of deformation for the statically indeterminate structure, i.e. $W\left(F, X^*_{1,1}, X^*_{1,2}, X^*_{1,3}, X^*_{2,1}, X^*_{2,2}, X^*_{2,3}\right) = W_{in}$.

beams AD and DB equal to zero, the load is carried only by beam CD. In that case, the work of deformation of the entire structure is equal to the work of the fundamental structure only composed by element CD, as described above.

As a result of the investigation previously proposed, a fundamental structure subjected to external loads that has a work of deformation close to the one of the original statically indeterminate structure (under the same loads) can be considered as a representative description of the original structure. Referring to the previous example, a different load distribution, like an horizontal load in D, would imply a different conclusion.

Different quantities can be considered for describing the performance of the structure. Many authors have used properties of the stiffness matrix as indicators (Starossek and Haberland, 2011, Biondini et al., 2008). In that sense, unfortunately, the stiffness matrix contains quantities that cannot be compared because they have different physical meaning. Moreover, the stiffness matrix can describe the connections between the elements but does not consider the effects due to the magnitude and direction of the loads acting on the structure. Displacement field would be another possible solution. Anyway, rotations and translations posses different physical units and cannot be compared. Hence, the work of deformation is chosen as a performance indicator because of the following aspects:

- pure elastic structures (linear and non-linear) are conservative systems. Hence, the work of deformation is not affected by load history but only by the initial and final positions;

- the work of deformation in linear elastic structures is equal to the work performed by external forces and can be easily computed by Clapeyron's Theorem. In case of non-linear

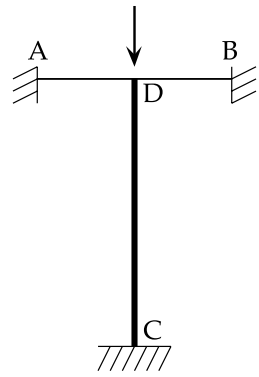

Figure 5.6: Beam CD has larger cross-section. Two fundamental structures can be imagined: one represented by horizontal beams ADB, the other one by vertical beam CD. For the applied external load, the former exhibits larger work of deformation than the latter. The predominant force path is represented by column CD.

elasticity, the work of deformation has to be computed by a step-by-step approach;

- the work performed by the structure merges into a single quantity the stiffness of the structure and the loads acting on it.

Each fundamental structure represents a link between the elevation and the foundation, a load path between the loaded nodes and the foundation nodes. The performance of each load path, intended as the discrepancy between the work of deformation in the fundamental structure and the original statically indeterminate structure, is connoted as a descriptor of the load path.

In particular, a performance factor ψ_i referred to the i-th fundamental structure can be defined as

$$\psi_i = \frac{W_{in}}{W_{\mathcal{S}_i}} \tag{5.23}$$

where, as previously stated, W_{in} is the work of deformation of the loaded statically indeterminate structure and $W_{\mathcal{S}_i}$ is the work of deformation of the i-th load path (e.g. a statically determinate structure), $\mathcal{S}_i$. The previous discussions can be related to the value assumed by ψ_i.

- $\psi_i \approx 1$, i.e. the fundamental structure and the original structure have almost the same work of deformation. The load path is thus representative of the behaviour of the structure.

- $\psi_i \approx 0$, i.e. the work of deformation performed by the fundamental structure is much

greater than the one performed by the original structure. The load path is not representative of the behaviour of the structure.

- Intermediate values of ψ_i are possible depending upon the proximity to one of the two limit conditions.

As stated in the introduction, an entropy-based measure allows quantifying the amount of information required to describe a system. As much as the system shows defined patterns in the structural response, the entropy of the system should decrease. That concept implies, obviously, that all the possible load paths are taken into account in the analysis. However, a continuous element can be cut in ∞ different ways and, therefore, there are ∞^e possible fundamental structures, where e is the number of elements. Because of that, we suppose that just the nodes are loaded. Despite that hypothesis may appear restraining in the analysis, it allows to take into account distributed loads by considering equivalent loads at nodes. Therefore, because the position of the cut in the element is not relevant, the number of fundamental structures is finite and is named s in the following.

5.6 Structural Complexity Indices

The structural complexity index, SCI, which takes into account the definition of information entropy previously recalled, can be computed by the following formula:

$$\mathrm{SCI} = -\sum_{i=1}^{s} \frac{\psi_i}{\sum_{j=1}^{s} \psi_j} \log_2 \left(\frac{\psi_i}{\sum_{j=1}^{s} \psi_j} \right) \tag{5.24}$$

where s is the (finite) number of load paths, i.e. fundamental structures, and ψ_i the performance index of the i-th load path linked to the work of deformation performed on the i-th fundamental structure. Since the ratio

$$\frac{\psi_i}{\sum_{j=1}^{s} \psi_j}$$

is smaller or equal to one, it can be alternatively considered a measure of probability. In that sense, Eqn. (5.24) is very similar to the expression proposed by Dehmer (2008a) and reported in Eqn. (5.6) where the information functional is based on metrical graph properties. In the structural case herein proposed, the information functional is a parameter that identifies the performance of the fundamental structure.

The value of SCI is affected not only by the distribution of the ψ_i values but also by the size of the structure. Therefore, in order to compare complexities of different structures, it is useful to introduce a normalised quantity, called the Normalised Structural Complexity Index, NSCI, ranging from 0 to 1 which can be expressed as

$$\mathrm{NSCI} = \frac{\mathrm{SCI}}{-\log_2 (1/s)} = \frac{\mathrm{SCI}}{\log_2 (s)}. \tag{5.25}$$

The denominator of the previous expression is the maximum value of complexity for a structure with s mechanisms with the same performance, as stated in the introduction of the chapter. In particular, the NSCI parameter reflects the complexity of the structure in such a way that:

- if $\mathrm{NSCI} \approx 0$, i.e. minimum complexity, the frame has a prevailing resisting mechanism which can be identified as the one with performance index ψ_i close to one;
- if $\mathrm{NSCI} \approx 1$, i.e. maximum complexity, all the mechanisms have the same weight in the overall behaviour of the structure;
- intermediate values reflect the tendency towards particular resisting schemes.

5.7 Complexity of frames

The procedure illustrated in the previous paragraphs can be summarised in the following steps:

1. for a given loaded statically indeterminate structure, compute the work of deformation W_{in};
2. create cuts (or remove the beams if the loads are applied at nodes) in such a way to turn the structure into a series of statically determinate schemes, $\mathcal{S}$, called fundamental structure, which play the role of admissible load paths;
3. compute the work of deformation $W_{\mathcal{S}}$ for each fundamental structure;
4. compare W_{in} and $W_{\mathcal{S}}$ in order to put into evidence the presence of a possible preponderant mechanism.
5. compute the SCI and the NSCI values in order to evaluate the overall complexity of the scheme.

The concepts previously illustrated can be applied to the analysis of a frame structure. This kind of scheme is characterised by a large degree of static indeterminacy caused by the jointed connections of the elements. There is, usually, a wide distribution of stiffnesses between the elements, which are conceived for performing different functions: the beams are characterised by large flexural inertia, while the columns have large cross-section area. The complexity analysis of a large structure with an high number of connection might be difficult, in particular in deriving the set of fundamental structures. Anyway, once this step is done, it is straightforward to compute the performance indices ψ via force matrix methods (typical of frame analysis) and then apply Eqns. (5.24) and (5.25) to get the complexity indices.

The most complicated step in the procedure is represented by the definition of the set of the fundamental structures of the scheme (i.e. of the load paths). This problem can be overcome by using graph theory, as described below.

5.7.1 Graph theory and structural analysis

Any frame structure composed by beams linked with each other by connections can be described by means of graph theory. This approach is not novel in structural mechanics.

The first (implicit) applications of graph theory in the field of applied sciences were provided by Kirchhoff and Maxwell in the analysis of electrical networks. The first applications of topology and graph theory to structural mechanics is due to Carter (1944) and Kron (1962) who first made an explicit analogy between electrical networks and elastic structures. In the same period, Langefors (1950, 1956a,b) presented a framework for the analysis of statically indeterminate continuous frames by means of algebraic graph theory. An alternative approach was proposed by Samuelsson (1962) for skeletal structures, and Wiberg (1970) for continuum problems.

Henderson and Bickley (1955) related the degree of static indeterminacy of a rigid-jointed frame to the First Betty Number and Kaveh (1988) applied many graph theoretical concepts to structural mechanic and, in particular, to structural optimisation (Kaveh, 2004). Others applications of graph theory to elastic systems can be found in Kaveh (2006).

5.7.2 Fundamental structures of a frame

A frame structure is a skeletal structure, i.e. a structure that can be ideally represented by linear members appropriately connected at point nodes (Henderson and Bickley, 1955), with fixedly connected elements at nodes. In our analysis we suppose that all nodes are loaded. That hypothesis, recalling Section 5.6, is not restraining in such a way that distributed loads can be condensed with equivalent nodal loads. On top of that, any real structure possesses self-weight and, therefore, at any node a dead load apply.

The associated graph G of the frame can be drawn remembering that the foundation node is unique in the mathematical model (Kaveh, 2006). Comparing the original scheme with any fundamental structure, the latter can be considered as a subgraph of G spanning on it. The static determinacy of the fundamental structures implies that any spanning subgraph will be a rooted tree of G, i.e. a spanning tree. Mathematically, the search of the set of rooted tree of a graph coincides with the extraction of the set of all possible fundamental structures of the scheme, since the elements are jointed at the nodes. If the elements were hinged in the nodes, the approach would not operate and a more complicated reasoning should be used.

In order to perform the analysis, the few basic definitions on graphs are reported in Chapter 2. In order to implement structural schemes into a graph theoretical framework, the following definitions are made:

1. A *frame associated graph* is a graph whose edges and nodes are in a one-to-one correspondence with the beams and the connections of a structural frame.

2. A *loaded node* is a node of the frame associated graph corresponding to a loaded connection of the frame.

3. A *foundation node* is that node of the frame associated graph corresponding to the external constrain of the frame. The foundation node is unique, in our first approximation.

In this sense, a help is given by algebraic graph theory: the number of spanning trees in a graph G is determined by its Laplacian. As a lemma of Kirchhoff's Theorem, let n be the number of vertices of G and let $\lambda_1, \ldots, \lambda_n$ be the ordered eigenvalues of the Laplacian of G. The number of spanning trees, s, is thus defined as

$$s = \frac{1}{n} \prod_{i=2}^{n} \lambda_i. \tag{5.26}$$

At the same time, it is necessary to define the degree of static indeterminacy of the frame. That quantity would be important for the determination of the number of cuts necessary for turning the statically indeterminate scheme into a statically determined one. In that sense, the Cyclomatic Number by Henderson and Bickley (1955) that associates the First Betti Number of the frame associated graph to the indeterminacy number, can be used. For a graph with n nodes and e edges, the Cyclomatic Number $\mathcal{C}$ is equal to

$$\mathcal{C} = e - n + 1 \tag{5.27}$$

The degree of static indeterminacy (Γ) of the frame is given by

$$\Gamma = 3 \times \mathcal{C} = 3\,(e - n + 1)\,. \tag{5.28}$$

The generation of all the possible s fundamental structures can be automatised. The first step is to assign to each element of the structure a progressive number. The $\mathcal{C}$-combinations of e elements are generated. Within the previous list, as illustrated later, there are combinations that cannot be considered in the analysis and have to be removed. The remaining part represents the set of the possible load-carrying fundamental structures. The steps of the algorithm are listed below:

1. The vertices (i.e. the nodes) and the edges (i.e. the beams) of the graph are numbered progressively.
2. The incidence matrix $\mathbf{B}$ of the original structure is computed, see Section 2.1.2 for the details on what an incidence matrix is.
3. By means of Kirchhoff's Theorem, the number of spanning trees, s, is determined. The Cyclomatic Number, $\mathcal{C}$, representing the number of necessary cuts is computed.
4. Since e is the number of beams in the structure, the $\mathcal{C}$-combinations of e elements are generated. These represent the indices of the elements of the graph of the structure that have to be removed. The number of combinations is greater or equal than s. That is

$$\binom{e}{\mathcal{C}} \leq s.$$

In fact, within all possible combinations, two different situations might occur. On one side, it is possible that one or more nodes are isolated; otherwise, it is possible that the number of connected spanning subgraphs is greater than one. The counter parameter i is set to 1, $i = 1$.

5. The i-th combination is considered. The incidence matrix of the structure is modified by means of the combination, i.e. null values are assigned to all the elements of the columns indexed in the combination. The Laplacian is computed and, by means of Kirchhoff's Theorem, the number of spanning trees is determined. Two situations are possible:
   - the number of spanning trees is equal to one. In that case there is only one connected component that is also a tree;
   - the number of spanning trees is equal to zero. If it is not possible to derive a tree that spans the entire structure, it implies that the frame-associated graph is composed by two, or more, components.
6. If the previous control is satisfied, i.e. the number of spanning trees is equal to one, the indices correspond to a feasible statically determinate structure and the counter parameter is increased, $i = i + 1$.

At the end of the algorithm application, s combinations have been isolated. The results can be stored in an extraction matrix. The following Section 5.9.1 reports all the calculations.

5.8 Beam Importance Factor

The contribution of each element to the overall complexity of the scheme is now evaluated. From the set of the performance indices, we define a beam importance factor, β_i, relative to the i-th element, which can be expressed as

$$\beta_i = \frac{\sum_{j=1}^{s} \psi_j \rho_{ij}}{\sum_{j=1}^{s} \psi_j} \tag{5.29}$$

where ρ_{ij} is a discriminant parameter that is equal to 1 if and only if the i-th element belongs to the graph of the j-th fundamental structure $\mathcal{S}_j$, i.e.

$$\rho_{ij} = \begin{cases} 1 & i \in \mathcal{S}_j \\ 0 & \text{otherwise} \end{cases}. \tag{5.30}$$

The physical meaning of β_i reflects the importance of each single element in the frame. In particular, $\beta_i \approx 1$ if the beam belongs to fundamental structures with high performance factor ψ or, if the beam represents a common and unique path connecting its ends, as shown in Section 5.9.3. On the contrary, $\beta_i \approx 0$ if the beam belongs to fundamental structures with low performance factor ($\psi_i \approx 0$). Intermediate values are possible.

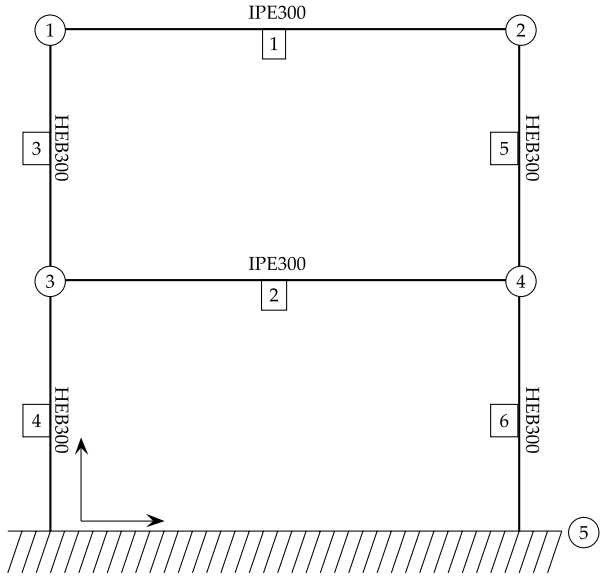

Figure 5.7: The two-stories frame analysed.

5.9 Simple examples

In the following, three examples are presented. The first example, reported in Section 5.9.1, illustrates the basic ideas of the metric of complexity, the second (Section 5.9.2 extends the concepts to the parametric analysis of a simple frame. The main resisting mechanism of a frame appears to change as much as the distance between the columns increases. The last example, reported in Section 5.9.3 analyses in detail the beam importance factor showing that values of β_i close to the unity implies both that a specific beam belongs to fundamental structures with high performance factor and that the element may belong to all the fundamental structures.

5.9.1 A two-stories frame

Consider the frame structure in Figure 5.7. It is made of of HEB 300 (EU 53-62) columns and IPE 300 (EU 19-57) beams. The properties of the elements are listed in Table 5.1.

The frame associated graph of the scheme is depicted in Figure 5.8. Vertices and edges are numbered progressively. Considering that the foundation node is unique, there are $e = 6$

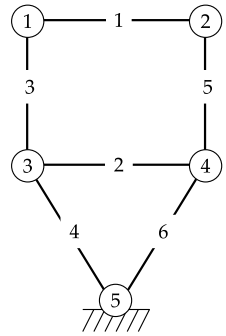

Figure 5.8: Frame associated graph of the structure in Figure 5.7.

Element	ℓ [m]	A [m^2]	J [m^4]	E [GPa]
1	5.0	5.381 $\times 10^{-3}$	8.356 $\times 10^{-5}$	210
2	5.0	5.381 $\times 10^{-3}$	8.356 $\times 10^{-5}$	210
3	3.0	1.491 $\times 10^{-2}$	2.517 $\times 10^{-4}$	210
4	3.0	1.491 $\times 10^{-2}$	2.517 $\times 10^{-4}$	210
5	3.0	1.491 $\times 10^{-2}$	2.517 $\times 10^{-4}$	210
6	3.0	1.491 $\times 10^{-2}$	2.517 $\times 10^{-4}$	210

Table 5.1: Geometrical and mechanical properties of the frame depicted in Figure 5.7.

edges and $n = 5$ nodes. The incidence matrix $\mathbf{B}$ of the original structure is:

$$\mathbf{B} = \begin{bmatrix} -1 & 0 & 1 & 0 & 0 & 0 \\ 1 & 0 & 0 & 0 & 1 & 0 \\ 0 & -1 & -1 & 1 & 0 & 0 \\ 0 & 1 & 0 & 0 & -1 & 1 \\ 0 & 0 & 0 & -1 & 0 & -1 \end{bmatrix}.$$

The eigenvalues of the Laplacian, which is $\mathbf{Q} = \mathbf{B}\mathbf{B}^T$, are ordered and reported in the following sorted vector $\lambda = \lambda(\mathbf{Q})$

$$\lambda = \begin{bmatrix} 0.0000 \\ 1.3820 \\ 2.3820 \\ 3.6180 \\ 4.6180 \end{bmatrix}$$

The number of fundamental structures is given by Eqn. (5.26. Hence,

$$s = \frac{1}{5}\prod_{i=2}^{5}\lambda_i = 11.$$

The number of necessary cuts to turn the graph into a tree is given by the Eqn. (5.27, that is

$$\mathcal{C} = 6 - 5 + 1 = 2.$$

The 2-combinations of 6 elements (15 in total) are represented by the following list.

$$\begin{array}{lllll} \{1,2\} & \{1,3\} & \{1,4\} & \{1,5\} & \{1,6\} \\ \{2,3\} & \{2,4\} & \{2,5\} & \{2,6\} & \{3,4\} \\ \{3,5\} & \{3,6\} & \{4,5\} & \{4,6\} & \{5,6\} \end{array}$$

Note that the combinations $\{1,3\}$ and $\{1,5\}$ implying the cut of beams 1 and 3, or 1 and 5, isolate nodes 1 and 2, respectively. On the other hand, combinations $\{3,5\}$ and $\{4,6\}$ separate the structure in such a way that the spanning trees are more than one. Hence, four combinations have to be neglected. The eleven admissible fundamental structures are reported in Table 5.2.

In order to examine the complexity indices and the beam importance factor, two different loading schemes are considered. The first loading scheme is reported in column LS1 of Table 5.3: only vertical loads act on nodes. Due to the symmetry of the structure and of the loads, the structure transfers almost the totality of the loads through the columns. The work of deformation of the original structure is calculated using Clapeyron's Theorem and is equal to

$$W_{in} = 4.791 \times 10^{1}\text{Nm}.$$

The analysis of the performance of each fundamental structure deriving from the eleven spanning trees of Table 5.2 gives that the Structural Complexity and the Normalised Structural Complexity Indices are, respectively,

$$\text{SCI} = 0.0976,$$

$$\text{NSCI} = 0.0282.$$

The last parameter denotes that the scheme is not complex (NSCI very close to zero) and that there is a specific mechanism, which is preponderant. As can be seen in Table 5.4, the ratio between $W_{\mathcal{S}_1}$ and W_{in} is 1.00, while the others are very close to zero. Because of that, F.S 1 can be considered as the preponderant load path in the frame. The beam indices, calculated with Eqn. (5.29), are reported in Table 5.5.

The second loading scheme LS2 takes into account horizontal and vertical forces at nodes. Thus, the results are different. The work of deformation of the whole structure is equal to

$$W_{in} = 2.230 \times 10^{3}\text{Nm}$$

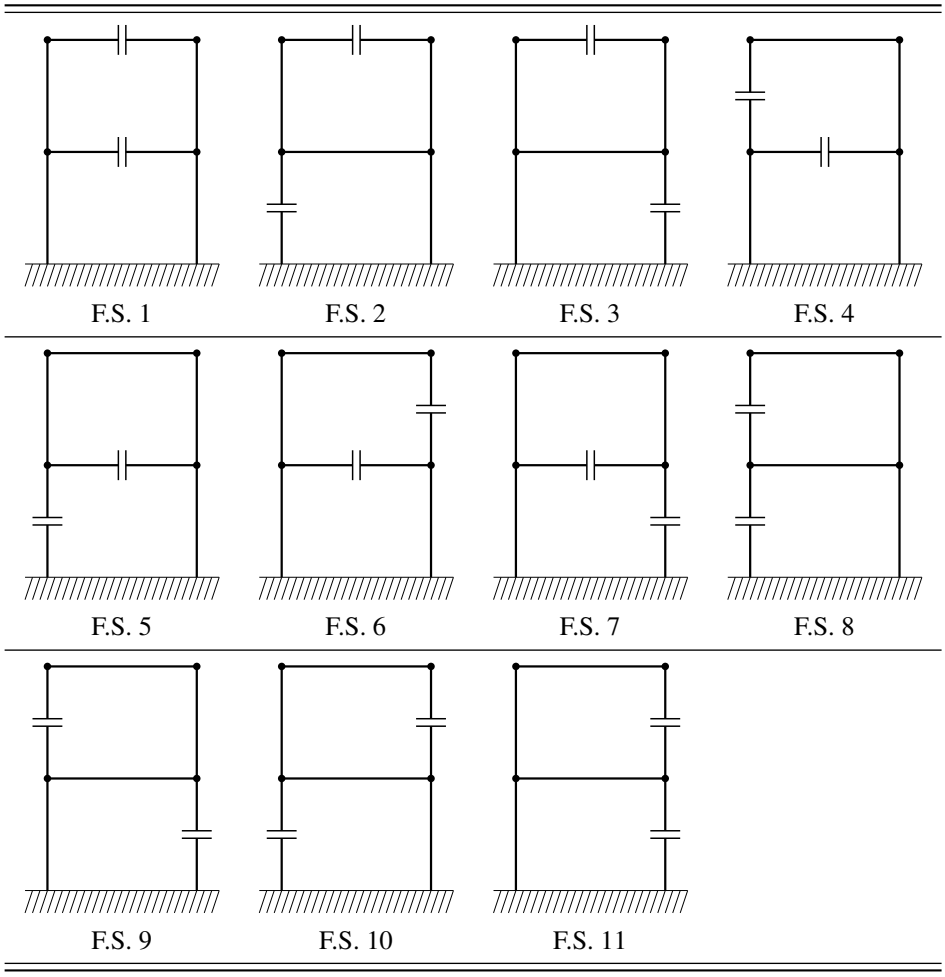

Table 5.2: The eleven fundamental structures (F.S.) obtained from the frame of Example of Section 5.9.1.

Node	LS1		LS2	
	vertical	horizontal	vertical	horizontal
1	-100 kN	0 kN	-100 kN	60 kN
2	-100 kN	0 kN	-100 kN	60 kN
3	-100 kN	0 kN	-100 kN	30 kN
4	-100 kN	0 kN	-100 kN	30 kN
5	0 kN	0 kN	0 kN	0 kN

Table 5.3: The two considered loading schemes LS1 and LS2 on the frame of Figure 5.7. Loads are in kN and their direction of application follows the reference system reported in Figure 5.7.

Fund. Strct.	LS1	LS2
F.S. 1	1.0000	0.3360
F.S. 2	0.0006	0.0702
F.S. 3	0.0006	0.0144
F.S. 4	0.0018	0.1401
F.S. 5	0.0005	0.0253
F.S. 6	0.0018	0.0376
F.S. 7	0.0005	0.0150
F.S. 8	0.0008	0.0705
F.S. 9	0.0006	0.0130
F.S. 10	0.0006	0.0381
F.S. 11	0.0008	0.0197

Table 5.4: $\psi_i = W_{\mathcal{S}_i}/W_{in}$ ratio for LS1 and LS2 for the frame of Figure 5.7. Values close to 1.00 indicate that the fundamental structure plays a relevant role in the structural behaviour of the frame. On the contrary, values close to 0.00 indicate that the fundamental structure has a marginal role as a load path in the structural behaviour of the frame.

Element	LS1	LS2
1	0.0073	0.4607
2	0.0040	0.2898
3	0.9968	0.7133
4	0.9975	0.7382
5	0.9968	0.8777
6	0.9975	0.9204

Table 5.5: Beam importance factors β_i for the frame of Figure 5.7 for loading schemes LS1 and LS2.

and the Structural Complexity and the Normalised Structural Complexity Indices are, respectively,

$$\mathrm{SCI} = 2.6273,$$

$$\mathrm{NSCI} = 0.7595.$$

The last parameter demonstrates that there are no single preponderant mechanisms. That result can be seen in the right-hand side column of Table 5.4: no value is close to one. Anyway, the most relevant load path is represented by fundamental structure F.S. 4, which has the highest ψ value. The presence of more than one preponderant mechanisms involving different sets of distinct elements is a good starting point for the analysis of the presence of different load paths.

5.9.2 A two-stories frame – parametric analysis

Consider again the structural scheme reported in Figure 5.7 and previously analysed in Section 5.9.1. The structure, whose material properties (cross-section area and inertia and elastic modulus) are reported in Table 5.1, is loaded with the Loading Scheme 2 (LS2) of Table 5.3. A parametric analysis can be performed. The controlling parameter is represented by a shape factor ζ (cell aspect), that is

$$\zeta = \frac{L}{h},$$

where h is the length of the columns and L is the distance between columns. The value of ζ ranges from 0.033 to 4. In other words, saying that h is kept constant at 3.00 m, $L_{min} = 0.10$ m and $L_{max} = 12.00$ m. In this analysis, the monitored quantities are the performance factors ψ_i, the Normalised Structural Complexity Index, NSCI, and the work of deformation of the original statically indeterminate structure, W_{in}.

In Figure 5.9, the performance factors of the eleven fundamental structures are plotted as functions of ζ. As can be seen, the most relevant load paths are the structures 1, 2, 4 and 8 respectively. Since the loads act on nodes vertically (down) and horizontally (right), these schemes are the ones for which both the statically determined structure shows high stiffness and the mutual works are less relevant. For example, taking the F.S. 5 of Table 5.2, the load applied to node 3 generates large displacements on the remaining nodes and, thus, the work of deformation increases. As illustrated, for $\zeta \to 0$, that is as the distance between the columns reduces, all the fundamental structures, except F.S.1, tend to have performance factor ψ equal to 0.50. F.S. 1 has $\psi_1 \approx 1$ showing that the frame can be reduced to a cantilever loaded at the top and at half height. This predominance is shown for $\zeta \leq 0.35$. As much as ζ increases, other load paths become predominant. In particular, for $0.35 < \zeta \leq 1.10$ the fundamental structures F.S. 8 and F.S. 2 attain higher performance index. This result can be attributed to the frame behaviour of the structural scheme. In that sense, the loads are transferred from one column to the other through the horizontal beams. For ζ-values larger than 1.10, ψ_1 increases while all the others performance factors decrease. This tendency highlights the fact that the

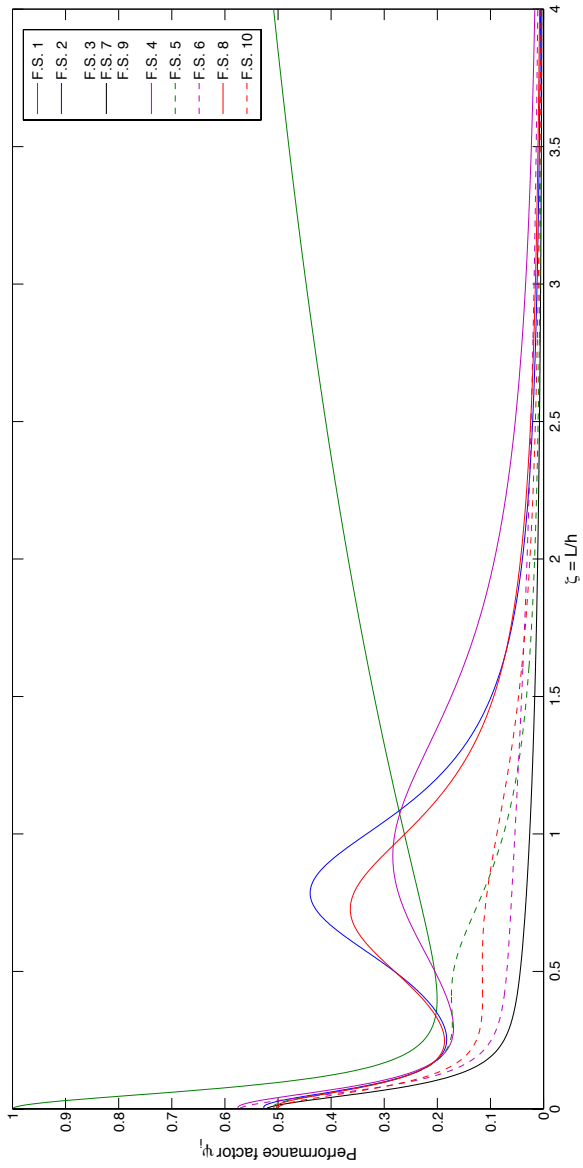

Figure 5.9: Performance factor of the eleven fundamental structures as functions of the ζ ratio. Three regions in which different fundamental structures have higher performance index are shown: for $0 < \zeta \leq 0.35$ the fundamental structure F.S. 1 prevailing, for $0.35 < \zeta \leq 1.10$ the fundamental structures F.S. 8 and F.S. 2 are predominant, for $\zeta > 1.10$ the fundamental structure F.S. 1 is again the predominant load path.

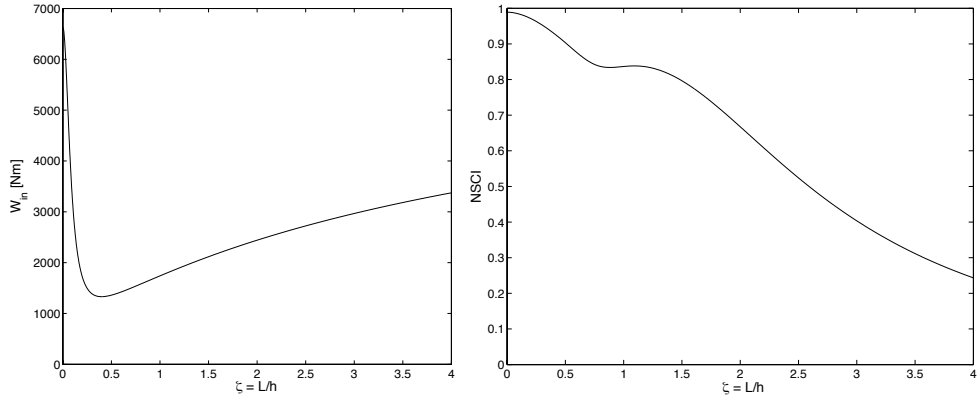

Figure 5.10: In the right-hand side part, the Normalised Structural Complexity Index (NSCI) is plotted as a function of ζ. For $\zeta \approx 0$, the NSCI is roughly equal to one. As ζ increases, NSCI decreases. At about $\zeta = 0.80$, a local minimum is shown and, then, a local maximum is recorded at $\zeta = 1.10$. Then, the NSCI monotonically decreases towards zero showing that the complexity reduces for large ζ. In the left-hand side part, the work of deformation of the original structure is plotted as a function of ζ. A minimum is shown at $\zeta \approx 0.35$ representing a well-developed frame behaviour, i.e. the load is transferred from the columns through an efficient effort of the horizontal beams. Since the forces are kept constant throughout the parametric analysis, this last configuration represents the optimal if the displacements of the scheme have to be limited, like in a real design (the lower the work of deformation, the more reduced the displacements).

structural scheme behaves like a double cantilever, independently loaded. The stiffness of the horizontal beams is not able to guarantee the efficient sharing of the loads between the columns.

The previous observations can be deduced from the analysis of the Normalised Structural Complexity Index. In Figure 5.10, NSCI is plotted versus ζ ratio. For $\zeta \to 0$ the complexity is maximum because all the ψ_i are equal, except $\psi_1 \approx 1$. The maximum complexity reflects the properties of entropy measures reported in the introduction. In the range $0.35 < \zeta \leq 1.10$, the NSCI is almost constantly equal to 0.80. The constancy represents a well-developed frame behaviour. As much as ζ increases, then, the NSCI decreases showing that the statically indeterminate structure turns into a simpler scheme, which corresponds to the fundamental structure F.S.1 (e.g. the role of beams vanishes).

The value of W_{in} versus ζ ratio is represented in the left-hand side plot of Figure 5.10. The interesting behaviour of this quantity confirms the previous suppositions on the functioning of the structural scheme. In particular, for $\zeta \to 0$ the work of deformation increases because the internal lever arm represented by the two columns is small enough and the scheme globally

	β_{III}	NSCI	W_{in}
Stage I	0.7146	0.9673	1.154×10^5 Nm
Stage II	0.4359	0.9122	1.215×10^5 Nm

Table 5.6: Beam importance factors of element III in the initial condition (Stage I) with nominal geometrical properties and in the final condition (Stage II) with reduced geometrical properties. β_{III} reduces in the second stage showing that the element contributes marginally to the overall static behaviour.

behaves like a double cantilever. At $\zeta \approx 0.35$, value at which a developed frame behaviour was obtained; the work of deformation reaches a minimum. For increasing ζ-values, the work of deformation increases monotonically. This behaviour can be explained by means of considerations on the influences of the singular fundamental structures on the whole loaded scheme. First, at $\zeta = 0$, the following situation is present: the statically indeterminate structure is, ideally, a single vertical cantilever (composed by two superposed cross sections). On one hand, F.S.1 has a work of deformation very close to the one of the original structure. On the contrary, the other ten F.S. have larger works of deformation, say roughly twice W_1, because columns are partially cut and, thus, the bending moment generated by the horizontal forces is supported, alternatively, by only one column (i.e. the work of deformation duplicates because the cross-section halves).

As much as ζ increases, the horizontal beams starts to be subjected to internal forces. Anyway, F.S.1 continues to behave in exactly the same manner (the horizontal beams are off the scheme). On the contrary, the work of deformation of the other mechanisms, e.g. F.S.(2, 4, 5, 8), reduces gradually, as shown by the relative ratio $\psi_{2,4,5,8}/\psi_1$. The presence of various mechanisms with similarly (low) works of deformation is, in our opinion, the cause of the minimum of W_{in}.

5.9.3 A single-column frame

In order to investigate the physical meanings of the beam importance factor β_i, the following example is proposed. Consider the scheme reported in Figure 5.11. Shaded nodes, i.e. all nodes except node A and foundation node, are loaded. The particularity of the frame is represented both by element I which is the only connection between the elevation nodes and the foundation node and by element II which links the unloaded node A to the remaining part of the scheme and, thus, to the foundation. All beams are 3.00 m length and cross-section area and moment of inertia are 5381 mm^2 and 8356×10^4 mm^4, respectively (IPE 300). Elements are made of steel, i.e. $E = 210$ GPa.

Attention is now focused on the values of the beam importance factor β with reference to elements I and II. The results of the analysis show the following aspects:

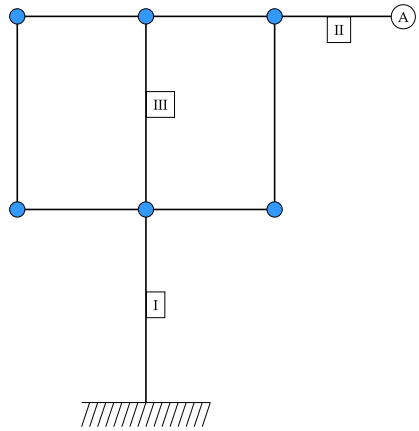

Figure 5.11: Frame of Example 3. The structural scheme presents one column (indicated with boxed letter I) linking the foundation node with the elevation structure. Another particularity of the scheme is represented by node A which is connected to the remaining structure by the cantilever element II, alone. Loaded nodes are shaded.

- $\beta_I = 1.00$ because element I is the only connection between the foundation node and the elevation structure. Therefore, all the fundamental structures have element I in common. Remembering Eqn. (5.29, $\rho_{Ij} = 1$ for any $j = 1, .., s$ and therefore the numerator is equal to the denominator, that is $\beta_I = 1$;

- in the same way, $\beta_{II} = 1.00$ because element II is the only connection between node A and the foundation, independently of the fact that node A is unloaded.

Following the results of the above example, it can be derived that the beam importance factor β does not take into account the presence, or not, of loads upon the nodes. The factor is identical both for the element I, which is really fundamental for the functioning of the scheme, and element II, which has no importance for the overall behaviour in the sense that it links the structure with an isolated and unloaded node.

The analysis focuses now on the importance factor of element III when its mechanical properties are strongly reduced. In particular, at that stage (named Stage II, see caption of Table 5.6 for details), the cross-section area and inertia of element III are set at 1.03×10^{-3} m^2 and 1.71×10^{-6} m^4. Material is unchanged. The values of β_{III} are reported in Table 5.6. The beam importance factor reduces as well as the mechanical properties of the element, hence the performance of those fundamental structures containing beam III diminishes. This trend reflects the fact that lower mechanical properties imply higher work of deformation both in the whole structure and in the element. The former aspect is highlighted by the value of W_{in} increasing in Stage II, the latter can be derived from the value of β_{III} at Stage II

since the number and the topology of the fundamental structures remain unchanged in both the monitored stages. It can be derived that low beam importance factors imply that the corresponding elements contribute only marginally to the overall structural behaviour.

Chapter 6

Digression on structural complexity

Although the examples illustrated in the previous chapter give an idea about the capabilities of the novel metric, some questions are still unanswered. This chapter of the dissertation deals, first, with some properties of the NSCI. The importance of external loads on the scheme, the scaling and an idea of targeted complexity are then considered in a theoretical and experimental ways. Then, in Section 6.4, an answer on what a fundamental structure is proposed. The theoretical approach follows the idea of stiffness reduction first on axially loaded schemes and then the idea is extended to moment resisting frames. This is the basis for damage studies on complex frames, further illustrated in Chapter 7.

Since the "mood" of this chapter is a digression, a fixed structural scheme is proposed and, then, various numerical an mathematical tests are performed.

The chosen reference structural scheme is constituted by 15 beams (6 horizontal beams and 9 columns) joined together in 9 elevation nodes and by a unique foundation node, see the sketch in Figure 6.1. Figure 6.2 illustrates the corresponding frame associated graph. All the elements of the arbitrary scheme are made of linear elastic material with Young's Modulus equal to 25 GPa, squared cross-section (40×40 cm).

The frame is exclusively loaded with nodal forces applied on all elevation nodes, i.e. A…I. That is

$$\begin{aligned} V_i = &\quad 100 \text{ kN} \\ H_i = &\quad 100 \text{ kN} \end{aligned} \tag{6.1}$$

with $i = \text{A,}\ldots, \text{I}$. The number s of fundamental structures is found from Eqn. (5.26) and is about 1183.

The structural complexity parameters are computed with Eqns. (5.24) and (5.25) and are

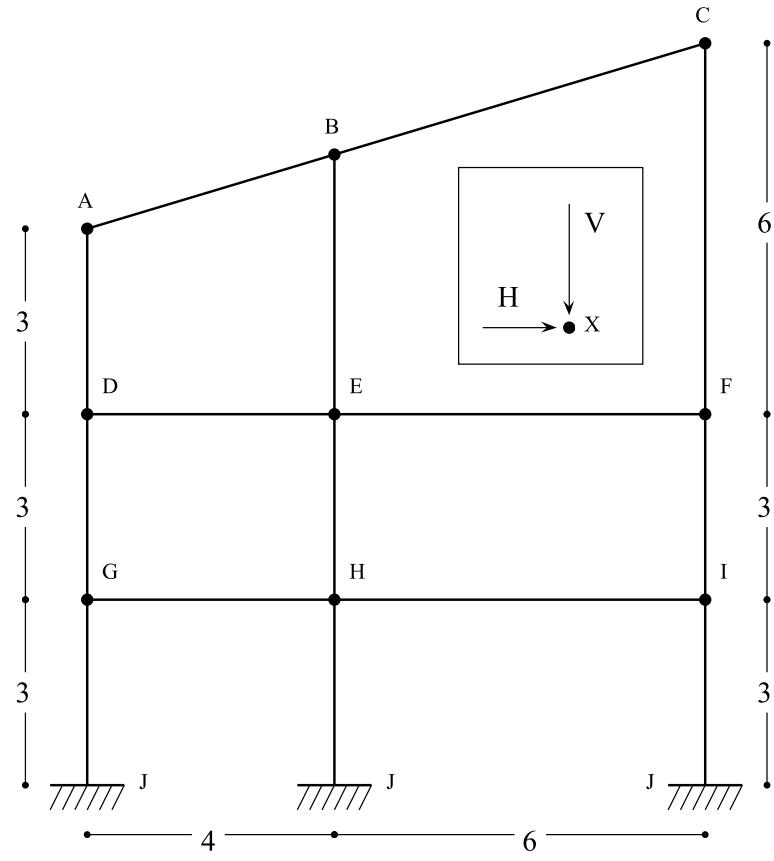

Figure 6.1: Sketch of the frame used in the working examples of Chapter 6. Lengths are in meters.

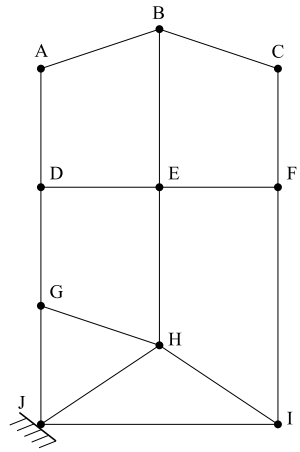

Figure 6.2: Frame associated graph of the structural scheme of Figure 6.1.

equal to

$$\begin{aligned} \mathrm{SCI} = &\quad 9.5849 \\ \mathrm{NSCI} = &\quad 0.9389 \end{aligned} \tag{6.2}$$

6.1 Loads[1]

The performance ratios, computed with Eqn. (5.23), indicate the load paths in the structure and its efficiency. The highest value of the performance ratio is 0.2064 and relates to the fundamental structure depicted in Figure 6.3(a).

A parametric analysis on the external loads is now performed. In particular, the ratio between the magnitude of the horizontal force acting on the elevation nodes is reduced up to zero.

Suppose a ratio $H/V = 0.50$, that means that $H = 50$ kN. In this case, the values of the complexity parameters reduce, showing that the structural behaviour is turning into a simpler one. In particular, we get

$$\begin{aligned} \mathrm{SCI} = &\quad 9.3588 \\ \mathrm{NSCI} = &\quad 0.9168. \end{aligned} \tag{6.3}$$

As reported in Chapter 5, the analysis of the performance ratios gives an idea on how the

[1]The present section is part of the Proceedings of FraMCos–8 conference hold in Toledo (De Biagi and Chiaia, 2013b).

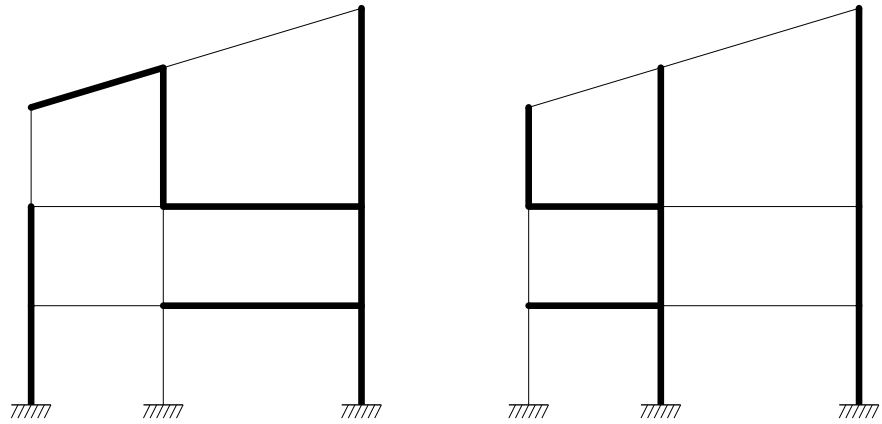

(a) $H/V = 1.00$ (b) $H/V = 0.50$

Figure 6.3: Fundamental structure with highest performance factor for $H/V = 1.00$ (a) and $H/V = 0.50$ (b). The fundamental structures are represented by thick lines.

loads are transmitted to the foundation. In this case, differently from before, the fundamental structure which exhibits the highest performance ratio, $\psi = 0.1716$, is different from before, as can be seen in Figure 6.3(b). The main differences refer to the upper-left part: the contribution of the columns becomes more relevant as much as the horizontal force reduces, i.e. the resultant nodal force tends to be vertical. As a limit situation, the case $H = 0$ kN is considered. In this sense, the NSCI is equal to 0.4527 and the fundamental structure with higher performance index is the one constituted by the columns alone. The associated ψ-value is, as expected, 0.9999.

In order to study the contribution of different fundamental structures, we ordered the ψ-

	H/V			
ψ^*/ψ_{max}	1.00	0.50	0.10	0.00
≥ 0.90	6	5	1	1
≥ 0.80	9	9	1	1
≥ 0.50	69	27	1	1
≥ 0.20	262	82	2	1
≥ 0.10	581	256	4	1

Table 6.1: Number of fundamental structures with performance ratio greater than a given percentage of the maximum value, ψ_{max}. Values are cumulative.

values obtained from the analysis of the 1183 statically determinate structures in ascending order. To control easily if there are more than one mechanisms with relevant ψ, I normalise each order position by dividing it by the number of fundamental structures. Plotting these data on a graph like the one of Figure 6.4(a), it is possible to asses the percentage of mechanisms with performance ratio smaller than a given value ψ^*. The loading cases considered refer to H/V values equal to 1.00, 0.50, 0.10 and 0.00. Referring to cases 1.00 and 0.50, there are many mechanisms with relatively high performance indexes. In Figure 6.4(b) the values of ψ^* are normalised to the maximum value. There are six fundamental structures in the range $0.90 - 1.00\,\psi_{max}$ in the case $H/V = 1.00$, which reduces to five in the case $H/V = 0.50$. There is only one in the cases $H/V = 0.10$ and 0.00. These data are reported in Table 6.1. The representativeness of a particular load path in the case of $H/V = 0.00$ is clearly visible. This aspect makes the corresponding NSCI low.

6.2 Scaling[2]

The effects of scaling are well known in structural engineering. The first attempts in searching the relationship between size and nominal strength date back to Renaissance and to the experiments of Leonardo Da Vinci on cords resistance (Bazant and Chen, 1997). Although the first researches on fracture mechanics date at the first decades of 20th century (Griffith, 1921), size effects on materials and constructions have been outlined at the end of the century (Carpinteri, 1994a,b) and are still a research topic of interest.

The purpose of the present section is to illustrate the effects of scaling on the measure of structural complexity. As a summary of the following, different trends emerge. In case of consistent load set, i.e. either forces or bending moments at nodes, the complexity results invariant to scaling operations. Otherwise, in case of non-consistent load set, a transition in the way the structural elements interact each others is shown. In particular, as much as the structure reduces its size, setting-aside the forces, the overall behaviour is governed by the torques applied at the nodes and the axial stiffnesses. On the contrary, for large structures, the situation is the opposite: the major contribution on load transfer is due to the forces and the flexural stiffnesses of the structure. Loading scaling is analysed independently from geometric scaling, as reported below.

6.2.1 Loads scaling

As stated in Section 6.1, complexity is dependent on the load set acting on the structure. In the following, the effects due to a proportional scaling of the magnitude of the applied loads are presented. A brief remind on stiffness matrix is necessary. In the simplest analysis possible,

[2]The present section has been published on Complexity (De Biagi and Chiaia, 2014).

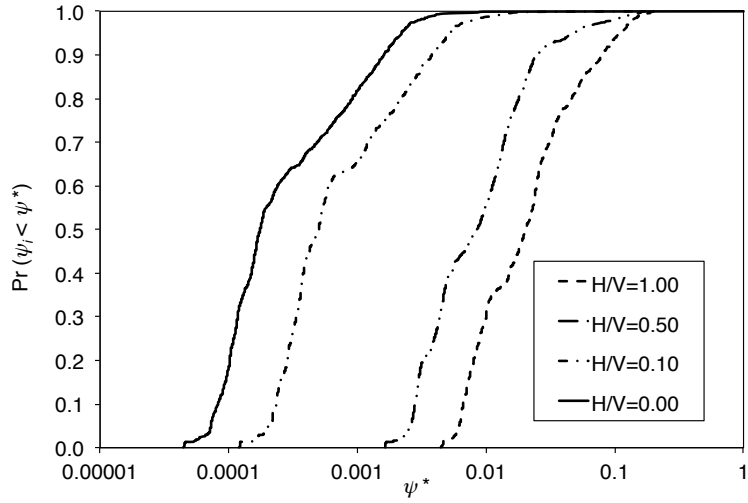

(a)

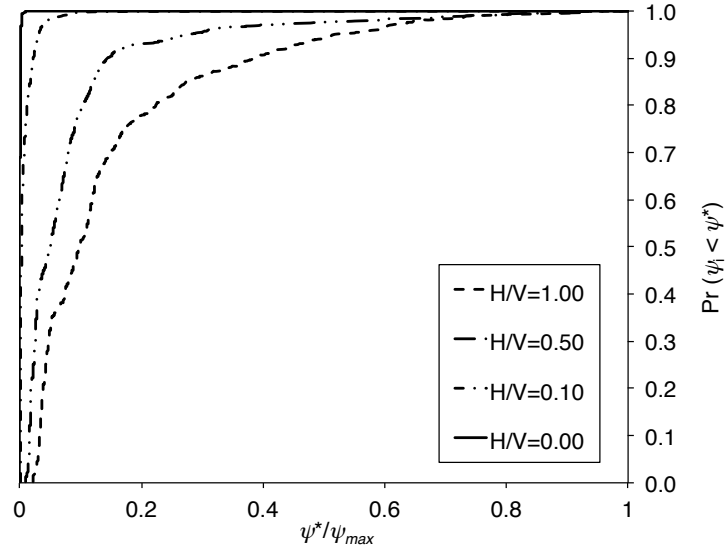

(b)

Figure 6.4: Cumulative probability plots. Probabilities of occurrence of mechanisms with performance ratio smaller than ψ^*, i.e. $\Pr(\psi_i \leq \psi^*)$. On plot (a), the values of ψ^* are absolute, on plot (b) the values are normalised to the maximum ψ-value of each load case. The considered load cases are $H/V = 1.00, 0.50, 0.10$ and 0.00.

the response of a structure is governed by the following expression,

$$\mathbf{f} = \mathbf{K}\mathbf{d}, \tag{6.4}$$

where $\mathbf{d}$ represents the displacement field, $\mathbf{f}$ contains the external loads applied to the scheme, $\mathbf{K}$ is the so-called *stiffness matrix* and gives information about the ability of external loads to displace the structural scheme (Felippa, 2001). The stiffness matrix is positive defined and symmetric. The elements in the matrix reflect the topology of the scheme and the geometrical and material properties of the elements. In general, it is more convenient to speak about tangent stiffness matrix, since in many problems the matrix evolves as much as the structure deforms towards the collapse. Supposing the structure to be made of linear elastic material, the components of the stiffness matrix do not change during the loading process. Under an arbitrary loading scheme, $\mathbf{f}_0$, the work of deformation, W_0, can be easily computed by means of Clapeyron's Theorem. Inverting Eqn. (6.4), the displacements are computed

$$\mathbf{d}_0 = \mathbf{K}^{-1}\mathbf{f}_0. \tag{6.5}$$

The work of deformation is thus equal to

$$W_0 = \frac{1}{2}\mathbf{f}_0^T\mathbf{d}_0 = \frac{1}{2}\mathbf{f}_0^T\mathbf{K}^{-1}\mathbf{f}_0, \tag{6.6}$$

where the superscript ^{T} indicates the transposed of the vector.

Suppose to modify the intensity of the load through a scaling parameter ξ. Thus, the load vector becomes

$$\mathbf{f}_\xi = \xi\mathbf{f}_0. \tag{6.7}$$

As much as the load increases, the displacements increase proportionally, as can be clearly noticed by substituting Eqn. (6.7) into Eqn. (6.5) getting

$$\mathbf{d}_\xi = \mathbf{K}^{-1}\mathbf{f}_\xi = \xi\mathbf{K}^{-1}\mathbf{f}_0 = \xi\mathbf{d}_0. \tag{6.8}$$

The work of deformation made by scaled forces is equal to

$$W_\xi = \frac{1}{2}\mathbf{f}_\xi^T\mathbf{d}_\xi = \frac{1}{2}\xi^2\mathbf{f}_0^T\mathbf{K}^{-1}\mathbf{f}_0 \tag{6.9}$$

and can be rewritten as

$$W_\xi = \xi^2 W_0. \tag{6.10}$$

Since the algorithm for evaluating the complexity considers the ratio between two work of deformations, see Eqn. (5.23), the scaling factor, ξ^2, simplifies, leaving the complexity unchanged, i.e.

$$\mathrm{SCI}_\xi = \mathrm{SCI}_0, \tag{6.11}$$

where SCI_0 is the Structural Complexity Index of the scheme under the arbitrary load set. Similarly, $\mathrm{NSCI}_\xi = \mathrm{NSCI}_0$.

6.2.2 Geometric scaling

In the current section, the loads are kept constant and the geometric properties of the structure, i.e. elements length, cross-sections size, area and inertia, are scaled by a scaling factor η. In this sense, given an arbitrary scheme to which element lengths and cross-section sizes are assigned, the corresponding properties of the scaled scheme are

$$\ell_{i,\eta} = \eta \ell_{i,0} \tag{6.12}$$
$$A_{i,\eta} = \eta^2 A_{i,0} \tag{6.13}$$
$$J_{i,\eta} = \eta^4 J_{i,0}, \tag{6.14}$$

where $\ell_{i,0}$, $A_{i,0}$ and $J_{i,0}$ are length, cross-sectional area and inertia of the i-th element of the arbitrary scheme. Differently from the previous scaling situation in which $\mathbf{K}$-matrix remains unchanged, now, the factor acts directly on the components of the stiffness matrix. In general, since the elements of $\mathbf{K}$ have different physical units, a non-linear behaviour emerges because of the dependence of the work of deformation on the inverse of the stiffness matrix, see Eqn. (6.6).

In order to discuss the problem and its limit situations, consider a simple structural system in which the degrees of freedom are a rotation, φ, and a linear displacement, v. The dual static quantities are a bending moment, M, and a generic force, F. Eqn. (6.4) can be rewritten as

$$\begin{bmatrix} M \\ F \end{bmatrix} = \begin{bmatrix} \hat{a} & \hat{b} \\ \hat{b} & \hat{c} \end{bmatrix} \begin{bmatrix} \varphi \\ v \end{bmatrix}, \tag{6.15}$$

where $\hat{a}$, $\hat{b}$ and $\hat{c}$ are the components of the stiffness matrix $\mathbf{K}$. The rotation measured in radians is physically dimensionless and, in parallel, bending and pure forces are measured as $[\text{Force} \times \text{Length}]$ and $[\text{Force}]$, respectively, the components of the stiffness matrix have the following physical units:

$$\begin{aligned} [\hat{a}] &= [\text{Force} \times \text{Length}] \\ \left[\hat{b}\right] &= [\text{Force}] \\ [\hat{c}] &= \left[\text{Force} \times \text{Length}^{-1}\right]. \end{aligned} \tag{6.16}$$

The solution of the algebraic system of equations gives the displacement vector

$$\begin{bmatrix} \varphi \\ v \end{bmatrix} = \frac{1}{\hat{a}\hat{c} - \hat{b}^2} \begin{bmatrix} \hat{c} & -\hat{b} \\ -\hat{b} & \hat{a} \end{bmatrix} \begin{bmatrix} M \\ F \end{bmatrix}, \tag{6.17}$$

The first two terms of the right-hand side of Eqn. (6.17) represent the inverse of the stiffness matrix, i.e. $\mathbf{K}^{-1}$. The work performed by the external loads, W_0, is computed by means of Clapeyron's Theorem and is equal to

$$W_0 = \frac{1}{2\left(\hat{a}\hat{c} - \hat{b}^2\right)} \begin{bmatrix} M & F \end{bmatrix} \begin{bmatrix} \hat{c} & -\hat{b} \\ -\hat{b} & \hat{a} \end{bmatrix} \begin{bmatrix} M \\ F \end{bmatrix}, \tag{6.18}$$

which simplifies into

$$W_0 = \frac{1}{2\left(\hat{a}\hat{c} - \hat{b}^2\right)}\left(\hat{c}M^2 - 2\hat{b}MF + \hat{a}F^2\right). \tag{6.19}$$

Introducing a scaling on the lengths, the terms of the stiffness matrix are rewritten following their physical unit in such a way the lengths are multiplied by the scaling factor η. Thus, thee stiffness matrix of the scaled scheme, $\mathbf{K}_\eta$, is

$$\mathbf{K}_\eta = \begin{bmatrix} \eta\hat{a} & \hat{b} \\ \hat{b} & \frac{\hat{c}}{\eta} \end{bmatrix}. \tag{6.20}$$

The work of deformation performed by the loads acting on the scaled scheme is evaluated with Eqn. (6.19) and is equal to

$$W_\eta = \frac{1}{2\left(\hat{a}\hat{c} - \hat{b}^2\right)}\left(\frac{\hat{c}}{\eta}M^2 - 2\hat{b}MF + \eta\hat{a}F^2\right). \tag{6.21}$$

The following two limit situations are clearly visible. If F is null, i.e. the external load is a bending moment exclusively, the work of deformation in the arbitrary scheme is

$$W_0 = \frac{\hat{c}}{2\left(\hat{a}\hat{c} - \hat{b}^2\right)}M^2, \tag{6.22}$$

and the corresponding quantity in the scaled scheme is

$$W_\eta = \frac{\hat{c}}{2\left(\hat{a}\hat{c} - \hat{b}^2\right)}\frac{M^2}{\eta}. \tag{6.23}$$

Thus, the two energies are linked through the following expression

$$W_\eta = \frac{W_0}{\eta}. \tag{6.24}$$

On the contrary, if M is null, i.e. the external load is a generic force, the two energies are proportional, that is

$$W_\eta = \eta W_0. \tag{6.25}$$

Since the complexity is governed by the performance factor, the value of the ratio remains unchanged if both numerator and denominator are multiplied by the same quantity. This results in complexity invariance to scaling operations.

In the case in which neither M and F are null, the relationship between W_η and W_0 depends on the stiffness of the structure — $2\hat{b}$ in the round brackets of Eqns. (6.19) and (6.21) — and the magnitude of the loads.

Referring to the last case, the loading set is not consistent, i.e. there are both external forces and moments. Each component of $\mathbf{K}_\eta$ plays a role in the behaviour of the structure. Comparing the scaled stiffness matrix, i.e. $\mathbf{K}_\eta$ of Eqn. (6.20), and the non-scaled one, i.e. $\mathbf{K}$ of Eqn. (6.15), two trends emerge. In case of small scaling factor ($\eta \to 0$), the flexural stiffness, represented by component $\hat{a}$ in Eqn. (6.15), tends to reduce and, in parallel, the axial stiffness, represented by component c in Eqn. (6.15), increases. The opposite situation emerges for large scaling factors. The effects on the work of deformation invert. Analysing the first term ($\hat{c}/\eta$) of the trinomial in the round brackets of Eqn. (6.21), the contribution of the axial stiffness increases as much as η tends to zero and, in parallel, the last term ($\eta\hat{a}$), representing the contribution of the flexural stiffness, decreases. In this case, the contribution of the force, F, is not important for the evaluation of the work of deformation and, thus, the complexity. In case of large scaling factor, the situation is reversed: the term $\hat{c}/\eta$ tends to zero, while $\eta\hat{a}$ increases, showing the preponderance of the force load to the detriment of the moment M.

Geometric scaling with non-consistent load sets

In the LOADING EXPERIMENT NO.1, three different load sets are applied to the structural scheme of Figure 6.1. In loading situation (i) called "Force", a vertical force, V, equal to 100 kN is applied to all elevation nodes (A to I) and three horizontal forces, H, are applied to node A (100 kN), D (50 kN) and G (50 kN). Loading situation (ii) called "Bending" is composed by an anti-clockwise torque applied to node A (100 kNm). Loading situation (iii) called "Force + Bending" is the mere sum of the previous two. Load-cases (i) and (ii) are consistent, since are composed by either forces or torques. Load-case (iii) is not consistent because possesses both forces and torques. Torques applied on the bidimensional plane of the structure result in bending in the elements.

In order to show the effects of geometric scaling, a set of 15 values of parameter η logarithmically spaced are generated in the range $\left[10^{-5}; 10^{3}\right]$. For each value of the scaling parameter, the Normalised Structural Complexity Index related to the three load-cases is evaluated. Before commenting the results, it is important to state that geometric scaling has no effects on Young's Modulus, since all components of the stiffness matrix are multiplied by the same quantity (right Young's Modulus, or a fraction of it in case of homogenised elastic modulus).

The results of the complexity analysis are reported in Table 6.2 and plotted in Figure 6.5(a). As expected, scaling on scheme with consistent load-cases has no effects on the value of the Normalised Structural Complexity Index. The loading situation composed by "Force" has a NSCI equal to 0.8817, the loading situation composed by "Bending" has a NSCI equal to 0.9824. The most interesting issue is represented by the variation of NSCI-value in the loading situation composed by "Force + Bending". Making clear that the complexity analysis serves for estimating the amount of diversity of the load-paths through the structure, an interaction between structural behaviour and size of the structure is clearly visible. In this sense,

η	"Force"	"Force + Bending"	"Bending"
0.00001	0.8817	0.9824	0.9824
0.00004		0.9823	
0.00014		0.9822	
0.00052		0.9815	
0.00193		0.9786	
0.00720		0.9650	
0.02683		0.9373	
0.10000		0.9142	
0.37276		0.9010	
1.38950		0.8875	
5.17947		0.8832	
19.3070		0.8821	
71.9686		0.8818	
268.270		0.8818	
1000.00	0.8817	0.8818	0.9824

Table 6.2: LOADING EXPERIMENT NO.1: NSCI as a function of the scaling parameter η for three different load-cases. For the load-case "Force", no dependency is shown since the NSCI is constant at 0.8817. Similar consideration for the load-case "Bending" at 0.9824. The sum of the two load-cases, i.e. the load-case "Force + Bending", shows a transition between the two previous situations, which act as bounds.

for small scaling parameters, i.e. small structural schemes, the behaviour of the system tends to be similar to the one in which only the torques are applied, even if the loading scheme includes forces. On the contrary, for large scaling parameters, i.e. big, say huge, structural schemes, the behaviour of the system tends to be similar to the one in which only the forces are applied, even if the loading scheme includes torques. At intermediate sizes there is a transition between the two limit behaviours.

In the LOADING EXPERIMENT NO.2, three different load sets are applied to the structural scheme of Figure 6.1. In loading situation (i) called "Force", a vertical force, V, equal to 100 kN is applied to nodes F, G, H and I and a horizontal forces, H, equal to 100 kN is applied to nodes A, B, C, D and E. Loading situation (ii) called "Bending" is composed by an anti-clockwise torque applied to node A (100 kNm) and by an anti-clockwise torque applied to node E (10 kNm). Loading situation (iii) called "Force + Bending" is the mere sum of the previous two. Load-cases (i) and (ii) are consistent, since are composed by either forces or torques. Load-case (iii) is not consistent because possesses both forces and torques. As before, a set of 15 values of parameter η logarithmically spaced are generated in the range $\left[10^{-5}; 10^{3}\right]$. Obviously, as expected, the NSCI-values are different from the loading experiment no.1. In this case, the pure "Force" NSCI is equal to 0.9613, while the pure "Bending"

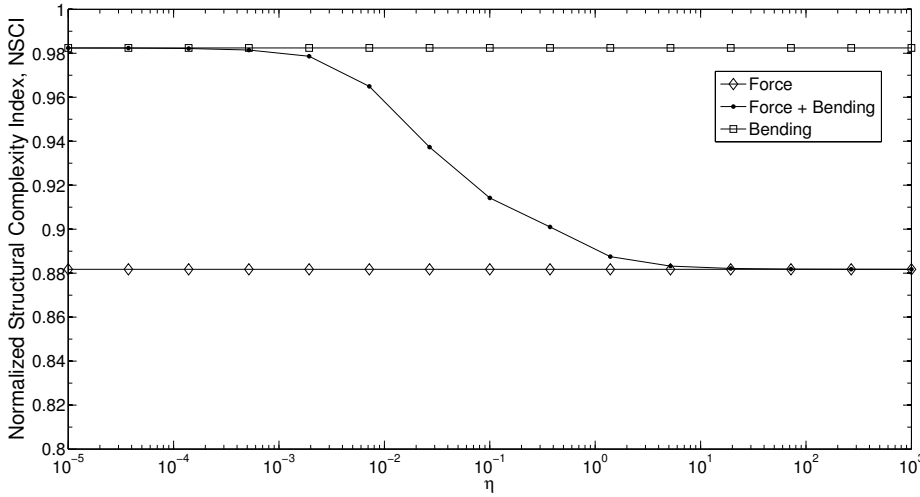

(a) LOADING EXPERIMENT NO.1

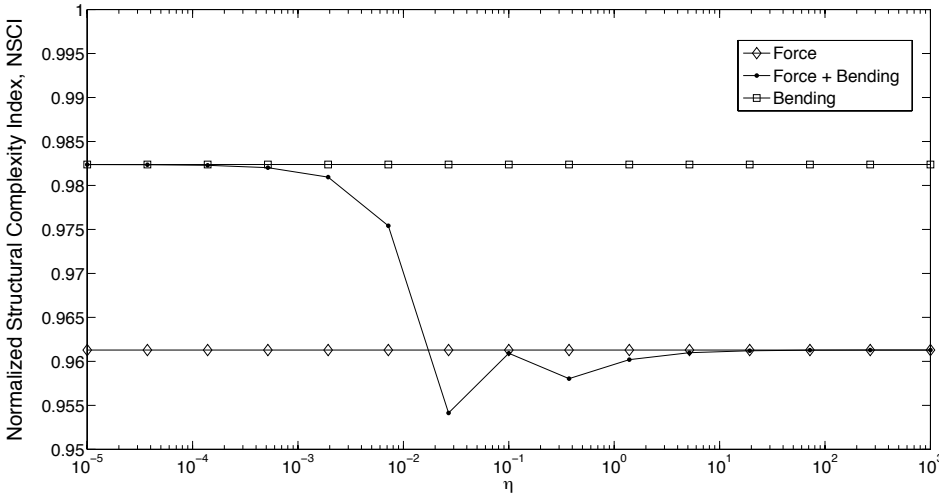

(b) LOADING EXPERIMENT NO.2

Figure 6.5: Normalised Structural Complexity Index, NSCI, for different values of the scaling factor η. Diamonds refer to the load-case "Force", plain dots to the load-case "Force + Bending" and squares to the load-case "Bending".

η	"Force"	"Force + Bending"	"Bending"
0.00001	0.9613	0.9824	0.9824
0.00004		0.9824	
0.00014		0.9823	
0.00052		0.9820	
0.00193		0.9809	
0.00720		0.9754	
0.02683		0.9541	
0.10000		0.9609	
0.37276		0.9580	
1.38950		0.9602	
5.17947		0.9610	
19.3070		0.9612	
71.9686		0.9613	
268.270		0.9613	
1000.00	0.9613	0.9613	0.9824

Table 6.3: LOADING EXPERIMENT NO.2: NSCI as a function of the scaling parameter η for three different load-cases. For the load-case "Force", no dependency is shown since the NSCI is constant at 0.8817. Similar consideration for the load-case "Bending" at 0.9824. The sum of the two load-cases, i.e. the load-case "Force + Bending", shows a transition between the two previous situations, which act as bounds.

NSCI is equal to 0.9824. The transition between the two, representing the "Force + Bending" NSCI is plot by plain dots in Figure 6.5(b). It clearly that, in the transition between the two limit regimes, the NSCI is lower than the pure "Force" NSCI, showing that this value does not represent a lower limit for the complexity of the loaded scheme under scaling. The results of the complexity analysis are reported in Table 6.3 and plotted in Figure 6.5(b).

6.3 Targeting complexity[3]

It would be interesting to find the most complex and the simplest structures. Or, in a more general problem, to target the value of the complexity of the structure. Different strategies are possible:

1. keeping fixed the position of the elevation nodes and the topology of the structure and changing the stiffnesses of the single elements;

2. keeping fixed the geometrical and material properties of the elements and changing the

[3]The present section is a part of IABSE 2013 workshop hold in Helsinki (De Biagi and Chiaia, 2013c).

position of the nodes (nodal coordinates);

3. keeping fixed the position of the elevation nodes and changing the topology of the structure by adding/removing elements.

Obviously, a combination of the previous approaches can be done. Anyway, practically, the position of the loads is fixed and thus solution 2. is not applicable. Analogously, it is not possible to increase the number of the elements of the structure, since the cost increases. The more feasible solution seems to be the one that consider stiffness variation across the elements.

In this sense, the distribution of stiffnesses in the structural scheme for which the complexity is minimised or maximised is worked out in the following.

The strategy for the solution of the problem takes into account the fact that the values of NSCI can be found only after the distribution of stiffnesses is given. In other words, as detailed in the examples of Chapter 4, the evaluation of NSCI is made by:

1. giving geometry and material properties of the elements of the structure;

2. computing the work of deformation of the whole structure;

3. evaluating the work of deformation of the set of fundamental structures and, consequently, the ψ-ratios;

4. determining SCI and NSCI values.

Because of the impossibility of inverting the problem and getting a possible distribution of sizes for a given value of complexity, since the problem is highly nonlinear and has a large number of variables, an evolutionary optimisation algorithm is used. This is an implementation of a metaheuristic[4] modelled on the behaviour of biological evolution.

The idea at the base of the evolution strategies sprouted in the Sixties at the Technical University of Berlin (TUB) in Germany (Rechenberg, 1965, Schwefel, 1965). The solution algorithm is based on the collective learning process within a population of individuals, each of which represents a search point in the space of potential solutions to a given problem. The population is arbitrarily initialised and it evolves toward better and better regions of the search space by means of randomised processes of selection, mutation, and recombination. The environment delivers quality information (fitness value) about the search points, and the selection process favours those individuals of higher fitness to reproduce more often than those of lower fitness. The recombination mechanism allows the mixing of parental information while passing it to their descendants, and mutation introduces innovation into the population (Bäck and Schwefel, 1993). Evolution techniques are used in many fields, even in structural engineering for topological cost optimisation, see Hajela and Lee (1995) and further publications.

[4]Wikipedia defines a metaheuristic as an higher-level procedure designed to find, generate, or select a lower-level procedure or a partial search algorithm that may provide a sufficiently good solution to an optimisation problem

In the optimisation problem herein discussed, the dimensions of the element cross-sections are the unknown parameters, the length of the beams and the coordinates of the connections are fixed. In order to simplify the computations, a square cross-section is supposed. As demonstrated in Section 6.2, since the load set represented in Eqn. (6.1) is consistent, the value of the complexity is geometric and loading scale free. In this sense, the size of the elements identifies a class of structures. Because of that, there are ∞^1 possible solutions to the problem of complexity maximisation (or minimisation). To overcome this fact, the cross-section size of beam joining nodes A and B is set equal to a reference length (say one). Therefore, the sizes of the other elements are related to the one of the reference beam.

The evolution strategy implemented is based on a simple mutation following a random vector generator. The following procedure is applied: (i) a population of random solutions is generated (as said, element AB is set equal to one throughout the optimisation process). For each solution, (ii) the corresponding structure is defined and its complexity is computed. To achieve complexity maximisation, (iii) the structures are ordered in decreasing order based on their complexity. A subset of cardinality q of the population is chosen (the best q structures) and, randomly, one element Φ of the subset is selected as "father" of the future generation of parameters. (iv) The parameters of structure Φ are varied using a normally distributed random number generator ($\sigma = 0.005$) and a novel population (generation) of solutions, i.e. structures, is found. The evolution process, consisting of steps (ii) to (iv) is repeated until the cost function, i.e. the NSCI, does not change between subsequent generations and optimisation is achieved. The initial population is about 24 structures; the size of the bests is about 12 structures ($q = 12$). The process is stopped at the 750th generation. The following structures are obtained. The structure with minimum complexity has $\mathrm{NSCI} = 1.6 \times 10^{-6}$, while the structure with maximum complexity has a $\mathrm{NSCI} = 0.9936$. The schemes are presented in Figures 6.6 and 6.7.

As shown in the histogram of Figure 6.8, the grey bars indicate that an extremely large number of performance factors is equal to zero (logarithmic scale does not represent properly that the performance factors are 1×10^{-8}) except one that has performance factor equal to one. It is possible to identify the load path in Figure 6.6 with the largest beams. The structure with maximum complexity has a NSCI equal to 0.9936. As reported in the histogram of Figure 6.8, white bars shows that the performance factors are, more or less, around the order of magnitude 10^{-2}. Few structures have ψ-values larger or smaller.

Throughout the years, quicker and more precise evolution techniques have been developed by mathematicians and physicians. For complexity optimisation, the procedure implemented is based on the Covariance Matrix Adaptation Evolution Strategy (CMA-ES), which has been promoted by Hansen and Ostermeier (1996). Briefly and without claiming to be complete, in order to minimise a nonlinear objective function that is a mapping from search space $S \subseteq \mathbb{R}^n$ to $\mathbb{R}$, the search steps are are taken by stochastic variation by means of a normally distributed random vector that is adjusted following the covariance matrix of the population of parents. The effectiveness of the procedure has been tested and the results are positive in terms of computation time (Hansen and Ostermeier, 2001, Hansen and Kern, 2004). Implementing

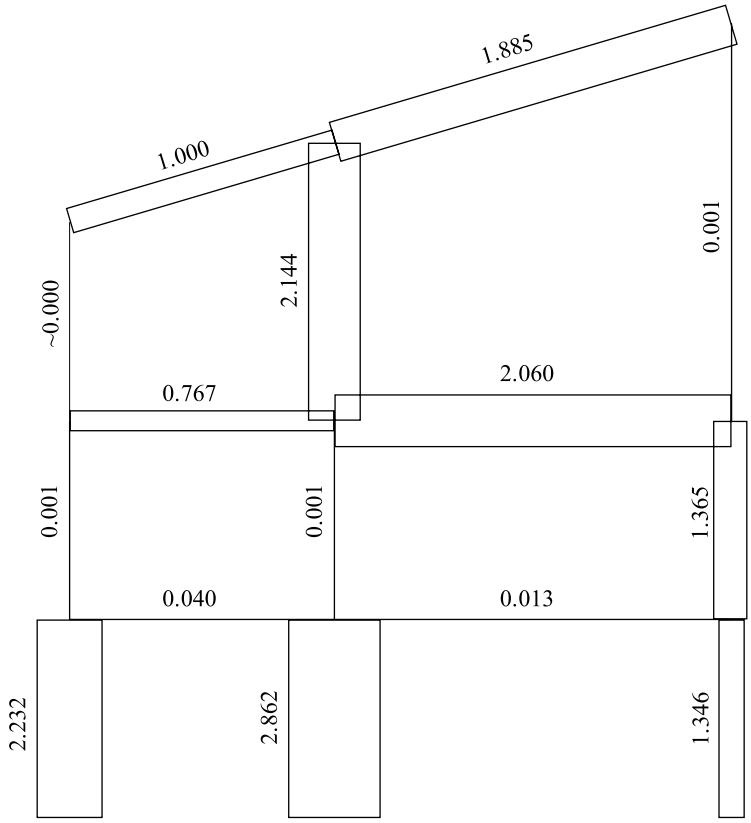

Figure 6.6: Cross-section dimensions for the reference structure of Figure 6.1 for which the NSCI is minimised (NSCI = 1.6×10^{-6}). The size of the beams (which is reported on each element) is proportional to the value of the multiplier of the reference length, i.e. the size of beam AB which is equal to one (top right of both schemes). The scheme is loaded similarly to the one of Figure 6.7.

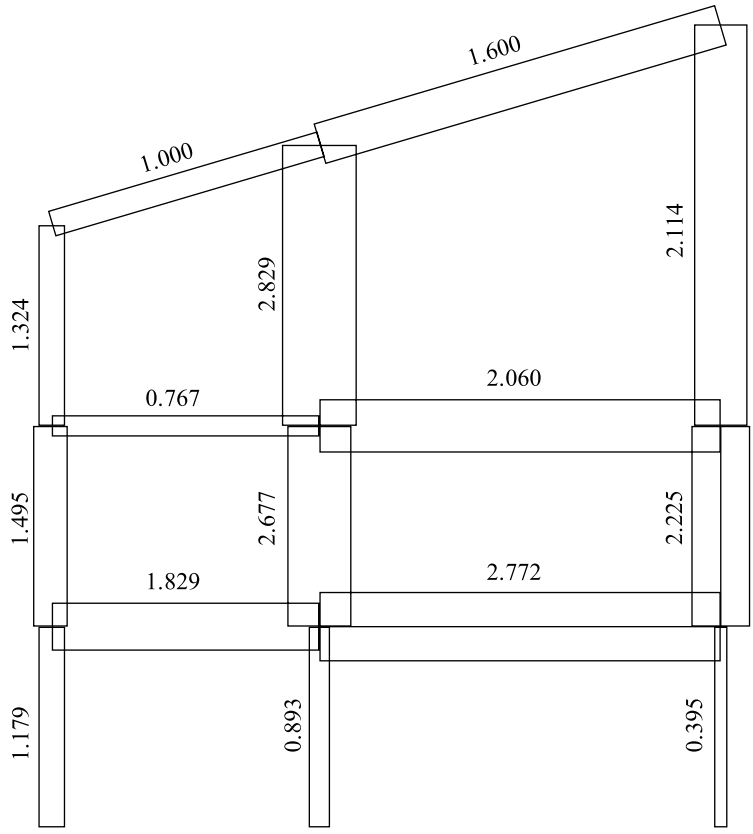

Figure 6.7: Cross-section dimensions for the reference structure of Figure 6.1 for which the NSCI is minimised (NSCI = 0.9936). The size of the beams (which is reported on each element) is proportional to the value of the multiplier of the reference length, i.e. the size of beam AB which is equal to one (top right of both schemes). The scheme is loaded similarly to the one of Figure 6.6.

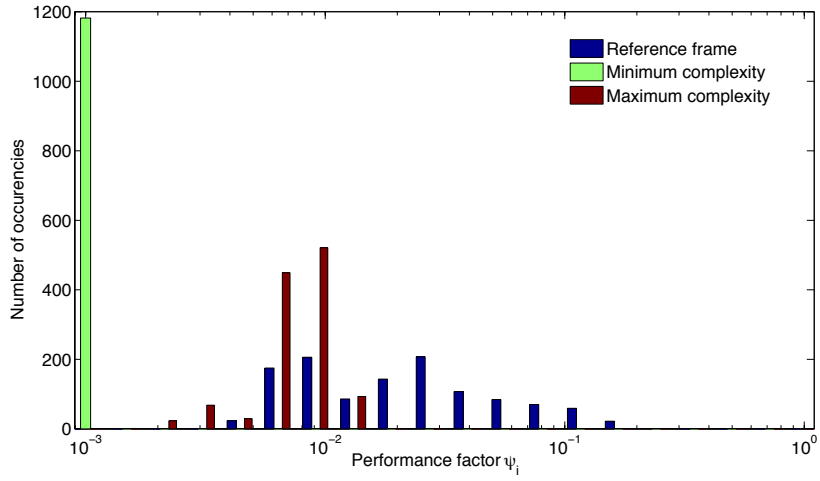

Figure 6.8: Histogram nesting the performance factors of the reference structure (NSCI = 0.9389), the maximum complex structure (NSCI = 0.9936) and the minimum complex structure (NSCI = 1.6×10^{-6}).

the algorithm for solving the problem of complexity maximisation and minimisation, better computational times are recorded. This strategy is suited for large structures requiring large computational effort.

6.4 Discussion on fundamental structures

The present section serves for answering the important question "what a fundamental structure is?". Before that, it is necessary to state some properties of frames once subjected to stiffness variation. In particular, some questions arise: what does happen to a system of rods if the stiffness of one of its elements reduces? How does this reduction influence the work of deformation of the whole structure?

Proceeding step-by-step in the analysis, if a material is linear elastic, e.g. a linear spring, a force, F, required for the elongation of the body is proportional to the variation of distance between the ends of the spring, δ, based on the following relationship

$$F = k\delta. \tag{6.26}$$

In case of a system composed by many springs, this variation is directly linked to the way the bodies are disposed in the system. In this sense, the value of k would reflect the topology of the connections.

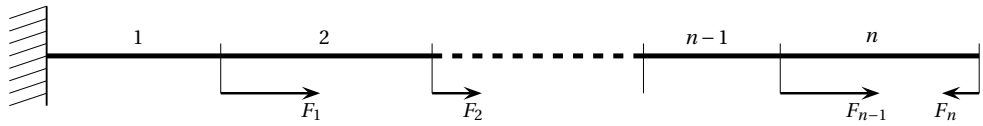

Figure 6.9: Sketch of the rods in series. The forces, F_i, act on right-hand end of each element.

6.4.1 Structural schemes with rods in series

Consider a system of linear elastic rods in series, as shown in Figure 6.9. The scheme is composed by n rods connected the ones to the others. The left-hand side end of rod no.1 is hinged, i.e. the horizontal displacement is set to zero and, consequently, a horizontal reaction is generated once the system is loaded. On the contrary, the right-hand side end of the system, that is the top end of the n-th rod, is free. The system is loaded with horizontal forces, F_i, acting on the right-hand side end of each element.

Further to the application of the loads, the elastic system deforms. It is possible to compute the displacement of rod right-hand side ends as

$$\delta_1 = \frac{1}{k_1}\sum_{i=1}^{n} F_i, \tag{6.27a}$$

$$\delta_2 = \delta_1 + \frac{1}{k_2}\sum_{i=2}^{n} F_i, \tag{6.27b}$$

$$\dots \tag{6.27c}$$

$$\delta_{n-1} = \delta_{n-2} + \frac{1}{k_{n-1}}\sum_{i=n-1}^{n} F_i, \tag{6.27d}$$

$$\delta_n = \delta_{n-1} + \frac{1}{k_n}F_n. \tag{6.27e}$$

where k_i is the axial stiffness of the i-th rod.

In general, the displacement of the right-hand side end of the α-th rod is

$$\delta_\alpha = \frac{1}{k_1}\sum_{i=1}^{n} F_i + \frac{1}{k_2}\sum_{i=2}^{n} F_i + \dots + \frac{1}{k_{\alpha-1}}\sum_{i=\alpha-1}^{n} F_i + \frac{1}{k_\alpha}\sum_{i=\alpha}^{n} F_i, \tag{6.28}$$

and can be rewritten in a compact form as

$$\delta_\alpha = \sum_{j=1}^{\alpha}\left(\frac{1}{k_j}\sum_{i=j}^{n} F_i\right). \tag{6.29}$$

The elastic work of deformation, W_T, is computed by means of Clapeyron's Theorem as half the product between the external forces and the displacements of the points of application. It can be expressed as

$$W_T = \frac{1}{2}F_1\delta_1 + \frac{1}{2}F_2\delta_2 + \cdots + \frac{1}{2}F_{n-1}\delta_{n-1} + \frac{1}{2}F_n\delta_n = \frac{1}{2}\sum_{w=1}^{n}\left(F_w\delta_w\right). \tag{6.30}$$

Substituting Eqn. (6.29) in Eqn. (6.30), it follows

$$W_T = \frac{1}{2}\sum_{w=1}^{n}\left[F_w\sum_{j=1}^{w}\left(\frac{1}{k_j}\sum_{i=j}^{n}F_i\right)\right]. \tag{6.31}$$

Global effect due to a local stiffness variation

The variation of the elastic work of deformation, ∂W_T, due to a variation of the stiffness of the q-th rod, ∂k_q, is now computed. For sake of simplicity, the components of W_T are separated following the position of the forces: first, the forces applied on the left-hand side of the q-th rod; then, the forces applied on the right-hand side of the q-th rod. Therefore, Eqn. (6.31) can be rewritten as

$$W_T = \frac{1}{2}\sum_{w=1}^{q-1}\left[F_w\sum_{j=1}^{w}\left(\frac{1}{k_j}\sum_{i=j}^{n}F_i\right)\right] + \frac{1}{2}\sum_{w=q}^{n}\left[F_w\sum_{j=1}^{w}\left(\frac{1}{k_j}\sum_{i=j}^{n}F_i\right)\right]. \tag{6.32}$$

One can easily note that the first sum does not contain k_q component, while the second contains component $(1/k_q)\sum_{i=q}^{n}F_i$, representing the elongation of the q-th rod due to the loads applied on the system at its right-hand side. This can be observed expanding Eqn. (6.31), which can be rewritten as

$$\begin{aligned} W_T = {} & \frac{1}{2}F_1\left(\frac{1}{k_1}\sum_{i=1}^{n}F_i\right) + \frac{1}{2}F_2\left(\frac{1}{k_1}\sum_{i=1}^{n}F_i + \frac{1}{k_2}\sum_{i=2}^{n}F_i\right) + \cdots + \\ & + \frac{1}{2}F_{q-1}\left(\frac{1}{k_1}\sum_{i=1}^{n}F_i + \cdots + \frac{1}{k_{q-1}}\sum_{i=q-1}^{n}F_i\right) \\ & + \frac{1}{2}F_q\left(\frac{1}{k_1}\sum_{i=1}^{n}F_i + \cdots + \frac{1}{k_{q-1}}\sum_{i=q-1}^{n}F_i + \frac{1}{k_q}\sum_{i=q}^{n}F_i\right) + \cdots + \\ & \frac{1}{2}F_n\left(\frac{1}{k_1}\sum_{i=1}^{n}F_i + \cdots + \frac{1}{k_{q-1}}\sum_{i=q-1}^{n}F_i + \frac{1}{k_q}\sum_{i=q}^{n}F_i + \cdots + \frac{1}{k_n}F_n\right). \end{aligned} \tag{6.33}$$

The partial derivative of the elastic work of deformation with respect to the stiffness variation on the q-th rod of the first term of Eqn. (6.32) is zero. Hence, its final expression is

$$\frac{\partial W_T}{\partial k_q} = \frac{1}{2}F_q\left(-\frac{1}{k_q^2}\sum_{i=q}^{n}F_i\right) + \frac{1}{2}F_{q+1}\left(-\frac{1}{k_q^2}\sum_{i=q}^{n}F_i\right) + \cdots + \frac{1}{2}F_n\left(-\frac{1}{k_q^2}\sum_{i=q}^{n}F_i\right). \tag{6.34}$$

Isolating the common terms, Eqn. (6.34) can be rewritten as

$$\frac{\partial W_T}{\partial k_q} = -\frac{1}{2}\frac{1}{k_q^2}\left(F_q + F_{q+1} + \cdots + F_n\right)\left(\sum_{i=q}^{n}F_i\right), \tag{6.35}$$

which compact expression is

$$\frac{\partial W_T}{\partial k_q} = -\frac{1}{2k_q^2}\left(\sum_{i=q}^{n}F_i\right)^2. \tag{6.36}$$

Since Eqn. (6.36) is composed by squared components, necessarily positive, the following inequality follows

$$\frac{\partial W_T}{\partial k_q} < 0. \tag{6.37}$$

Local effects due to a local stiffness variation

The response of the system in terms of variation of the elastic work of deformation on an arbitrary element due to a stiffness variation on q-th rod is now evaluated. If Saint-Venant's Theory applies, the elastic work of deformation made by the axially loaded α-th rod is

$$W_\alpha = \frac{1}{2}\int_{\ell_\alpha}\frac{N_\alpha^2}{E_\alpha A_\alpha}dz, \tag{6.38}$$

where ℓ_α is the length of the rod, N_α is the axial load on the rod, E_α and A_α are Young's Modulus and cross-section area, respectively.

Supposing the axial force N_α constant throughout the length of the considered element (and similarly Young's modulus and cross-section area, E_α and A_α), Eqn. (6.38) becomes

$$W_\alpha = \frac{1}{2}\frac{N_\alpha^2}{k_\alpha}, \tag{6.39}$$

remembering that $k_\alpha = E_\alpha A_\alpha/\ell_\alpha$.

Considering the α-th rod, the total axial force is equal to the sum of the forces acting on the ends of the elements on the right-hand side of the examined rod, that is

$$N_\alpha = \sum_{i=\alpha}^{n} F_i. \tag{6.40}$$

Hence, the elastic work of deformation on the α-th rod is computed by substituting Eqn. (6.40) into Eqn. (6.39), getting

$$W_\alpha = \frac{1}{2}\frac{1}{k_\alpha}\left(\sum_{i=\alpha}^{n} F_i\right)^2. \tag{6.41}$$

The effects of a local stiffness variation are evaluated through the partial derivative of the work of deformation made by α-th with respect to the variation of stiffness on q-th rod, $\partial W_\alpha / \partial k_q$. Two situations are possible.

- If the stiffness variation occurs on a rod different than the one considered, in other words $q \neq \alpha$, the partial derivative is null, i.e.

$$\frac{\partial W_\alpha}{\partial k_q} = 0. \tag{6.42}$$

- If the considered element is the one on which the stiffness variation occurs, $q = \alpha$, the partial derivative becomes

$$\frac{\partial W_\alpha}{\partial k_\alpha} = -\frac{1}{2}\frac{1}{k_\alpha^2}\left(\sum_{i=\alpha}^{n} F_i\right)^2 \tag{6.43}$$

  and is negative, i.e.

$$\frac{\partial W_\alpha}{\partial k_\alpha} < 0. \tag{6.44}$$

6.4.2 Structural schemes with rods in parallel

Consider a system of linear elastic rods in parallel, as shown in Figure 6.10. The scheme is composed by n rods connected, on their right-hand side ends, to a rigid body on which a force Q is applied. The left-hand side ends are constrained and, thus, their displacements are prohibited. The rigid body is externally restricted in such a way that no rotational effects occur. That is, the point of application of Q is irrelevant.

Following the application of the external force, the system displaces. The force on each rod, N_i, is proportional to its axial stiffness, k_i and its elongation which is equal for all ele-

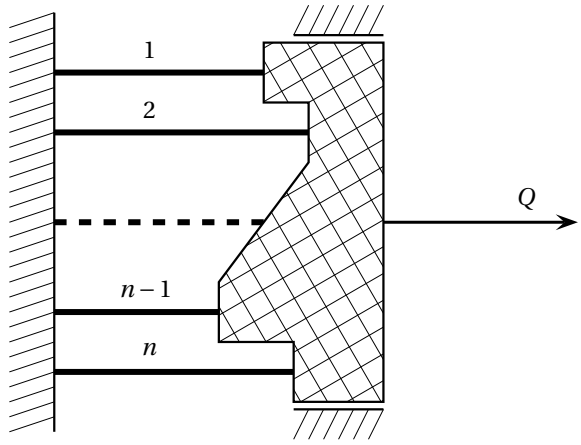

Figure 6.10: Sketch of the rods (thick lines) in parallel. The infinitely stiff element is dashed.

ments since the rigid body cannot deform, δ. That is

$$N_1 = k_1\delta \tag{6.45a}$$
$$N_2 = k_2\delta \tag{6.45b}$$
$$\dots \tag{6.45c}$$
$$N_\alpha = k_\alpha\delta \tag{6.45d}$$
$$\dots \tag{6.45e}$$
$$N_{n-1} = k_{n-1}\delta \tag{6.45f}$$
$$N_n = k_n\delta. \tag{6.45g}$$

In the equilibrium equation, the sum of the axial forces on the rods, $\sum_i N_i$, is equal and opposite to force Q, see Figure 6.11. Summing member contributions of Eqns. (6.45), the total force is equal to

$$Q = \sum_{i=1}^{n} N_i = \delta \sum_{i=1}^{n} k_i. \tag{6.46}$$

The term $\sum_{i=1}^{n} k_i$ is defined as the equivalent stiffness, k_{eq}. Getting the displacements from Eqn. (6.46),

$$\delta = \frac{Q}{\sum_{i=1}^{n} k_i}. \tag{6.47}$$

The elastic work of deformation of the system of rods, W_T, is expressed as

$$W_T = \frac{1}{2} Q\delta = \frac{1}{2} \frac{Q^2}{\sum_{i=1}^{n} k_i}. \tag{6.48}$$

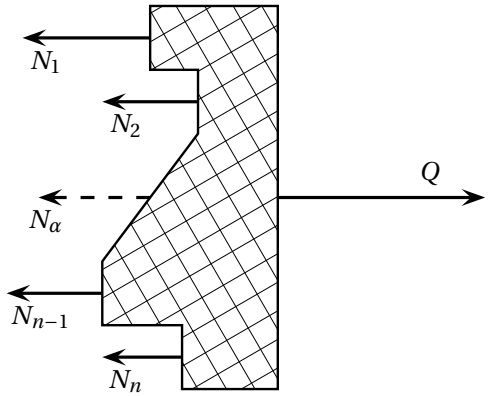

Figure 6.11: Equilibrium of the infinitely stiff body.

Global effect due to a local stiffness variation

The variation of the elastic work of deformation, ∂W_T, due to a variation of the stiffness of the q-th rod, ∂k_q, is computed by differentiating Eqn. (6.48) and is equal to

$$\frac{\partial W_T}{\partial k_q} = -\frac{1}{2}\frac{1}{\left(\sum_{i=1}^{n} k_i\right)^2} Q^2. \tag{6.49}$$

Since the components of the previous expression are squared quantities, the variation is negative, i.e.

$$\frac{\partial W_T}{\partial k_q} < 0. \tag{6.50}$$

Local effects due to a local stiffness variation

The response of the system in terms of variation of the elastic work of deformation on an arbitrary element due to a stiffness variation on q-th rod is now evaluated. As already stated, if Saint-Ventant's Theory hypotheses apply, the elastic work of deformation made by α-th rod can be expressed as a ratio between axial force and axial stiffness, see Eqn. (6.39). Substituting Eqns. (6.45d) and (6.47) into Eqn. (6.39), the following expression is obtained

$$W_\alpha = \frac{1}{2} k_\alpha \frac{Q^2}{\left(\sum_{i=1}^{n} k_i\right)^2}. \tag{6.51}$$

The partial derivation is made considering two different situations, as done in the previous section.

- If the stiffness variation occurs on a rod different than the one considered, in other words $q \neq \alpha$, the partial derivative is

$$\frac{\partial W_\alpha}{\partial k_q} = \frac{1}{2} k_\alpha Q^2 \frac{-2}{\left(\sum_{i=1}^n k_i\right)^3} = -\frac{k_\alpha Q^2}{\left(\sum_{i=1}^n k_i\right)^3} \tag{6.52}$$

  and it is negative, that is

$$\frac{\partial W_\alpha}{\partial k_\alpha} < 0. \tag{6.53}$$

- If the considered element is the one on which the stiffness variation occurs, $q = \alpha$, the partial derivative becomes

$$\frac{\partial W_\alpha}{\partial k_\alpha} = \frac{1}{2} Q^2 \left[\frac{1}{\left(\sum_{i=1}^n k_i\right)^2} + k_\alpha \frac{-2}{\left(\sum_{i=1}^n k_i\right)^3} \right]. \tag{6.54}$$

  The sign of Eqn. (6.54) depends on the quantity into square brackets, which can be rewritten as

$$\frac{1}{\left(\sum_{i=1}^n k_i\right)^2} + k_\alpha \frac{-2}{\left(\sum_{i=1}^n k_i\right)^3} = \frac{1}{\left(\sum_{i=1}^n k_i\right)^3} \left[\sum_{i=1}^n k_i - 2k_\alpha \right]. \tag{6.55}$$

  Since the term $\left(\sum_{i=1}^n k_i\right)^3$ is positive (the stiffness is a positive quantity), Eqn. (6.54) is negative if

$$\sum_{i=1}^n k_i - 2k_\alpha < 0, \tag{6.56}$$

  i.e. if the equivalent stiffness of the system composed by the n except the considered rods, $\sum_{i=1}^n k_i - k_\alpha$, is smaller than the stiffness of the α-th rod,

$$\sum_{i=1}^n k_i - k_\alpha < k_\alpha. \tag{6.57}$$

6.4.3 General considerations

Table 6.4 shows the expressions of $\frac{\partial W_T}{\partial k_q}$, $\frac{\partial W_\alpha}{\partial k_q}$ and $\frac{\partial W_\alpha}{\partial k_\alpha}$ for the previously considered situations. Consider, first, the response of the system to a variation of stiffness of one of its part. Two situation are clearly visible.

- In case of systems with rods in parallel, the global effect is independent on the element that varies its stiffness. The global response depends uniquely on the magnitude of the external force and on the equivalent stiffness , $k_{eq} = \sum_{i=1}^n k_i$.

Scheme	$\dfrac{\partial W_T}{\partial k_q}$	$\dfrac{\partial W_\alpha}{\partial k_q}$	$\dfrac{\partial W_\alpha}{\partial k_\alpha}$
Series	$-\dfrac{1}{2k_q^2}\left(\sum_{i=q}^{n} F_i\right)^2$	0	$-\dfrac{1}{2k_\alpha^2}\left(\sum_{i=\alpha}^{n} F_i\right)^2$
Parallel	$-\dfrac{Q^2}{2\left(\sum_{i=1}^{n} k_i\right)^2}$	$-\dfrac{k_\alpha Q^2}{\left(\sum_{i=1}^{n} k_i\right)^3}$	$\dfrac{Q^2}{2\left(\sum_{i=1}^{n} k_i\right)^3}\left(\sum_{i=1}^{n} k_i - 2k_\alpha\right)$

Table 6.4: Summary of $\frac{\partial W_T}{\partial k_q}$, $\frac{\partial W_\alpha}{\partial k_q}$ and $\frac{\partial W_\alpha}{\partial k_\alpha}$ for systems of rods in series and in parallel.

- In case of systems with rods in series, the global effect depends on the element that varies its stiffness and on the internal forces on it, $\sum_{i=q}^{n} F_i$. If the stiffness of each element is proportional to the axial force on it, i.e.

$$\frac{\left(\sum_{i=1}^{n} F_i\right)^2}{k_1^2} = \frac{\left(\sum_{i=2}^{n} F_i\right)^2}{k_2^2} = \cdots = \frac{\left(\sum_{i=n-1}^{n} F_i\right)^2}{k_{n-1}^2} = \frac{\left(F_n\right)^2}{k_n^2}, \tag{6.58}$$

  an equal response to the system, independently from the element that varies its stiffness, is possible. The amount of variation of the elastic work of deformation increases as much as the element varying its stiffness is close to the restrained end of the system, as can be clearly seen in Figure 6.9.

Before analysing the case of local response to stiffness variation, it is necessary to remember that the total elastic work of deformation, W_T, has to be equal to the sum of the single contributions on each element of the system, i.e.

$$W_T = W_1 + W_2 + \cdots + W_{n-1} + W_n. \tag{6.59}$$

Derivating the previous Eqn. (6.59), the total variation of work of deformation is still the sum of the variations on each element, i.e.

$$dW_T = dW_1 + dW_2 + \cdots + dW_{n-1} + dW_n, \tag{6.60}$$

noting that the variation on one component may be due to something happening in other parts of the structural scheme.

The disparity in the response of the systems in series and in parallel still emerges in the components of Eqn. (6.60). In case of a system of rods in series, there is a direct link between the element that varies its internal energy and the one on which the stiffness variation occurs. The local energetic variation coincides with the variation of the elastic work of deformation

Scheme	$\frac{\partial W_T}{\partial k_q}$	$\frac{\partial W_\alpha}{\partial k_q}$	$\frac{\partial W_\alpha}{\partial k_\alpha}$
Series	< 0	0	< 0
Parallel	< 0	< 0	$\mathrm{sgn}\left(\sum_{i=1}^{n} k_i - 2k_\alpha\right)$

Table 6.5: Sign of the derivatives of the work of deformation in case of stiffness variations in systems in series and in parallel.

of the whole system. In other words, substituting α-index with q-index, Eqn. (6.43) becomes Eqn. (6.36).

On the contrary, in systems with rods in parallel, all the elements compete to the variation of the elastic work of deformation of the whole system. In this sense, it is easy to probe that the sum of the variations on each element coincides with the total variation. In fact, one gets

$$\sum_{\alpha=1}^{n} \frac{W_\alpha}{W_q} = \left\{ \sum_{j=1}^{n} \left[-\frac{k_j Q^2}{\left(\sum_{i=1}^{n} k_i\right)^3} \right] - \left[-\frac{k_\alpha Q^2}{\left(\sum_{i=1}^{n} k_i\right)^3} \right] \right\} + \frac{Q^2}{2\left(\sum_{i=1}^{n} k_i\right)^3} \left(\sum_{i=1}^{n} k_i - 2k_\alpha \right), \tag{6.61}$$

which can be simplified into

$$\sum_{\alpha=1}^{n} \frac{W_\alpha}{W_q} = -\frac{\sum_{i=1}^{n} k_i}{2\left(\sum_{i=1}^{n} k_i\right)^3} Q^2 = -\frac{Q^2}{2\left(\sum_{i=1}^{n} k_i\right)^2}. \tag{6.62}$$

Eqns. (6.62) and (6.49) are identical.

Observing the columns of Table 6.5, it is possible to deduce that, in the majority of cases, the ratio between variation of the elastic work of deformation and variation of stiffness is negative, or null. The only case in which the ratio assumes positive sign is represented by the case of rods in parallel provided that the distribution of stiffnesses across the system respects the constraints of Eqn. (6.57).

6.4.4 Towards a general solution of the problem

The reasoning for a general and comprehensive treatment of the problem, that is the relationship between a variation of stiffness and variation of energy in the elastic system, for any linear elastic structure (with elements both in series ad in parallel) takes ideas from Castigliano's Second Theorem. Then an extension to the problem follows.

Castigliano's Second Theorem: statement and proof

Castigliano's Second Theorem states that

In a structure made by linear elastic material, the first partial derivative of the total internal energy in a structure with respect to the force applied at any point is equal to the deflection at the point of application of that force in the direction of its line of action.

Suppose that a structure is in equilibrium under a system of forces $F_1, F_2, \ldots, F_n$. The application of these forces on the system generate displacements $\delta_1, \delta_2, \ldots, \delta_n$ of the points of application. The forces perform a certain amount of external work, W_e, and generate an equal quantity of deformation energy, U, that is stored in the structure. An infinitesimal increment dF_n of force F_n increments the total deformation energy, which becomes

$$U' = U + \frac{\partial U}{\partial F_n} dF_n. \tag{6.63}$$

Invert the process, i.e. apply first the increment dF_n on the unloaded structure and, then, the system of forces $F_1, F_2, \ldots, F_n$. Since the structure is linear elastic, the total deformation energy does not change from one situation to the other and it is equal to U'.

The force increment, dF_n, previously applied produces and infinitesimal displacement, $d\delta_n$. The corresponding external work performed by dF_n during the application of F_n is a second order quantity, $\frac{1}{2} dF_n d\delta_n$, and is neglected. Analogously, the external work performed by forces $F_1, F_2, \ldots, F_n$ when they are applied on the structure is not modified by dF_n. However, dF_n acts on the same direction as δ_n and a mutual work, $dF_n \delta_n$, is generated. Hence, the external work made by the system of forces on the structure during the loading process is equal to

$$W_e' = W_e + dF_n \delta_n. \tag{6.64}$$

The principle of conservation of the energy states that $W_e' = U'$, i.e.

$$W_e + dF_n \delta_n = U + \frac{\partial U}{\partial F_n} dF_n. \tag{6.65}$$

Since $W_e = U$, it is possible to state that

$$dF_n \delta_n = \frac{\partial U}{\partial F_n} dF_n, \tag{6.66}$$

that can be rewritten as

$$\frac{\partial U}{\partial F_n} = \delta_n, \tag{6.67}$$

that, mathematically, represents Castigliano's Second Theorem.

What does happen if the stiffness varies?

In the present section the following statement is proved.

In a structure made by linear elastic material, a local decrease in stiffness cannot produce other than an increment of the strain energy stored in the system, or can at least leave it unaltered. In any case NO *decrements of strain energy can be recorded.*

The first part of the proof is identical to the one of Castigliano's Second Theorem. That is, suppose that a structure is in equilibrium under a system of forces $F_1, F_2, \ldots, F_n$. The application of these forces on the system generate displacements $\delta_1, \delta_2, \ldots, \delta_n$ of the points of application. The forces perform a certain amount of external work, W_e, and generate an equal quantity of deformation energy, U, that is stored in the structure, i.e.

$$W_e = U. \tag{6.68}$$

Following a variation of stiffness of an element of the structure, e.g. the flexural stiffness of the α-th beam, the deformation energy varies and becomes

$$U' = U + \frac{\partial U}{\partial k_\alpha} dk_\alpha. \tag{6.69}$$

The variation of stiffness, in general, implies a displacement of the points of application of the external forces, which do not vary their magnitude. Because of that, the external work changes,

$$W'_e = W_e + \sum_{i=1}^{n} d\delta_i F_i. \tag{6.70}$$

Due to the stiffness variation on the α-th beam, the i-th displacement varies. For small stiffness variations, the displacement increment (or decrement) can be computed as

$$d\delta_i = \frac{\partial \delta_i}{\partial k_\alpha} dk_\alpha. \tag{6.71}$$

Remembering that stiffness is the link between an external action and the displacement of the corresponding point of application, Eqn. (6.26) becomes

$$d\delta_i = \frac{\partial}{\partial k_\alpha} \left(\frac{F_i}{k_i} \right) dk_\alpha. \tag{6.72}$$

Applying the rules of derivation of composite functions,

$$d\delta_i = \left[\frac{\dfrac{\partial F_i}{\partial k_\alpha} k_i - F_i \dfrac{\partial k_i}{\partial k_\alpha}}{k_i^2} \right] dk_\alpha. \tag{6.73}$$

Since the external actions are constant throughout the stiffness variation process, the term $\frac{\partial F_i}{\partial k_\alpha}$ is null. Substituting Eqn. (6.73) into Eqn. (6.70), the following expression is got

$$W'_e = W_e + \sum_{i=1}^{n} \left(-\frac{F_i}{k_i^2} \frac{\partial k_i}{\partial k_\alpha} F_i \right) dk_\alpha. \tag{6.74}$$

The principle of conservation of the energy states that $W_e' = U'$, i.e.

$$W_e + \sum_{i=1}^{n} \left(-\frac{F_i^2}{k_i^2} \frac{\partial k_i}{\partial k_\alpha} \right) dk_\alpha = U + \frac{\partial U}{\partial k_\alpha} dk_\alpha. \tag{6.75}$$

Since $W_e = U$, it is possible to state that

$$\frac{\partial U}{\partial k_\alpha} = -\sum_{i=1}^{n} \left(\frac{F_i^2}{k_i^2} \frac{\partial k_i}{\partial k_\alpha} \right). \tag{6.76}$$

Stiffness k_i is the sum of many terms, as can be shown in the assembly procedure in finite element methods. Because force and displacement are concomitant, the contributions for stiffness k_i are positively defined, that is

$$k_i = k_{i,1} + k_{i,2} + \cdots + k_{i,\alpha} + \cdots + k_{i,m-1} + k_{i,m}, \tag{6.77}$$

where $k_{i,j}$ is the contribution to the i-th stiffness due to j-th beam. Because of the addition property of Eqn. (6.77), a variation in one of the addends produces a concomitant variation in k_i. In other words, the sign of the variation is equal, e.g. a decrease of $k_{i,2}$ produces a decrease of k_i. The following can be stated

$$\frac{\partial k_i}{\partial k_\alpha} \geq 0. \tag{6.78}$$

Therefore, Eqn. (6.76) is negative or, at least, zero, i.e.

$$\frac{\partial U}{\partial k_\alpha} \leq 0. \tag{6.79}$$

The case in which the previous expression is null rises if the contribution to the i-th stiffness of the α-th element is null, i.e. $k_{i,\alpha} = 0$.

6.4.5 What is a fundamental structure?

As a result of the simple observations and the proof reported in the present chapter, as much as the stiffness of one element of the structure reduces, the internal energy of the system increases.

The structural scheme with an arbitrary degree of static indeterminacy, during the stiffness reduction process, turns into a similar one with lower degree of static indeterminacy. In graph theoretical fields, this procedure is something similar to pass from a graph (representing the original scheme) to a one of its spanning subgraphs (i.e. the result of the maximum possible reduction of the stiffness on one element of the scheme – $EJ = 0$, coinciding with element removal).

Since the elimination of one element of the scheme coincides, ideally, with the progressive decrease of its stiffness to zero, the total work of deformation tends to increases or, at least, to remain unchanged, but never decreases, as proved.

Thus, it is possible to imagine a fundamental structure as one of the possible configurations after the removal of a $\mathcal{C}$ number of elements in such a way that the statically indeterminate scheme becomes statically determinate.

That is, the "fundamental structures" introduced in Chapter 5 are nothing but the possible ultimate situations that a structural system can experience in term of damage, intended as stiffness reduction, or element removal, of its members. Since the framework for analysing the complexity of a frame considers the external loads applied only on the nodes, it does not matter where the cuts of Figure 5.3 are made, neither if the whole element is removed, since both situations are equivalent (for equilibrium no forces act on the halved element).

Chapter 7

Damage on frame structures[1]

The damage can be considered as an unplanned variation of the properties (Mises, 1923) or of the geometry of one or more parts of a structure, which entails a weakening and, usually, negative consequences. The methods usually used in the evaluation of damage on a structure consider its static or dynamic (Andreaus et al., 2007, Andreaus and Baragatti, 2009, Roveri and Carcaterra, 2012) response, or both (Irschik, 2002). Previous researches shown that the former is more sensitive to damage than the latter (Hjelmstad and Shin, 1997) and stressed the fact that the instrumental equipment for static measures is economic and easy to install (He and Hwang, 2007, Wang et al., 2001). Anyhow, the interpretation of deflection, rotations and strains is not straightforward for a direct evaluation of the health of the structure (Housner et al., 1997). The main problems in the usage of static data rise when the damage acts on an element that has no or fairly little contribution to structural deformation under a certain load case. Wang et al. (2001) spoke about "concealed damage" and suggested an optimisation of the loading scheme according to a pre-analysis. In the same manner, He and Hwang (2007) considered two different load cases in their damage simulations.

The response of the structure, under its elastic phase, is a function of the distribution of stiffnesses and the position and magnitude of the external loads. In structures with high degree of static indeterminacy, e.g. frames, the overall behaviour is determined by the contribution of all the elements belonging to the scheme. For example, in a three stories frame subjected to vertical loads and horizontal wind forces, the actions at the foot of one of the columns are highly dependent upon the way the stiffnesses are distributed on the whole structure, rather than on the neighbourhood of the column under consideration. The distribution of stiffnesses on the frame has its main result in the presence of a non-trivial way with which the loads are transferred from the elevation to the foundation (Ghali and Neville, 1997).

In parallel, the presence of various load paths is a strategy for ensuring the robustness

[1]The introduction of the chapter is part of a publication on Zeitschrift für Angewandte Mathematik und Mechanik (Cennamo et al., 2014).

of the structure. Speaking about robustness to deterioration, the most natural definition has been given by Baker et al. (2008) which state that "robustness is taken to imply tolerance to damage from extreme loads or accidental loads, human error and deterioration". As a natural consequence, the robust structure may not be prone to show the effects of deterioration on one of its elements. On the contrary, in case of damage acting on a part of a statically determined structural scheme, it is generally possible to record an increase in displacements as much as the damage acts. For example, consider Figure 7.1. It represents a statically determinate reinforced concrete structure. The reinforcement of the joint is disposed following the common structural detailing and presents a tension rod embracing the angle of the beam, as represented in detail in the sketch. Because of localised carbonatation, the reinforcement is subjected to environmental attack and its cross section reduces progressively. Since the structure is statically determined, no alternative path exists between the point of application of the force and the feet of the column. As much as the degradation progresses, the rotation of the joint increases and, thus, the end of the horizontal beam moves downward. The damage would be assessed and determined as far as the rotation of the joint or the vertical displacement would have been monitored through the time. Moreover, remember that the total work, expressed as the scalar product of force and displacement vectors, increases progressively.

Consider now the structure depicted in Figure 7.2. It shows a structure similar to the one of the previous example; the only difference is represented by the presence of a vertical rod between the point of application of the force and the joint. As much as the damage progresses on the reinforcements, the resistance of the joint reduces but, despite this fact, the rotation does not increase since the compression force in the rod increases more and more. Ideally, when the bending resistance of the joint is null and a hinge is formed, the compression force in the rod is equal in magnitude to the tension force in the column and its intensity is proportional to the position of the external force and to the inverse of the distance between the vertical elements. The total work of deformation tends to remain constant in the first steps of the deteriorating process and, in the following, highly depends on the resistances in tension and compression of the vertical elements and on their axial stiffness. If the shear resistance of the horizontal beam is sufficient, the system collapse can be prevented. In the case in which one was interested in the progression of damage at the joint, the measurement of the vertical displacement of the point on which the external force is applied would have been ineffective. The best would have been the measurement of the compression force in the rod.

As explained before, the presence of multiple load paths is considered a powerful strategy for preventing large deformations due to local damages and for ensuring the robustness of the structure. In parallel, the robustness of the structure may be a good indicator on the possibility that the structure exhibits large or smaller displacements before the collapse. In these terms, it is important to assess whether a structure is robust or not. To further explain how much difficult can be assessing the progression of damages on a robust structure, shall we consider the structure represented in Figure 7.3. It is a three column-one storey frame on which a uniform load acts on the horizontal deep beam. The system is symmetric, thus, the bending moment in the central column is null: this element is simply loaded with a vertically

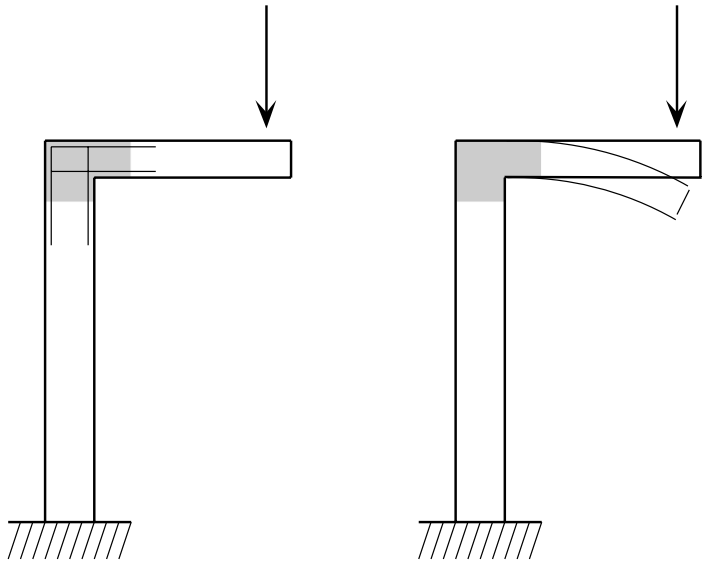

Figure 7.1: A cantilever with an horizontal beam: (a) undamaged structure with the load acting at the top of the horizontal element, (b) effects on the structure after the damage of the joint shaded in grey. As much as the damage progresses, the rotation of the joint and, by consequence, the vertical displacement under the point of application of the load increase.

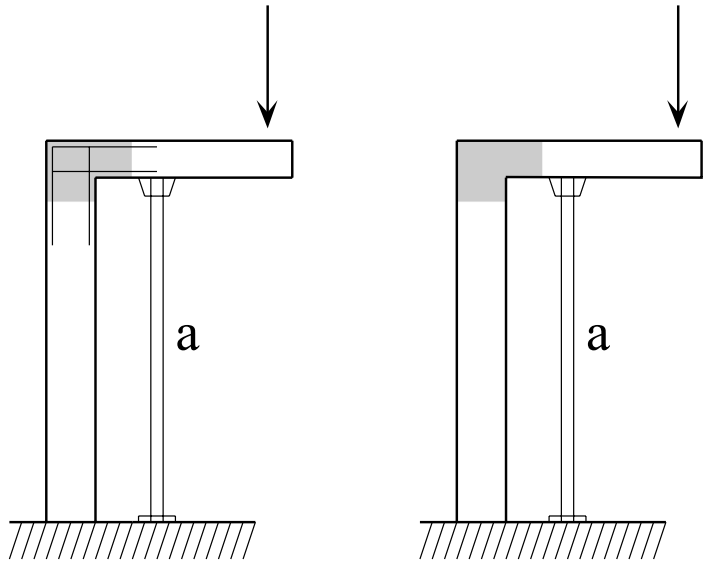

Figure 7.2: A cantilever with an horizontal beam and a vertical rod, **a**: (a) undamaged structure with the load acting at the top of the horizontal element, (b) effects on the structure after the damage of the joint shaded in grey. As much as the damage progresses, the joint exhibit the rotation of the joint and, by consequence, the vertical displacement under the point of application of the load increases.

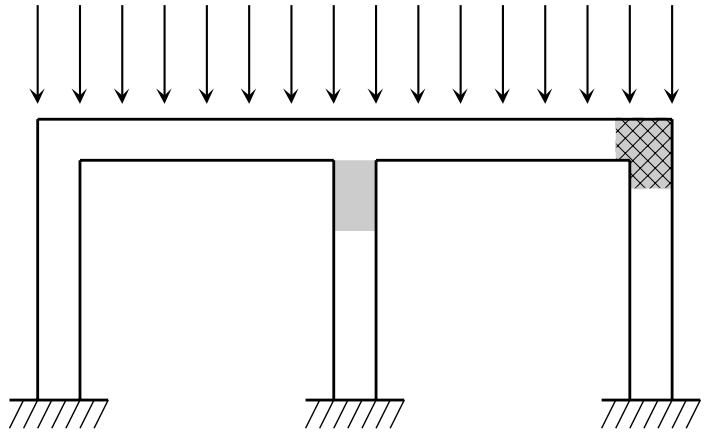

Figure 7.3: A three columns – one storey concrete frame. Two different damages are supposed to act, alternatively on the structure. The damage acting on the top right joint (indicated as grey shaded transversal black hatchings represents the first situation. Otherwise, the plain grey area represents the second damage situation.

axial force. The system exhibits various load paths: essentially, damaging progressively one column, the remaining is able to sustain the external actions, i.e. to transfer the loads from the elevation to the foundation. Suppose to monitor the vertical displacement at the two mid-spans of the top beam. In the case in which the damage interests the top right joint, the resisting bending moment at that point reduces and, thus, the bending of the top beam increases, i.e. the mid-span of the right beam moves down. On the contrary, if the damage interests the cross-section of the central column, which is only subjected to axial force, the stiffness reduction is smaller. This is essentially due to the fact that the flexural stiffness is several orders of magnitude higher to the respect to the axial one. Hence, the damage progresses and the system apparently behaves as undamaged. The collapse may occur in two distinct situations: (i) if compressive strength in the central column is exceeded and the element breaks in compression, (ii) if flexural strength is not sufficient for the additional horizontal force acting on the structure and generating bending in the columns.

The previous examples explain clearly that the presence of alternatives in the load paths, and the distribution of stiffnesses in the structure may affect the displacement field in a progressively damaged structure. Similar problems in damage assessment can be expected in those structures that, on the opposite, present distinct parts and reduced interaction, as illustrated in the following section.

7.1 General behaviour of damaged frames[2]

The possibility of designing a structure in the framework of a consequence-based design has been shown to be a proper strategy for ensuring structural robustness. In the following, the robustness of a frame is assessed in the light of the complexity indices previously defined. As seen in the previous sections, for a given loading condition and stiffnesses distribution across the structure, an importance factor can be assigned to each element, see Table 5.5. Let us suppose now to change the topology of the frame by removing one or more elements. The attention is focused now on the effects of that removal. For example, it may happen that the removal of an element with high importance factor would affect the safety of the overall structure. Referring to the structure illustrated in Figure 5.11, a damage acting on element I will imply more severe effects, say collapse, than a damage acting on element III. The susceptibility of a structure towards damage is called robustness. This concept has been already detailed within a probabilistic framework by Baker et al. (2008). Direct consequences of damage, i.e. the ones associated with the initial damage, are compared with the indirect consequences, e.g. propagation towards system failure. The system fails if the damage occurs and propagates, then direct and indirect consequences sum together (Baker et al., 2008). In that sense, the study of collapse propagation plays a fundamental role for understanding such phenomenon (Masoero et al., 2010). Moreover, important considerations should be paid to the capacity of the structure to carry the loads while it is damaged. Design codes prescribe that the structure should be "tied together" in such a way that local collapses are avoided (CEN, 1994). In that sense, the outcomes of the previous sections on resistant mechanisms may be relevant. On the opposite side, compartmentalisation is preferable in certain situations: referring to the terrorist attack against Murrah Federal Building in Oklahoma City in 1995, the local collapse occurred after bomb explosion did not propagate into the remaining part of the structure because of efficient compartmentalisation.

The sources of damage, as presented, can be various: extreme values of design loads, extraordinary loads, i.e. explosions, or deterioration of the structure through environmental processes. In any case, susceptibility of the structure towards damage has to be assessed in order to design it properly and to prevent the consequences of such improbable events. In the following paragraphs, we illustrate how a loaded frame structure behaves when damage acts on one of its elements (beam or column). This is an initial issue for a more detailed analysis on the possibility of increasing robustness of the structure by a specific design strategy, e.g. a consequence-based design, see Section 7.3.

7.1.1 Damage models for structural members

In general, damage occurs when loading conditions are severe: Yao et al. (1986) underlined the fact that structural damage necessarily depends on (i) the material used (steel, reinforced

[2]The present section and the following ones are part of a paper published on International Journal of Solids and Structures (De Biagi and Chiaia, 2013a).

concrete, masonry or wood); (ii) structural configuration and construction (frame, shear wall, etc.); and (iii) loading conditions (static, dynamic). We add to this list (iv) the environmental conditions, which play a fundamental role in aging phenomena. Concrete, in fact, suffers undesirable degrees of change with time because of improper design and construction specifications, errors during the construction, or unexpected environmental conditions (International Atomic Energy Agency, 1998). Sometimes, due to inaccessibility of the direct structural component, this aspect is missed out (e.g. in dams). In particular, referring to buildings, this can be the case of foundations structures that are covered into the ground, or columns that are covered by architectural shedding, and so on. In International Atomic Energy Agency (1998), a summary of the degradation factors (and their relative primary manifestations) that potentially can impact the performance of the basic components of reinforced concrete buildings (i.e., concrete, steel reinforcement, post-tensioning system) is presented. This list can be straightforwardly related to other concrete civil structures. Although operational procedures, which do not relate directly to structural safety, are implemented for detecting ageing effects (International Atomic Energy Agency, 2009), the assessment of structural condition can be achieved by non-destructive techniques. Vibrations of the structure (Cawley and Adams, 1979, Chen, 2000) or acoustic emissions (Carpinteri et al., 2007) can be, for instance, related to the degree of damage.

Damage phenomena on civil structures are various. Because of that, it is difficult to adopt a uniform approach for quantification of structural damage (Yao et al., 1986). In the past, different approaches were suggested. Krätzig and Petryna (2001) observed the effects of damage on the overall structural stiffness: the degradation process proceeds until the stiffness matrix becomes singular and the structure collapse. In that sense, the tangent stiffness matrix, at least along one deformation mode, tends to zero (Krätzig, 1997). Although the choice of a function for structural damage is a challenging task (Petryna and Krätzig, 2005), specific approaches are possible only once damage causes are clearly identified. In order to assess structural robustness with respect to a progressive deterioration of the structural components, two different damage models for structural members are herein proposed. In the following paragraphs, subscript $_1$ refers to Damage Model no.1, while subscript $_2$ refers to Damage Model no.2.

Two degradation models are considered. On one side, damage on the structure acts at the material level (Damage Model no.1). As reported in Lemaître and Chaboche (1994), the phenomenon can be modelled by softening of material strength and/or stiffness. In the present work, the damage variable d_1, varying between 0 and 1, acts on the uniaxial stress-strain relationship as reported below

$$\sigma = (1 - d_1)\, E_{i0}\varepsilon \tag{7.1}$$

where E_{i0} is the Young's modulus of the undamaged i-th elements, σ and ε represent the stress and the strain in the material. For $d_1 = 0$ the element is undamaged, for $d_1 = 1$ the element is totally damaged, thus it is removed.

On the other side, progressive deterioration of material, such as spalling of concrete, or direct damage such as explosion, is considered (Damage Model no.2). Structural damage is now

Element	ℓ [m]	b [m]	h [m]	E [GPa]
1	5.0	0.40	0.60	30
2	5.0	0.40	0.60	30
3	4.0	0.50	0.50	30
4	4.0	0.50	0.50	30
5	4.0	0.50	0.50	30
6	4.0	0.50	0.50	30

Table 7.1: Geometrical and mechanical properties of the frame of Figure 7.4. b and h are the width and the height of the rectangular cross-section, respectively.

defined by means of a damage index d_2 that acts on cross-section area and inertia (Biondini et al., 2008) and varies between 0 and 1, as before. In particular, the damage model supposes that the cross-section of the damaged element reduces as much as the damage extends. Therefore, area and moment of inertia decrease according the following laws

$$\begin{cases} A = A_0 \left(1 - d_2\right)^2 \\ J = J_0 \left(1 - d_2\right)^4 \end{cases} \tag{7.2}$$

where A and J represent the damaged cross-section area and moment of inertia, respectively. A_{i0} and J_{i0} are the undamaged cross-section area and moment of inertia.

7.2 Damage on complex structures: effects of a specific damage

The behaviour of a frame structure under damage is now investigated. A structural scheme similar to the one of Figure 7.4 is analysed. Concrete beams and columns are jointed together with proper reinforcement at nodes. The elements are characterised by the geometrical and material properties reported in Table 7.1. External loads are represented by uniformly distributed loads acting on beams (50 kN/m) and horizontal forces applied to left-hand side nodes (20 kN upon each node). In this simple analysis, dead loads and service loads are considered together. In order to underline the behaviour of the statically indeterminate structure under damage, an elastic analysis is conduced and the effects of member capacity in the overall response of the system are not considered.

Let us suppose that a damage process originates on Element no.5, which is a base column. Both the damage models previously presented are taken into account; comparisons of the results are made. Before going further, few considerations are necessary. First, as much as the damage factor d_1, or d_2, increase from 0 to 1, the response of the structure in terms of bending moment, shear, and axial forces would tend to the situation in which Element no.5 is

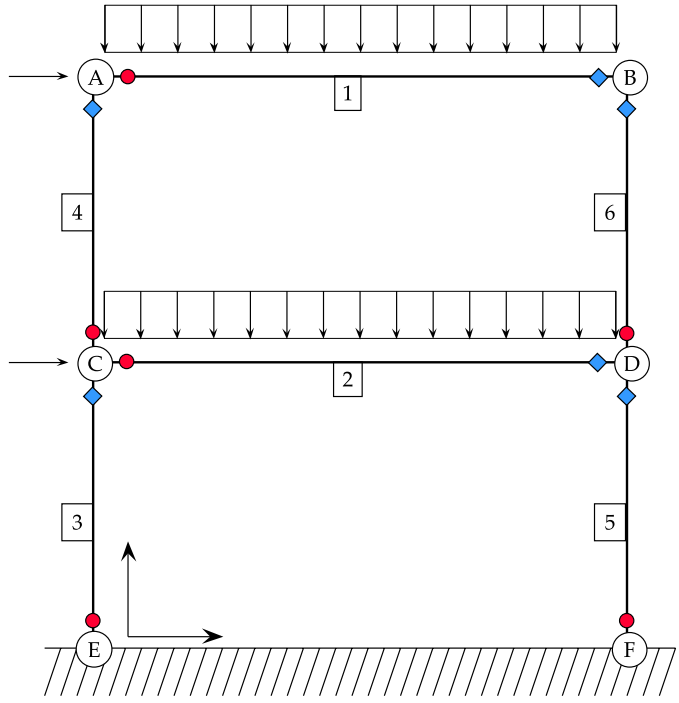

Figure 7.4: A two-stories concrete frame.

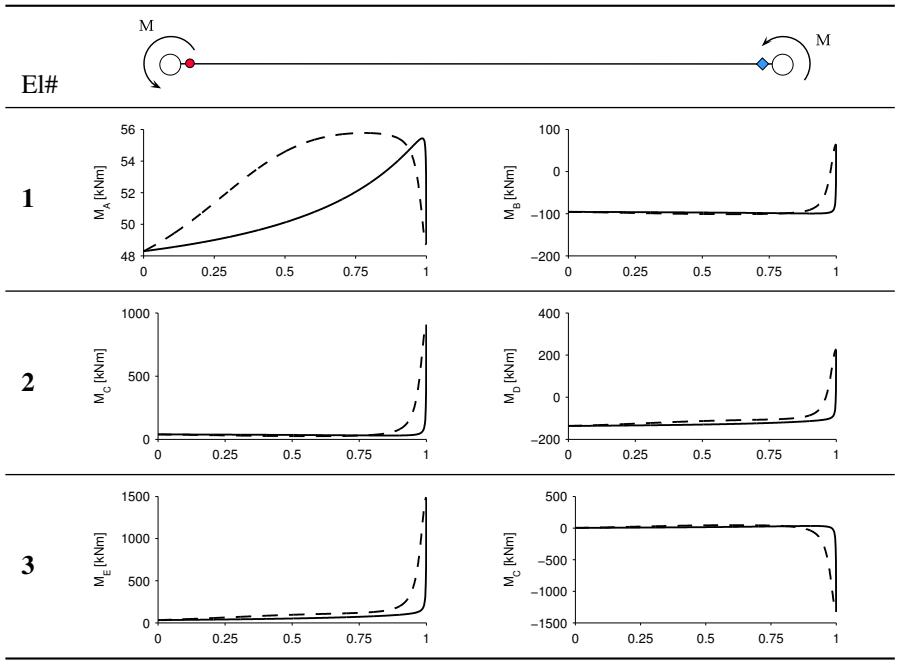

Table 7.2: Bending moments at the nodes of the elements during the damage process acting on Element no.5. Continuous line (–) refers to Damage Model no.1 (damage acting on the Elastic Modulus), dotted line (- -) refers to Damage Model no.2 (damage acting upon the cross-section geometry). On the X-axis the values of the Damage Factor d_1 and d_2 are plotted – Part 1.

absent. Since at maximum damage, that is $d_1 = 1$ or $d_2 = 1$, the same structural situation is implied, Element no.5 removed, the same force distribution upon surviving elements has to be found independently of the chosen damage model. The same consideration has to be made for the initial condition, that is $d_1 = 0$ or $d_2 = 0$, representing the undamaged state of the structure. In addition, we assume that damage is applied slowly to the structure. Therefore, no dynamical effects, which might change the response of the structure, are considered in this first approximation.

The structure is solved by means of the stiffness method. Bending moment and shear forces distribution are monitored as much as the damage propagates in Element no.5. In particular, in Tables 7.2 and 7.3, bending moments at nodes are plotted versus damage variable d_1 or d_2. In parallel, in Tables 7.4 and 7.5, shear forces at nodes are plotted versus damage variable d_1 or d_2. In both cases, plain line refers to Damage Model no.1 while dotted line refers to Damage Model no.2.

As can be seen in Tables 7.3 - 7.5, the choice of the damage model is relevant for the

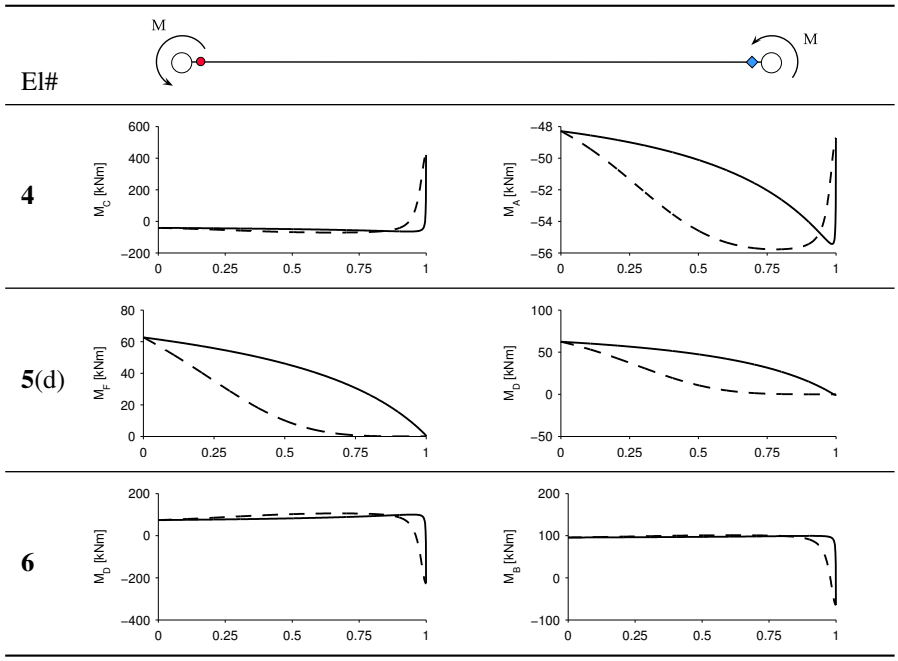

Table 7.3: Bending moments at the nodes of the elements during the damage process acting on Element no.5. Continuous line (–) refers to Damage Model no.1 (damage acting on the Elastic Modulus), dotted line (- -) refers to Damage Model no.2 (damage acting upon the cross-section geometry). On the X-axis the values of the Damage Factor d_1 and d_2 are plotted – Part 2.

response of the frame. Despite the fact that the behaviours seems to be similar, Damage Model no.2, which acts on the size of the damaged element, is generally more conservative than the other one. That is, equal values of bending moment (or shear) at the ends of the elements are usually monitored for $d_1 > d_2$. Although the damage modes give different results, for the initial and final values, that is $d_1 = d_2 = 0$ and $d_1 = d_2 = 1$, the bending moment distributions (and the shear distributions) are perfectly equal. Furthermore, other considerations can be made regarding the trends of each force as long as damage increases upon Element no.5.

- Force distributions do not vary linearly as the damage parameter increases. That phenomenon is independent of the chosen damage model. As can be seen, the values of each force have an initial plateau which extends from $d = 0$ to $d \approx 0.8$. In that range, the amount of variation is relatively small if compared with the trend for $d > 0.8$ (high damage).

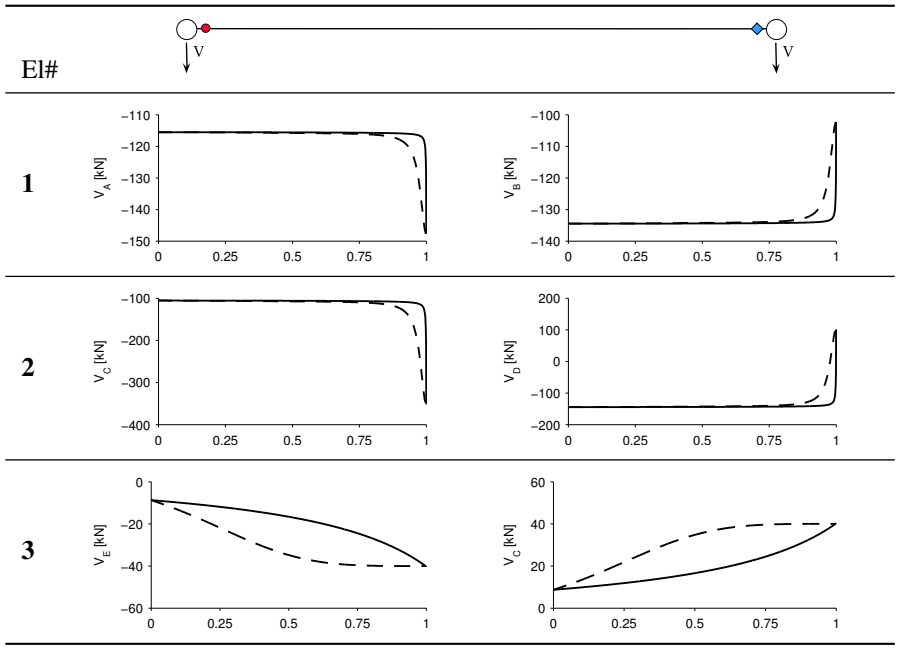

Table 7.4: Shears at the nodes of the elements during the damage process acting on Element no.5. Continuous line (–) refers to Damage Model no.1 (damage acting on the Elastic Modulus), dotted line (- -) refers to Damage Model no.2 (damage acting upon the cross-section geometry). On the X-axis the values of the Damage Factor d_1 and d_2 are plotted – Part 1.

- The diagram of the force versus the damage in Element no.5 is not monotonic. For example, referring to Node A increases as much as the damage process grows. The value reaches a maximum and then decreases. In fact, for $d_2 = 0.78$, M_1 is equal to 55.8 kNm, while the initial and final values are 48.3 kNm and 48.7 kNm, respectively.

In general, until the damage remains small, no direct consequences on the distribution of forces on the elements are recorded. The great changes in the distribution of forces occur when the damage parameter reaches values close to 0.8. In this case, depending on the damage model chosen, either Young's modulus is reduced at the 20% of the original value, or the dimensions of the element are reduced to 20%.

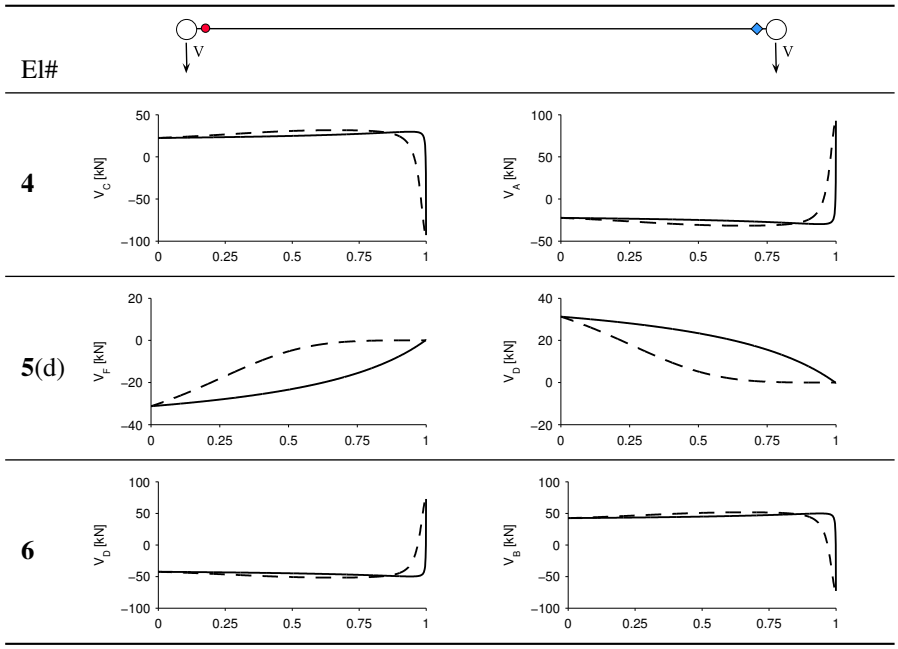

Table 7.5: Shears at the nodes of the elements during the damage process acting on Element no.5. Continuous line (–) refers to Damage Model no.1 (damage acting on the Elastic Modulus), dotted line (- -) refers to Damage Model no.2 (damage acting upon the cross-section geometry). On the X-axis the values of the Damage Factor d_1 and d_2 are plotted – Part 2.

7.3 Damage on complex structures: effects of elements resistance

As reported in the previous sections, some measures of robustness take into account the so-called "damage tolerance". Since the examples proposed in the literature focus on sudden damages, we consider, on the contrary, the effects of a progressive damage on frame structure. For each internal force (e.g. axial force, bending moment or shear), a specific value of damage parameter can be defined. In particular, consider the minimum

$$\hat{d}_i^p = \min \left\{ d^p \left| F_i^p \left(d^p \right) \leq F_i^- \text{ or } F_i^p \left(d^p \right) \geq F_i^+ \right. \right\}, \tag{7.3}$$

where $\hat{d}_i^p$ is the minimum value of the damage d^p on element p for which the value of internal force F_i^p exceeds the bounds F_i^+ and F_i^-. These bounds represent upper and lower limits in the resistance domain of the cross-section. Since each cross-section of the frame should be controlled, the number of monitoring forces F_i^p is arbitrary and reflects the geometry and the

topology of the structure. For example, referring to the frame of Figure 7.4, bending moments, shear and axial forces at the ends of each element are considered, that is, 36 forces in total.

For each element p, the following parameter can be computed,

$$\varpi_p = \min_i \hat{d}_i^p, \tag{7.4}$$

where ϖ_p represents the minimum value of the damage variable $\hat{d}_i^p$ for which any monitored force exceed its bounds. That value, which depends upon the structural response under the external loads and upon the limits of each internal force, serves as a measure of the frame robustness towards the damage on element p. A similar analysis should be conduced for all the elements composing the structure, if eventually subjected to damage.

An example

The methodology presented can be applied to a real case. Considering the frame structure represented in Figure 7.4, whose properties are reported in Table 7.1, the values of ϖ_p are computed for $p = 1, \dots, 6$. As stated before, the number of internal forces is 36, represented by bending moments, shear and axial forces at the ends of each element. In order to analyse the interaction between the forces as soon as the damage increases, e.g. the plots in Tables 7.2 - 7.5, variable bounds can be considered. That is, once a limit value B_i is defined, upper and lower bounds for each force F_i are computed as follows.

$$\begin{cases} F_i^+ = F_i\left(d^p = 0\right) + B_i \\ F_i^- = F_i\left(d^p = 0\right) - B_i \end{cases} \tag{7.5}$$

where $F_i\left(d^p = 0\right)$ represents the value of force i in the undamaged structure. A sketch showing the approach proposed is reported in Figure 7.5.

Values of B_i varying from 1 to 100 kNm, for bending moments, and from 1 to 100 kN, for shear and axial forces, are considered. For each simulation, equal values were assigned to the 36 monitored forces. Results of the robustness analysis are reported in the plots of Figure 7.6 that refer to Damage Model no.1 and no.2, respectively. The values of ϖ are plotted versus the limit value that is B_i. Each line corresponds to the removal of the corresponding element. Some considerations can be drawn.

- The results obtained with Damage Model no.2 are more conservative than those with Damage Model no.1. This behaviour reflects in the calculation of ϖ_p.
- The structure behaves differently depending on the choice of the damaged element. When damage acts on beams, e.g. on elements no.1 and 2, usually larger values of ϖ are obtained than the cases when the damage acts on columns. Both damage models show similar behaviour.

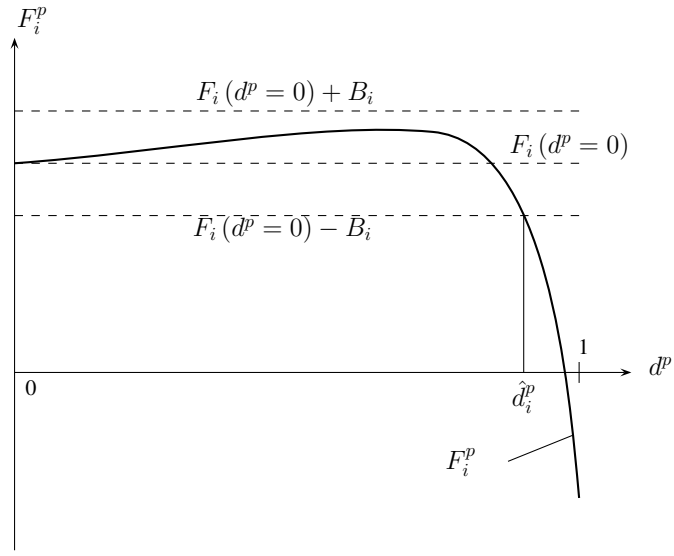

Figure 7.5: Sketch of the variable bounds: δ_i^p is the value of d^p for which $F_i^p\,(d^p)$ exceeds the bounds represented by $F_i\,(d=0)\pm B_i$.

- In both plots of Figure 7.6, curves referring to the removal of elements no.3 and 5 present some linear parts. That response is due to the interaction between the main resisting mechanisms composing the frame, as illustrated in the previous section of this paper.

- For any damaged element, there are values of B_i for which ϖ reaches a maximum and is constant. In that sense, once this value is reached, any increase of the bounds, that means an increase of the element capacity, would increase the robustness of the structure. This aspect is fundamental in design of the structure, as highlighted in the conclusions of this work.

As a preliminary result, it is possible to increase the robustness of the frame with respect to a specific damage by assigning a proper value of the bounds of the internal forces. A variation of B_i implies that the values of ϖ tend to 1. The plateau in the values of the forces, as shown in Tables 7.2 - 7.5, can be attributed to the capacity of the frame to redistribute the single-element damage to the rest of load paths in the structure.

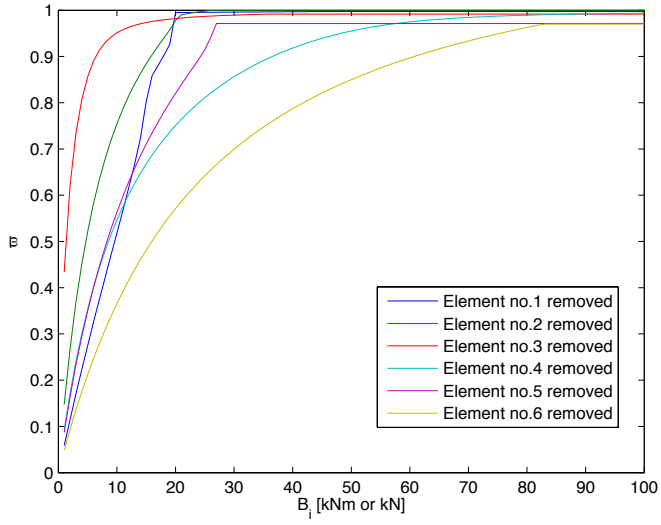

(a) Damage Model no.1

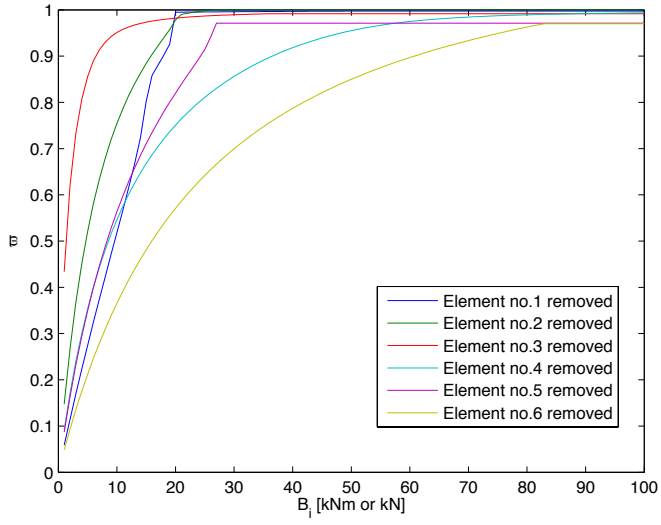

(b) Damage Model no.2

Figure 7.6: ϖ_p values for the damage acting on different elements at different values of the bound B_i. Damage Model no.1 analysis is illustrated in left-hand side plot; on the contrary Damage Model no.2 analysis is illustrated in right-hand side plot.

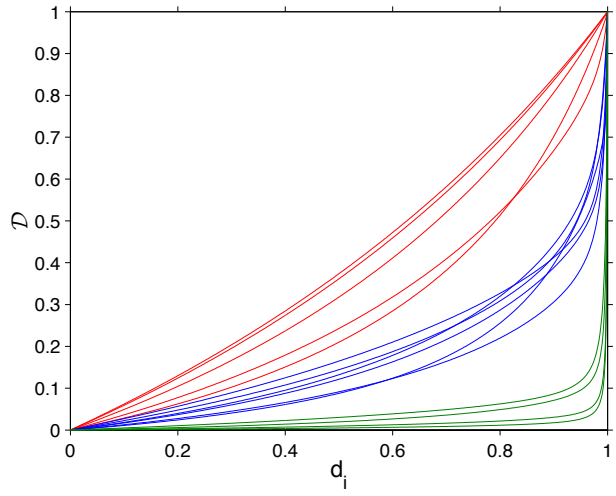

Figure 7.7: Values of parameter $\mathcal{D}$ for different element removal: red curves refer to elements AB, DE, EF, GH, HI removal, blue curves refer to elements AD, DG, DJ, BE, EH, HK removal, green curves refer to elements BC, CF, FI, IL removal.

7.4 Damage on complex structures: effects of complexity[3]

The effects of damage on the structure generate different behaviours. Following the metrics introduced by Biondini and Restelli (2008), in order to evaluate the impact of the damage progression on the structure, for the damage progression on each element i, a parameter $\mathcal{D}_i$ is formulated as

$$\mathcal{D}\left(d_i\right) = \left\{ \frac{W_d - W_0}{W_1 - W_0} \right\} \tag{7.6}$$

where W_d is the work of deformation computed at a value of damage variable equal to d_i, W_1 and W_0 are the work of deformation at $d_i = 1$ and $d_i = 0$, respectively. As a matter of evidence, W_0 is equal to W_{in} since the original structure is in an undamaged state. $\mathcal{D}_i$ ranges from 0, for the undamaged structure, to 1, when the damaged element is removed. In this section, the damage acts exclusively on material Young's Modulus, as explained before. Details on the differences between the two damage models are detailed in the following.

Consider the frame structure sketched in Figure 6.1 on which the load-set reported in Eqns. 6.1 is applied. Figure 7.7 plots the values of η for the 15 beams damaged alternatively. As reported, three different behaviours are shown. The progressive damage on elements AB,

[3]The present section is part of the proceedings of XXI AIMETA conference hold in Torino (De Biagi et al., 2013).

DE, EF, GH, HI (red lines in Figure 7.7), the progression of damage implies a proportional increase of the work of deformation from the initial value (undamaged scheme) to the final one (damaged). The previous behaviour, in other words, refers to all the horizontal beams except element BC. On the contrary, the progressive damage on elements AD, DG, DJ, BE, EH, HK, i.e. central and left-hand side columns, is plot with blue lines and a variable proportionality is clearly visible. Finally, the progressive damage on beam BC and on the right-hand side columns, in green in Figure 7.7, does not affect the overall behaviour of the structural scheme as long as the damage does not exceed a limit value, which is relatively close to 0.9.

In the following, the effects of complexity are taken into account and structures with different complexity are compared. Considering the two limit cases represented by the structural schemes of Figures 6.6 and 6.7, in which the NSCI-value is targeted to the minimum and to the maximum, respectively, the same damage analysis is performed. Figures 7.8 shows the values of $\mathcal{D}$ as a function of d_i.

In the case of minimum complexity, Figure 7.8(a), the scheme is essentially represented by beams AB, BC, BE, DE, EF and by columns BE, FI, IL, GJ, HK. The progressive damage on one of the previously listed elements entails a proportional increase of the work of deformation. The damage acting on the remaining elements, which have cross section size roughly null, does not affect the work performed by the loaded scheme. A totally different behaviour is shown in the case of maximum complexity, Figure 7.8(b). The curves are distributed uniformly in the bottom right of the plot. Note that there is still a curve for which there is a linear proportionality between the progress of damage and the increase of work of deformation. This curve corresponds to the damage on element AB and EF, beams that seem to play a relevant role in the transfer of loads to the foundation node.

Another important aspect to highlight is the fact that $\mathcal{D}$-curves refer to normalised values. The absolute values at $d = 1$ (and $\mathcal{D} = 1$) are reported in Table 7.6 for the three study cases. There are cases in which the removal of elements causes larger effect on the structure. For example, referring to the minimum complexity structure whose damage effects are proposed in the second column of Table 7.6, the suppression of elements belonging to the most effective (and unique) load path entails large increases in the work of deformation (values in round brackets). In parallel, the removal of elements not belonging to the most effective load path, does not involve an increase in work of deformation.

Since the effects of element removal play a fundamental role in the design of a "damage tolerant" structure, the complex and nonlinear behaviour that emerges from the plots of Figure 7.7 and Figures 7.8 gives an idea about the fact that the structure is not robust to progressive damages, as detailed below.

Suppose to monitor a real frame structure. The instrumentation installed is able to measure differential displacements that are supposed to be indicators of damage acting on the frame. It can be demonstrated that the reduction of stiffness on an element of the frame presupposes the increase of the global work of deformation of the structure. Therefore, since the work of deformation on the structure increases, without a change on the magnitude of the nodal loads, the displacements have necessarily to increase. What emerges from the analysis performed is

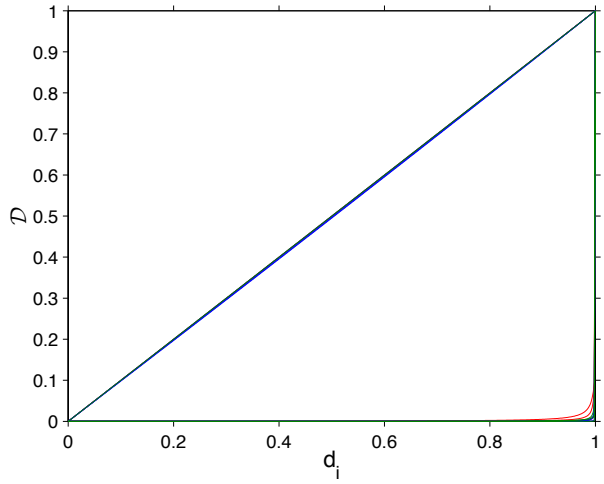

(a) Minimum complexity scheme

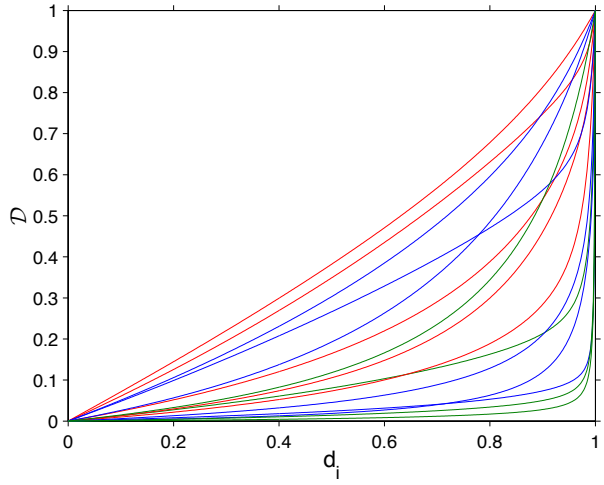

(b) Maximum complexity scheme

Figure 7.8: Values of parameter $\mathcal{D}$ for different element removal. The color of the curves is identical to the one of Figure 7.7. See Section 6.3 for the shape of the two schemes.

Rem.	Normalised Structural Complexity Index (NSCI)					
Element	1.6×10^{-6}		0.9389		0.9936	
Original	36.13		23.00		9.55	
AB	16524	(457.3)	26.15	(1.14)	9.72	(1.02)
BC	9960	(275.7)	33.14	(1.44)	10.32	(1.08)
DE	9943	(275.2)	30.06	(1.31)	10.74	(1.12)
EF	59464	(1645.8)	25.49	(1.11)	9.59	(1.00)
GH	36.13	(1.0)	30.04	(1.31)	17.34	(1.82)
GI	36.19	(1.0)	27.63	(1.20)	10.58	(1.11)
AD	36.13	(1.0)	29.42	(1.28)	12.89	(1.35)
DG	36.15	(1.0)	26.23	(1.14)	9.68	(1.01)
GJ	881.79	(24.4)	31.92	(1.39)	29.25	(3.06)
BE	258870	(7165.0)	29.95	(1.30)	10.94	(1.15)
EH	36.13	(1.0)	34.14	(1.48)	12.12	(1.27)
HK	267.54	(7.4)	37.26	(1.62)	13.77	(1.44)
CF	36.13	(1.0)	41.07	(1.79)	12.79	(1.34)
FI	2228945	(61692.4)	46.96	(2.04)	14.95	(1.57)
IL	75194	(2081.2)	66.78	(2.90)	16.14	(1.69)

Table 7.6: The work of deformation after element removal for different schemes. Second column refers to minimum complexity structure, third column to initial structure, fourth column to maximum complexity structure. In round brackets the ratio between the damaged structure ($d = 1$) and the original structure. The values of the works of deformation are expressed in MJ.

that there are three limit situations. The less dangerous is the one for which the damage on the structure does not imply any increase on the work of deformation, and in this sense we refer to the removal of the elements not belonging to the effective load path in the minimum complexity structure. No changes in the work of deformation presuppose no displacement variation and no increase of forces in the residual elements. The most obvious situation is, on the contrary, the one represented by these elements which progressive damage is spotlighted by a progressive increase of work of deformation, i.e. increase of displacements. When the deformation of the structure exceeds a threshold limit, countermeasures shall be implemented to prevent collapse: the damaged element, which is partially damaged but still complete, can be repaired at a low cost. The most dangerous situation is represented by these cases in which the removal of the element presupposes an increase of the work of deformation, but this work of deformation is accumulated on the structure only when the progression of damage is at an advanced stage. Green lines in Figure 7.7 refer to this behaviour. The instrument installed on the frame will not record any sensible variation on the overall behaviour, just as a progressive damage is in act. This last situation is the one less robust since a small increase of the damage may cause the collapse of the structure since there is a sudden variation of the forces across the elements and the stresses on material are larger than the corresponding strengths. This response is likely to be attributed to the redistribution of loads that occurs in statically indeterminate structures. This aspect has to carefully taken into account in the design of frames able to resist to disproportionate actions.

Observing the ratios between the damaged and the undamaged cases, one notes that, as much as complexity increases, the values in the round brackets of Table 7.6 shifts towards one. In other words, the increase in complexity, which relates to uniformity in the performance of the fundamental structures, is able of “uniformity” in the response of the scheme when a damage occur. Is this true, or it is a simple coincidence? The answer to this question is the main issue debated in the following chapter.

Chapter 8

Conclusions

At the end of the previous chapter, an interesting trend in complex structures has been highlighted. The ratio between the works of deformation in the damaged and the undamaged loaded structural scheme is, globally, lower in case of complex structures. This observation relates to the comparative analysis between the scheme with maximum complexity and the reference scheme. Hence, a question arises: is this observation a pure coincidence, or do exist evidences that the impact of element removal is smaller in case of complex structures?

I choose a simple iterative procedure for answering the issue. Consider, once again, the 15-elements structural scheme depicted in Figure 6.1.

1. a random set of cross-section sizes, referring to all the elements of the frame except AB (which is set kept constant to a reference length, as in Section 6.3), is generated. External loads are applied to the scheme;

2. the work of deformation, W_{in}, and complexity of the structure, the NSCI, is computed;

3. alternatively, each element of the frame is removed, and the work of deformation, W_i, is computed on the resulting structure.

4. as expected, referring to the results of Section 6.4, for each damage situation, $W_i \geq W_{in}$. That is, the ratio
$$\nu_i = \frac{W_i}{W_{in}} \geq 1 \tag{8.1}$$
is computed.

The previous steps are repeated 9999 times and, then, the consistency of the set of random structures is 10000.

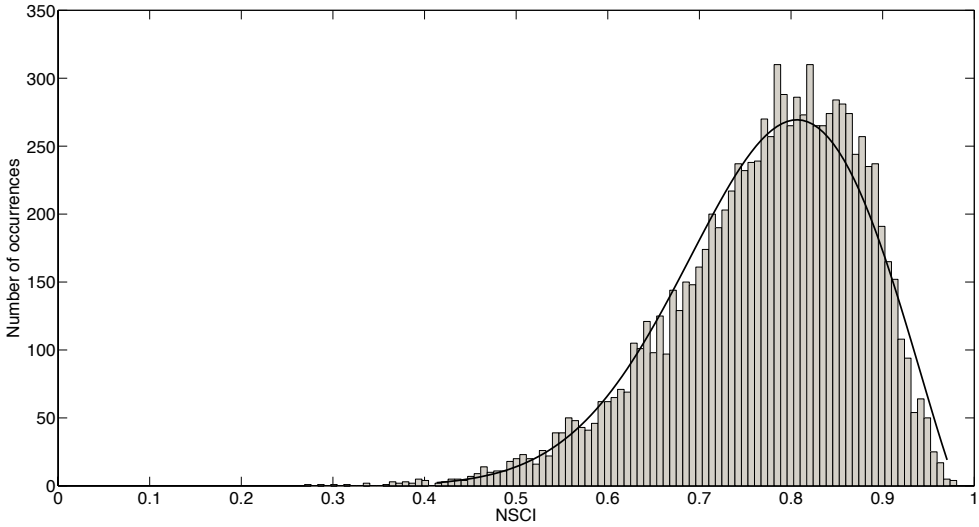

Figure 8.1: Number of occurrences for the random generation of size parameters. The total number of samples is 10000. The black thick line is the Generalised Extreme Value probability distribution that fits the histogram plot. Parameter evaluation of the GeV distribution derives from a maximum likelihood procedure for which the final expression of the distribution is $F(z) = \exp\left\{-\left[1 - 0.47\left(\frac{z-0.75}{0.11}\right)\right]^{2.13}\right\}$.

Various observations can be done. First, the Normalised Structural Complexity Indices derived from the generation of random structures range from 0.2691 to 0.9808. Obviously, structures, which NSCI is outside the previous bounds, do exist, but they were not generated. Counting the cardinality of a subset of structures having the complexity index ranging in a specific interval, Figure 8.1 is obtained. It seems that the associated probability distribution can be classified as an extreme values one. In this situation, considering the random generation, the median value of NSCI is equal to 0.7881.

Since the number of different undamaged schemes is equal to 10000 and the number of possible damage situations, i.e. element removal, is 15, 150000 values of ν_i are computed, ranging between 1 and 10^{13}. That is, there are damage situations that produce extremely high impacts on the scheme: despite their very reduced number, they affect the distribution of values since their magnitude is extremely elevated. Analysing the structural schemes belonging to the range $\mathrm{NSCI} = [0.80; 0.90]$, which are 3719 in number, one discovers that the

$$\min \nu_i = 1.00000008347837,$$

while

$$\max \nu_i = 1658849976505.83,$$

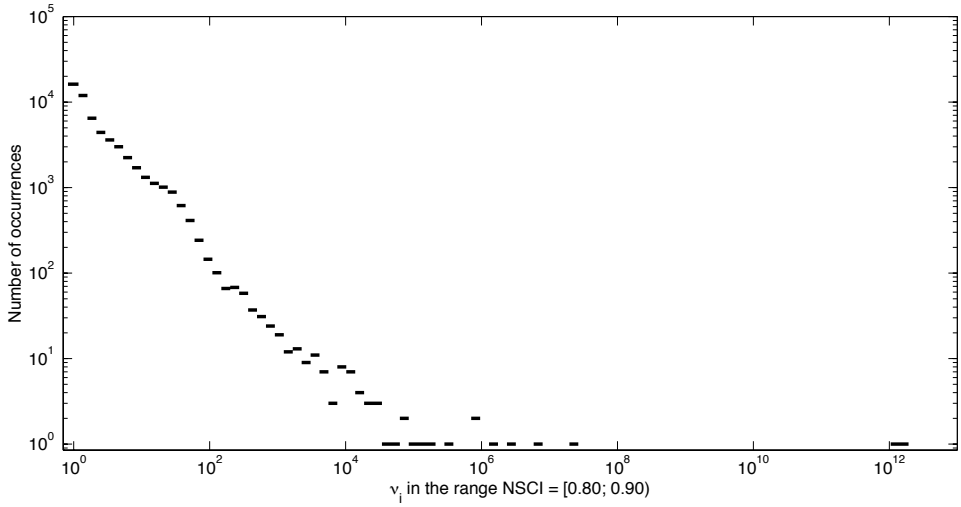

Figure 8.2: Histogram in a log-log scale plot showing the number of damaged structures with a given ν_i. The undamaged structures belong to the range $\mathrm{NSCI} = [0.80; 0.90]$.

i.e. a range of twelve order of magnitude. The histogram of Figure 8.2 shows the number of damaged structures with a given ν_i. Note the logarithmic scale in the ordinates. Observing the previous figure, one notes that as much as the ν_i increases, the number of occurrences diminishes. I therefore consider the set of ν_i to be composed by *outliers*, which are extreme or atypical data values that are notably different from the rest of the data. In presence of such values, the corresponding distribution is skewed. The skewness, K, is a measure of the asymmetry of the data around the sample mean and is computed as

$$K = \frac{E\left(x-\mu\right)^3}{\sigma^3}, \tag{8.2}$$

where μ is the mean of x, σ is the standard deviation of x, and $E\left(t\right)$ represents the expected value of the quantity t. If skewness is positive, the data are spread out more to the right. In case of normal distribution (or any perfectly symmetric distribution) the skewness is zero. For the ν_i in the range [0.80; 0.90), the computed skewness is $K_{[0.8;0.9)} = 171.5$.

In order to analyse the effects of the complexity on the values of ν, i.e. the effects of element removal, all the undamaged structures are grouped into bins following their NSCI, as detailed in Table 8.1.

Since the distributions of ν_i are skewed, the mean of the values is not representative of the distribution. This is a result of such asymmetric probability distribution, in which the

NSCI range	#
$[0.00; 0.10)$	0
$[0.10; 0.20)$	0
$[0.20; 0.30)$	3
$[0.30; 0.40)$	21
$[0.40; 0.50)$	109
$[0.50; 0.60)$	516
$[0.60; 0.70)$	1529
$[0.70; 0.80)$	3303
$[0.80; 0.90)$	3719
$[0.90; 1.00)$	800

Table 8.1: Number of structures with a NSCI ranging in a specific interval. The sum is 10000.

mean is generally 'pulled' in the direction of the tails by the outliers. In this sense, there is another statistical quantity that better describes the results: the median. This is one of the measures of central tendency, which are summary measures that attempt to describe a whole set of data with a single value. The median is the middle value in distribution (when the values are arranged in ascending or descending order). The mode is not used, herein, as a measure of central tendency since the set of data is not nominal.

The values of ν_i are statistically analysed. Consider the set of the fifteen ν_i obtained from the damaged of each of the 10000 undamaged structures. Four statistical parameters are evaluated in the sample of 15: the minimum, the maximum and 50 and 90 percentiles. Obviously, the presence of outliers would affect, locally, the previous parameters. Now, for each set of structures, grouped by the corresponding value of NSCI, the median of the parameters is computed, see Table 8.2. In other words, referring to the range [0.80; 0.90), the median is over a sample of 3719.

The results are plot in Figures 8.3. A clear trend emerges: as much as the complexity increases, the statistical parameter, which relates to the behaviour of ν, decrease. This gives an answer to the issue that raised at the beginning of the chapter: **as much as the complexity increases, the impact of element removal in the loaded structural scheme reduces**.

NSCI range	Min	p_{50}	p_{90}	Max
$[0.00; 0.20)$	——— No samples ———			
$[0.20; 0.30)$	1.0007	1.6152	580.95	1969.9
$[0.30; 0.40)$	1.0002	1.7216	69.638	2924.8
$[0.40; 0.50)$	1.0003	1.8357	76.371	1533.3
$[0.50; 0.60)$	1.0006	1.6722	31.800	552.43
$[0.60; 0.70)$	1.0009	1.6382	20.066	104.97
$[0.70; 0.80)$	1.0027	1.5963	14.012	42.332
$[0.80; 0.90)$	1.0077	1.5820	9.7578	27.005
$[0.90; 1.00)$	1.0140	1.5796	7.7895	22.734

Table 8.2: Medians of minimum, 50 and 90 percentiles and maximum of ν_i for each NSCI range.

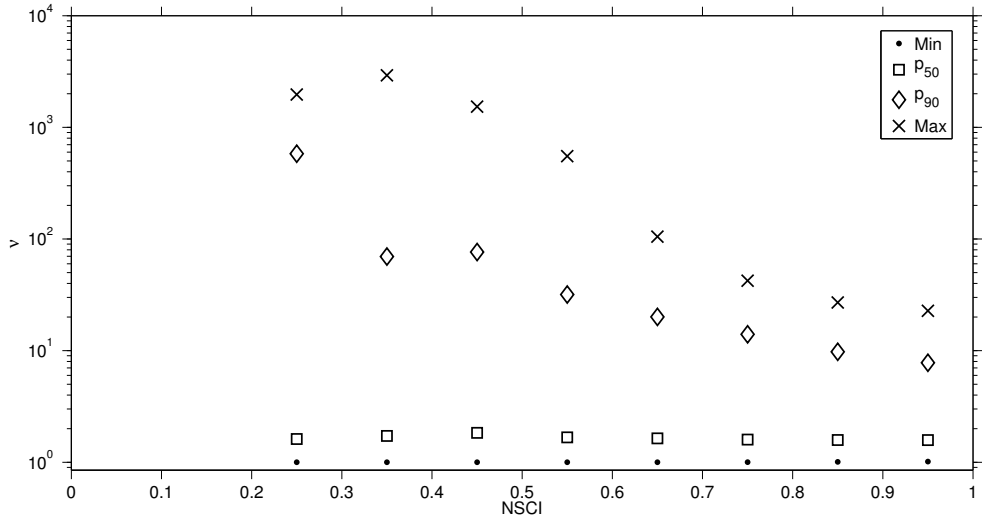

Figure 8.3: Plot of the median of minimum, 50 and 90 percentiles and maximum of ν_i for each NSCI range.

The first part of the dissertation focuses on the strategies Nature implemented and implements in order to survive to ordinary and extreme situations that may occur. Complexity is one of these: evidences of complexity are visible in biological, social and spontaneous systems. The connectedness between the components of the system has been shown to be a powerful way for ensuring the transfer between networks even if nodes are removed. Technology tries to take suggestion of this powerful strategy in order to induce robustness on human-made systems. For example, the World Wide Web was shown to be robust against random attacks, but not to targeted damages.

Complexity and connectedness concepts are implemented in applied sciences, but not in structural engineering. In the second part of this doctoral dissertation, a general framework for analysing complexity of structures was established. The properties of the proposed metric were evaluated both numerically and theoretically. By means of a simplified analysis on systems of rods, the operative definition of fundamental structure was given. Frame structures have been chosen as reference schemes for testing the ideas on connectedness and complexity. In such joined structural systems, the effect of element removal tends to be different, since redistribution of forces within the remaining elements occurs. Certainly, the effect of damage depends on the resistance of the members. Structural complexity was shown to play an important role in the overall behaviour of a damaged structure: as much as the complexity increases, the uniform distribution of load paths across the scheme tends to minimise the effects of random element removal.

References

Abrams, D. P., 2002. Consequence-based engineering approaches for reducing loss in mid-america. Conference on Apr 4, 2002 at Notre-Dame University.

Abrams, D. P., Elnashai, A. S., Beavers, J. E., 2002. A new engineering paradigm: Consequence-based engineering.

Achacoso, T. B., Yamamoto, W. S., 1992. AY's Neuroanatomy of C. elegans for Computation. CRC Press.

Adami, C., Cerf, N. J. J., 1996. Physical complexity of symbolic sequences. Physica D: Nonlinear Phenomena 137 (March), 12.

Agarwal, J., England, J., 2008. Recent developments in robustness and relation with risk. Proceedings of the ICE-Structures and Buildings 161 (4), 183–188.

Agarwal, J., Haberland, M., Holickỳ, M., Sỳkora, M., Thelandersson, S., 2012. Robustness of structures: Lessons from failures. Structural Engineering International 22 (1), 105–111.

Alam, M. S., Wahab, M. A., Jenkins, C. H., 2007. Mechanics in naturally compliant structures. Mechanics of materials 39 (2), 145–160.

Albert, R., Jeong, H., Barabási, A.-L., 1999. Internet: Diameter of the world-wide web. Nature 401 (6749), 130–131.

Albert, R., Jeong, H., Barabási, A.-L., 2000. Error and attack tolerance of complex networks. Nature 406 (6794), 378–382.

Alexander, D., 1993. Natural Disasters. UCL Press.

Alexander, S., 2004. New approach to disproportionate collapse. The Structural Engineer 7 (23), 14–18.

Alexanderson, G., 2006. About the cover: Euler and königsberg's bridges: A historical view. Bulletin of the American Mathematical Society 43 (4), 567–573.

Anderson, M. B., Woodrow, P. J., 1989. Rising from the ashes: development strategies in times of disaster. Westview Press.

Andreaus, U., Baragatti, P., 2009. Fatigue crack growth, free vibrations, and breathing crack detection of aluminium alloy and steel beams. The Journal of Strain Analysis for Engineering Design 44 (7), 595–608.

Andreaus, U., Casini, P., Vestroni, F., 2007. Non-linear dynamics of a cracked cantilever beam under harmonic excitation. International journal of non-linear mechanics 42 (3), 566–575.

ARA, 2003. Progressive collapse analysis and design guidelines for new federal office buildings and major modernization projects. Tech. rep., GSA.

ASCE/SEI, 2010a. ASCE/SEI 7: Minimum Design Loads For Buildings and Other Structures. American Society of Civil Engineers/Structural Engineering Institute.

ASCE/SEI, 2010b. Recommendations for Designing Collapse-Resistant Structures. American Society of Civil Engineers/Structural Engineering Institute, draft.

Ashby, W. R., 1955. An introduction to cybernetics. Taylor & Francis.

Aven, T., Renn, O., 2010. Risk Management and Governance. Concepts, Guidelines and Applications. Springer.

Ay, N., Olbrich, E., Bertschinger, N., 2006. A unifying framework for complexity measures of finite systems. Tech. Rep. 06-08-028, Santa Fe Institute.

Bäck, T., Schwefel, H.-P., 1993. An overview of evolutionary algorithms for parameter optimization. Evolutionary computation 1 (1), 1–23.

Bak, P., Tang, C., Wiesenfeld, K., 1987. Self-organized criticality: An explanation of 1/f noise. Physical Review Letters 59 (4), 381–384.

Baker, J., Schubert, M., Faber, M., 2008. On the assessment of robustness. Structural Safety 30 (3), 253–267.

Ball, P., 2011a. Branches: Nature's patterns: A tapestry in three parts. Vol. 3. Oxford University Press.

Ball, P., 2011b. Flow: Nature's patterns: A tapestry in three parts. Vol. 2. Oxford University Press.

Ball, P., 2011c. Shapes: Nature's patterns: A tapestry in three parts. Vol. 1. Oxford University Press.

Barabási, A.-L., Albert, R., 1999. Emergence of scaling in random networks. science 286 (5439), 509–512.

Bazant, Z. P., Chen, E.-P., 1997. Scaling of structural failure. Applied Mechanics Reviews 50, 593–627.

Bazant, Z. P., Zhou, Y., 2002. Why did the world trade center collapse?-simple analysis. Journal of Engineering Mechanics 128 (1), 2–6.

Beer, S., 1994. Decision and control: the meaning of operational research and management cybernetics. Stafford Beer classic library. John Wiley & Sons.

Below, R., Wirtz, A., Guha-Sapir, D., 2009. Disaster category classification and peril terminology for operational purposes. Tech. rep., Common Accord Centre for Research on the Epidemiology of Disasters (CRED) and Munich Re, Brussels, Belgium and Munich, Germany.

Biello, D., 2011. Anatomy of a nuclear crisis: A chronology of fukushima. Environment 360.

Bigg, N. L., Lloyd, E. K., Wilson, R. J., 1976. Graph Theory: 1736-1936. Oxford University Press.

Biondini, F., Frangopol, D. M., Restelli, S., 2008. On structural robustness, redundancy and static indeterminacy. Crossing Borders, 237–237.

Biondini, F., Restelli, S., 2008. Damage propagation and structural robustness. In: Life-Cycle Civil Engineering: Proceedings of the International Symposium on Life-Cycle Civil Engineering, IALCCE'08, Held in Varenna, Lake Como, Italy on June 11-14 2008. p. 131.

Blinder, P., Shih, A. Y., Rafie, C., Kleinfeld, D., 2010. Topological basis for the robust distribution of blood to rodent neocortex. Proceedings of the National Academy of Sciences 107 (28), 12670–12675.

Bollobás, B., 2001. Random graphs. Vol. 73. Cambridge University Press.

Bontempi, F., Giuliani, L., Gkoumas, K., 2007. Handling the exceptions: robustness assessment of a complex structural system. In: Proceedings of the 3rd International Conference on Structural Engineering, Mechanics and Computation (SEMC 2007), Cape Town, South Africa, 10–12 September 2007. pp. 1747–1752.

Bos, F. P., 2007. Towards a combined probabilistic/consequence-based safety approach of structural glass members. Heron 52 (1/2), 59.

Bos, F. P., Veer, F. A., 2007. Consequence-based safety requirements for structural glass members. In: Proceedings of Glass Processing Days. pp. 57–61.

Bosák, J., 1990. Decompositions of graphs. Mathematics and its applications (Kluwer Academic Publishers).: East European series. Kluwer Academic Publishers.

Briscoe, T., 1997. Robust parsing. In: Survey of the state of the art in human language technology. Cambridge University Press, pp. 121–123.

BRS, 1963. The Collapse of a precast concrete building under construction. London: HMSO.

Butts, R., Schaalje, G., 1997. Impact of subzero temperatures on survival, longevity, and natality of adult russian wheat aphid (homoptera: Aphididae). Environmental Entomology 26 (3), 661–667.

Calinescu, A., 2002. Manufacturing complexity: An integrative information-theoretic approach. Ph.D. thesis, University of Oxford.

Callaway, D. S., Newman, M. E. J., Strogatz, S. H., Watts, D. J., 2000. Network robustness and fragility: Percolation on random graphs. Physical review letters 85 (25), 5468.

Canisius, T. D. G., Diamantidis, D., Holicky, M., Markova, J., Vogel, T., 2011. Philosophy and principles of robustness. In: Canisius, T. (Ed.), Structural robustness design for practising engineers - COST Action TU0601 Robustness of structures. COST: European Cooperation in Science and Technology, pp. 13–30.

Cannon, W., 1932. The Wisdom of the Body. WW Norton & Company, New York.

Carlson, J., Doyle, J., 1999. Highly optimized tolerance: a mechanism for power laws in designed systems. Physical Review E 60, 1412–1427.

Carlson, J. M., Doyle, J., 2002. Complexity and robustness. Proceedings of the National Academy of Sciences of the United States of America 99 (Suppl 1), 2538–2545.

Carpinteri, A., 1994a. Fractal nature of material microstructure and size effects on apparent mechanical properties. Mechanics of Materials 18 (2), 89–101.

Carpinteri, A., 1994b. Scaling laws and renormalization groups for strength and toughness of disordered materials. International Journal of Solids and Structures 31 (3), 291–302.

Carpinteri, A., 2002. Structural Mechanics - a Unified Approach. Taylor & Francis.

Carpinteri, A., Lacidogna, G., Pugno, N., 2007. Structural damage diagnosis and life-time assessment by acoustic emission monitoring. Engineering Fracture Mechanics 74 (1-2), 273–289.

Carter, G., 1944. Network analyzer solution of the equivalent circuits for elastic structures. Journal of the Franklin Institute 238 (6), 443–452.

Castigliano, C., 1875. Intorno all'equilibrio dei sistemi elastici. In: Annali della Reale Accademia delle Scienze di Torino. Vol. 10. pp. 380–422.

Cawley, P., Adams, R. D., 1979. The location of defects in structures from measurements of natural frequencies. The Journal of Strain Analysis for Engineering Design 14 (2), 49–57.

CEN, 1994. EN 1991 (Eurocode 1): Actions on Structures. Comité Européen de Normalisation.

CEN, 2002. EN 1990 (Eurocode 0): Basis of structural design. Comité Européen de Normalisation.

CEN, 2006. Part 1-7: General actions - accidental actions.

Cennamo, C., Chiaia, B. M., De Biagi, V., Placidi, L., 2014. Monitoring and compartimentalized structures. Journal of Applied Mathematics and Mechanics / Zeitschrift für Angewandte Mathematik und Mechanik, in print.

Chen, H., 2000. Assessment of damage in continuum structures based on incomplete modal information. Computers Structures 74 (5), 559–570.

Chiaia, B. M., Masoero, E., 2008. Analogies between progressive collapse of structures and fracture of materials. International journal of fracture 154 (1-2), 177–193.

CIRIA, 1977. Rationalisation of safety and serviceability factors in structural codes. Vol. 63. Construction Industry Research and Information Association.

Clegg, J., 2001. Cryptobiosis - a peculiar state of biological organization. Comp Biochem Physiol B Biochem Mol Biol 128, 613–624.

Colbourn, C. J., Ling, A. C. H., 2003. Graph decompositions with application to wavelength add-drop multiplexing for minimizing sonet adms. Discrete Math. 261 (1-3), 141–156.

Colomer-de Simon, P., Boguñá, M., 2012. Clustering of random scale-free networks. Physical Review E 86 (2), 026120.

Corley, W. G., Sozen, M. A., Thornton, C. H., Mlakar, P. F., 1996. The oklahoma city bombing: Improving building performance through multi-hazard mitigation. Tech. rep., Federal Emergency Management Agency Mitigation Directorate, FEMA Report.

Corotis, R. B., 2003. Socially relevant structural safety. Applications of Statistics and Probability in Civil Engineering, Proc. ICASP 9, 15–26.

Cover, T. M., Thomas, J. A., 2006. Elements of information theory. Wiley Series in Telecommunications and Signal Processing. Wiley-Interscience.

Cranford, S. W., Tarakanova, A., Pugno, N. M., Buehler, M. J., 2012. Nonlinear material behaviour of spider silk yields robust webs. Nature 482 (7383), 72–76.

CRED, 2010. EM-DAT: The OFDA/CRED international disaster data base. centre for research on the epidemiology of disasters.

Crowe, J., Crowe, L. M., 2000. Preservation of mammalian cells-learning nature's tricks. Natural Biotechnology 18, 145–146.

Csete, M. E., Doyle, J. C., 2002. Reverse engineering of biological complexity. science 295 (5560), 1664–1669.

Cutter, S. H., Emrich, C. T., 2006. Moral hazard, social catastrophe: The changing face of vulnerability along the hurricane coasts. The Annals of the American Academy of Political and Social Science 604, 102–112.

Darwin, C., 1859. On the Origin of Species by Means of Natural Selection, or the Preservation of Favoured Races in the Struggle for Life, 1st Edition. John Murray, London.

De Biagi, V., Chiaia, B. M., 2013a. Complexity and robustness of frame structures. International Journal of Solids and Structures 50 (22), 3723–3741.

De Biagi, V., Chiaia, B. M., 2013b. Complexity of structures: a possible measure and the role for robustness. In: Van Mier, J. G. M., Ruiz, G., Andrade, C., Yu, R. C., Zhang, X. X. (Eds.), VIII International Conference on Fracture Mechanics of Concrete and Concrete Structures – FraMCoS-8. pp. 1–9.

De Biagi, V., Chiaia, B. M., 2013c. Robustness of structures: Role of graph complexity. In: IABSE Symposium Report. Vol. 100. International Association for Bridge and Structural Engineering, pp. 136–143.

De Biagi, V., Chiaia, B. M., 2014. Scaling in structural complexity. Complexity.

De Biagi, V., Chiaia, B. M., Placidi, L., 2013. Complexity and robustness of frame structures. In: Lacidogna, G., Carpinteri, A. (Eds.), XXI Congresso AIMETA, Torino, 17-20 settembre 2013. p. 131.

de Solla Price, D. J., 1965. Networks of scientific papers. Science 149, 510–515.

de Solla Price, D. J., 1976. A general theory of bibliometric and other cumulative advantage processes. Journal of the American Society for Information Science 27 (5), 292–306.

Dehmer, M., 2008a. Information processing in complex networks: Graph entropy and information functionals. Applied Mathematics and Computation 201 (1-2), 82–94.

Dehmer, M., 2008b. Information-theoretic concepts for the analysis of complex networks. Applied Artificial Intelligence 22 (7), 684–706.

Dehmer, M., Mowshowitz, A., 2011. A history of graph entropy measures. Information Sciences 181 (1), 57–78.

Derrible, S., Kennedy, C., 2010. The complexity and robustness of metro networks. Physica A: Statistical Mechanics and its Applications 389 (17), 3678–3691.

Diamantidis, D., Vogel, T., 2011. Designing for robustness. In: Structural robustness design for practising engineers - COST Action TU0601 Robustness of structures. COST: European Cooperation in Science and Technology, pp. 65–84.

Diestel, R., 2010. Graph theory. Graduate texts in mathematics. Springer.

Dorogovtsev, S. N., Mendes, J. F. F., Samukhin, A. N., 2000. Growing network with heritable connectivity of nodes. arXiv preprint cond-mat/0011077.

Easterling, D., Meehl, G., Parmesan, C., Changnon, S., Karl, T., Mearns, L., 2000. Climate extremes: Observations, modeling, and impacts. Science 289 (5487), 2068–2074.

Edmonds, B., 1995a. The evolution of complexity. Kluwer, Dordrecht, Ch. 1, pp. 1–18.

Edmonds, B., 1995b. What is complexity?-the philosophy of complexity per se with application to some examples in evolution. The evolution of complexity.

Ellingwood, B. R., 1994. Probability-based codified design: past accomplishments and future challenges. Structural Safety 13 (3), 159–176.

Ellingwood, B. R., 2011. Public perception and acceptance of risk in buildings and other structures. In: Structural robustness design for practising engineers - COST Action TU0601 Robustness of structures. COST: European Cooperation in Science and Technology, pp. 31–40.

England, J., Agarwal, J., Blockley, D., 2008. The vulnerability of structures to unforeseen events. Computers & Structures 86 (10), 1042–1051.

Erdös, P., Rényi, A., 1959. On random graphs i. Publ. Math. Debrecen 6, 290–297.

Erdös, P., Rényi, A., 1960. On the evolution of random graphs. Publ. Math. Inst. Hungar. Acad. Sci 5, 17–61.

Euler, L., 1741. Solutio problematis ad geometriam situs pertinentis. Commentarii Academiae Scientiarum Petropolitanae 8, 128–140.

Felippa, C. A., 2001. A historical outline of matrix structural analysis: a play in three acts. Computers & Structures 79 (14), 1313–1324.

Frangopol, D. M., Curley, J. P., 1987. Effects of damage and redundancy on structural reliability. Journal of Structural Engineering 113 (7), 1533–1549.

Frei, C., Schär, C., 2001. Detection probability of trends in rare events: Theory and application to heavy precipitation in the alpine region. Journal of Climate 14 (7), 1568–1584.

Fu, G., Frangopol, D. M., 1990. Balancing weight, system reliability and redundancy in a multiobjective optimization framework. Structural Safety 7 (2), 165–175.

Galton, F., 1886. Regression towards mediocrity in hereditary stature. The Journal of the Anthropological Institute of Great Britain and Ireland 15, 246–263.

Gell-Mann, M., 1995. What is complexity? Complexity 1 (1), 16–19.

Ghali, A., Neville, A. M., 1997. Structural analysis: a unified classical and matrix approach. Taylor & Francis Francis.

Gilbert, E. N., 1959. Random graphs. The Annals of Mathematical Statistics 30 (4), 1141–1144.

Godsil, C. D., Royle, G., 2001. Algebraic graph theory. Graduate texts in mathematics. Springer.

Goldberg, E., 1995. Rise and fall of modular orthodoxy. Journal of Clinical and Experimental Neuropsychology 17 (2), 193–208.

Gorman, M. R., 1984. Structural redundancy. In: Probabilistic Mechanics and Structural Reliability. ASCE, pp. 45–48.

Grassberger, P., 1986. Toward a quantitative theory of self-generated complexity. International Journal of Theoretical Physics 25 (9), 907–938.

Grave, P. R., Benvenuto, E., 1995. Entre Mecanique Et Architecture - Between Mechanics and Architecture. Birkhaüser Verlag.

Griffith, A. A., 1921. The phenomena of rupture and flow in solids. Philosophical transactions of the royal society of london. Series A, containing papers of a mathematical or physical character 221, 163–198.

Griffiths, H., Pugsley, A., Saunders, O. A., 1968. Report of the inquiry into the collapse of flats at Ronan Point, Canning Town: presented to the Minister of Housing and Local Government. London: HMSO.

Guare, J., 1990. Six Degrees of Separation: A Play. Vintage Books, New York.

Gulvanessian, H., 2002. Designers' Guide to EN 1990 Eurocode: Basis of structural design. Thomas Telford.

Gulvanessian, H., Vrouwenvelder, T., 2006. Robustness and the eurocodes. Structural engineering international 16 (2), 167–171.

Haberland, M., 2007. Progressiver Kollapse und Robustheit (progressive collapse and robustness). Hamburg University of Technology, Structural Analysis and Steel Structures Institute, Diploma thesis (in German).

Hai-Chang, H., 1954. On some variational principles in the theory of elasticity and the theory of plasticity. Acta Physica Sinica 10 (3).

Hajela, P., Lee, E., 1995. Genetic algorithms in truss topological optimization. International journal of solids and structures 32 (22), 3341–3357.

Hamburger, R. O., Foutch, D. A., Cornell, C. A., 2003. Translating research to practice: Fema/sac performance-based design procedures. Earthquake Spectra 19 (2), 255–267.

Hansell, M. H., 2005. Animal architecture. Oxford University Press Oxford.

Hansen, N., Kern, S., 2004. Evaluating the cma evolution strategy on multimodal test functions. In: Parallel Problem Solving from Nature-PPSN VIII. Springer, pp. 282–291.

Hansen, N., Ostermeier, A., 1996. Adapting arbitrary normal mutation distributions in evolution strategies: The covariance matrix adaptation. In: Evolutionary Computation, 1996., Proceedings of IEEE International Conference on. IEEE, pp. 312–317.

Hansen, N., Ostermeier, A., 2001. Completely derandomized self-adaptation in evolution strategies. Evol. Comput. 9 (2), 159–195.

Harding, G., Carpenter, J., 2009. Disproportionate collapse of 'class 3' buildings: the use of risk assessment. Structural Engineer 87 (15–16).

He, R.-S., Hwang, S.-F., 2007. Damage detection by a hybrid real-parameter genetic algorithm under the assistance of grey relation analysis. Engineering Applications of Artificial Intelligence 20 (7), 980–992.

Heisenberg, W., 1927. über den anschaulichen inhalt der quantentheoretischen kinematik und mechanik. Zeitschrift für Physik 43, 172–198.

Henderson, J. C., Bickley, W. G., 1955. Statical indeterminacy of a structure: A study of a necessary topological condition relating to the degree of statical indeterminacy of a skeletal structure. Aircraft Engineering and Aerospace Technology 27, 400–402.

Heylighen, F., Cilliers, P., Gershenson, C., 2006. Complexity and philosophy. arXiv preprint cs/0604072.

Hjelmstad, K. D., Shin, S., 1997. Damage detection and assessment of structures from static response. Journal of Engineering Mechanics 123 (6), 568–576.

Hlaváček, I., 1967. Derivation of non-classical variational principles in the theory of elasticity. Applications of Mathematics 12 (1), 15–29.

Holickỳ, M., Marková, J., Sỳkora, M., 2013. Forensic assessment of a bridge downfall using bayesian networks. Engineering Failure Analysis 30, 1–9.

Holland, J., 1996. Holland, Hidden order: how adaptation builds complexity. Addison Wesley Longman Publishing Co.

Housner, G. W., Bergman, L. A., Caughey, T. K., Chassiakos, A. G., Claus, R. O., Masri, S. F., Skelton, R. E., Soong, T. T., Spencer, B. F., Yao, J. T. P., 1997. Structural control: past, present, and future. Journal of engineering mechanics 123 (9), 897–971.

Huxley, J. S., 1942. Evolution: The modern synthesis. Evolution: The Modern Synthesis.

International Atomic Energy Agency, 1998. Assessment and management of ageing of major nuclear power plant components important to safety: concrete containment buildings. IAEA-TECDOC. IAEA.

International Atomic Energy Agency, 2009. Ageing management for nuclear power plants: safety guide. IAEA safety standards series. International Atomic Energy Agency.

International Strategy for Disaster Reduction, 2009. Global assessment report on disaster risk reduction: Risk and poverty in a changing climate invest today for a safer tomorrow.

International Strategy for Disaster Reduction, 2011. Global assessment report on disaster risk reduction. revealing risk, redefining development.

Irschik, H., 2002. A review on static and dynamic shape control of structures by piezoelectric actuation. Engineering Structures 24 (1), 5–11.

ISO, 1998. ISO 2394: General principles on reliability for structures. Internation Standard Organisation.

Jacquez, J. A., 1985. Compartmental analysis in biology and medicine. University of Michigan Press Ann Arbor.

JCSS, 2011. Probabilistic Model Code. Joint Committee on Structural Safety.

Jeong, H., Tombor, B., Albert, R., Oltvai, Z. N., Barabási, A.-L., 2000. The large-scale organization of metabolic networks. Nature 407 (6804), 651–654.

Jönsson, K. I., Bertolani, R., 2001. Facts and fiction about long-term survival in tardigrades. Journal of Zoology 255 (1), 121–123.

Kaveh, A., 1988. Topological properties of skeletal structures. Computers & Structures 29 (3), 403 – 411.

Kaveh, A., 2004. Structural mechanics: graph and matrix methods. Computational structures technology series. Research Studies Press.

Kaveh, A., 2006. Optimal structural analysis. RSP bird. John Wiley.

Kimura, M., 1968. Evolutionary rate at the molecular level. Nature 217 (5129), 624–626.

Kinali, K., Ellingwood, B. R., 2007. Seismic fragility assessment of steel frames for consequence-based engineering: A case study for memphis, tn. Engineering Structures 29 (6), 1115–1127.

Kirschner, M., Gerhart, J., 1998. Evolvability. Proceedings of the National Academy of Sciences 95 (15), 8420–8427.

Kitano, H., 2004. Biological robustness. Nature Reviews Genetics 5 (11), 826–837.

Kitano, H., 2007. Towards a theory of biological robustness. Molecular systems biology 3 (1), 137.

Knoll, F., Vogel, T., 2009. Design for Robustness. International Association for Bridge and Structural Engineering.

Kolmogorov, A. N., 1963. On tables of random numbers. Sankhyā: The Indian Journal of Statistics, Series A 25 (4), 369–376.

Körner, J., 1973. Coding of an information source having ambiguous alphabet and the entropy of graphs. Transactions of the 6-th Prague Conference on Information Theory, 411–425.

Kouvelis, P., Yu, G., 1997. Robust discrete optimization and its applications. Vol. 14. Springer.

Krakauer, D. C., 2006. Robustness in biological systems: a provisional taxonomy. In: Complex systems science in biomedicine. Springer, pp. 183–205.

Krakauer, D. C., Nowak, M. A., 1999. Evolutionary preservation of redundant duplicated genes. In: Seminars in cell & developmental biology. Vol. 10. Elsevier, pp. 555–559.

Krakauer, D. C., Plotkin, J. B., 2002. Redundancy, antiredundancy, and the robustness of genomes. Proceedings of the National Academy of Sciences 99 (3), 1405–1409.

Krapivsky, P. L., Redner, S., Leyvraz, F., 2000. Connectivity of growing random networks. Physical Review Letters 85, 4629.

Krätzig, W. B., 1997. Multi-level modeling techniques for elasto-plastic structural responses. In: et al., O. D. (Ed.), Computational Plasticity, Proc 5th Intern Conf Part 1, Barcelona: CIMNE. pp. 457–68.

Krätzig, W. B., Petryna, Y. S., 2001. Assessment of structural damage and failure. Archive of Applied Mechanics Ingenieur Archiv 71 (1), 1–15.

Kron, G., 1962. Elastic structures from the point of view of topological network theory. RAAG Memoirs 3, 329–337.

Langefors, B., 1950. Improvement in elastic complex networks for elastic structures. Tech. Rep. TN1, SAAB.

Langefors, B., 1956a. Algebraic methods for the numerical analysis of built-up systems. Tech. Rep. TN38, SAAB.

Langefors, B., 1956b. Algebraic topology and elastic networks. Tech. Rep. TN49, SAAB.

Latora, V., Marchiori, M., 2002. Is the boston subway a small-world network? Physica A: Statistical Mechanics and its Applications 314 (1), 109–113.

Lavell, A., Oppenheimer, M., Diop, C., Hess, J., Lempert, R., Li, J., Muir-Wood, R., Myeong, S., 2012. Climate change: new dimensions in disaster risk, exposure, vulnerability, and resilience. in: Managing the risks of extreme events and disasters to advance climate change adaptation. In: Field, C., Barros, V., Stocker, T. F., Qin, D., Dokken, D., Ebi, K., Mastrandrea, M., Mach, K., Plattner, G.-K., Allen, S., Tignor, M., Midgley, P. (Eds.), Managing the Risks of Extreme Events and Disasters to Advance Climate Change Adaptation. Cambridge University Press, pp. 25–64.

Lemaître, J., Chaboche, J. L., 1994. Mechanics of Solid Materials. Cambridge University Press.

Lind, N. C., 1995. A measure of vulnerability and damage tolerance. Reliability Engineering System Safety 48 (1), 1–6.

Lind, N. C., 1996. Vulnerability of damage-accumulating systems. Reliability Engineering and System Safety 53 (2), 217–219.

Lloyd, S., 2001. Measures of complexity: a nonexhaustive list.

Lomnitz, C., 1988. The 1985 mexico earthquake. In: Natural and Man-made Hazards. Springer, pp. 63–79.

Lu, H., Shi, Y., 2007. Complexity of public transport networks. Tsinghua Science & Technology 12 (2), 204–213.

Mandelbrot, B., 1963. The variation of certain speculative prices. The Journal of Business 36, 394–419.

Manrubia, S. C., Cuesta, J. A., 2010. Neutral networks of genotypes: Evolution behind the curtain. arXiv preprint arXiv:1002.2745.

Masoero, E., Wittel, F. K., Herrmann, H. J., Chiaia, B. M., 2010. Progressive collapse mechanisms of brittle and ductile framed structures. Journal of Engineering Mechanics 136 (8), 987.

Matsumoto, K., Nakayama, T., Sakai, H., Tanemura, K., Osuga, H., Sato, E., Ikeda, J.-E., 1999. Neuronal apoptosis inhibitory protein (naip) may enhance the survival of granulosa cells thus indirectly affecting oocyte survival. Molecular reproduction and development 54 (2), 103–111.

McCabe, T. J., 1976. A complexity measure. IEEE Transactions on Software Engineering 2 (4), 308–320.

McShea, D. W., Brandon, R. N., 2010. Biology's first law: the tendency for diversity and complexity to increase in evolutionary systems. University of Chicago Press.

Menabrea, L. F., 1858. Nouveau principe sur la distribution des tensions dans les systemes elastiques. In: Comptes Rendus Hebdomadaires des Sciences de l'Académie des Sciences. Vol. 48. pp. 1056–1061.

Mendel, G., 1866. Versuche über pflanzenhybriden. Verhandlungen des naturforschenden Vereines in Brunn 4, 3–47.

Meyer, B., 1988. Object-oriented software construction. Vol. 2. Prentice hall New York.

Milgram, S., 1967. The small world problem. Psychology Today 2, 60–67.

Mises, R. V., 1923. Über die stabilitätsprobleme der elastizitätstheorie. ZAMM-Journal of Applied Mathematics and Mechanics/Zeitschrift für Angewandte Mathematik und Mechanik 3 (6), 406–422.

Mitchell, M., 1992. Complexity: The emerging science at the edge of order and chaos. Simon & Schuster New York.

Mlakar, P., Dusenberry, D., Harris, J., Haynes, G., Phan, L., Sozen, M., 2003. Pentagon Building Performance Report. American Society of Civil Engineers.

Moan, T., 2009. Development of accidental collapse limit state criteria for offshore structures. Structural Safety 31 (2), 124–135.

Mowshowitz, A., 1968. Entropy and the complexity of the graphs I: An index of the relative complexity of a graph. Bull. Math. Biophys. 30, 175–204.

Nafday, A. M., 2008. System safety performance metrics for skeletal structures. Journal of Structural Engineering 134 (3), 499–504.

Nafday, A. M., 2011. Consequence-based structural design approach for black swan events. Structural Safety 33 (1), 108–114.

Pearson, C., Delatte, N., 2005. Ronan point apartment tower collapse and its effect on building codes. Journal of Performance of Constructed Facilities 19 (2), 172–177.

Petryna, Y. S., Krätzig, W. B., 2005. Compliance-based structural damage measure and its sensitivity to uncertainties. Computers Structures 83 (14), 1113–1133.

Porter, K. A., 2003. An overview of peer's performance-based earthquake engineering methodology. In: Conference on Applications of Statistics and Probability in Civil Engineering (ICASP9). Civil Engineering Risk and Reliability Association (CERRA) San Francisco, CA, pp. 6–9.

Rechenberg, I., 1965. Cybernetic solution path of an experimental problem. Farnsborough Hants: Ministery of Aviation, Royal Aircraft Establishment 1122.

Reid, S. G., 2000. Acceptable risk criteria. Progress in structural engineering and materials 2 (2), 254–262.

Reissner, E., 1961. On some variational theorems in elasticity. In: Problems of continuum mechanics (Muskhelishvili anniversary volume). SIAM, Philadelphia, Pa., pp. 370–381.

Roveri, N., Carcaterra, A., 2012. Damage detection in structures under traveling loads by hilbert–huang transform. Mechanical Systems and Signal Processing 28, 128–144.

Samuelsson, A. G., 1962. Linear analysis of frame structures by use of algebraic topology. Ph.D. thesis, Chalmer Tekniska Hogskola.

Santa Fe Institute, 2001. Working definitions of robustness. Rs-2001-009 Edition.

Schmieder, C., Kinda, T., Taleb, N. N., Loukoianova, E., Canetti, E., 2012. A new heuristic measure of fragility and tail risks: application to stress testing. Andrews McMeel Publishing.

Schwefel, H.-P., 1965. Kybernetische evolution als strategie der experimentellen forschung in der strömungstechnik. Master's thesis, Technical University of Berlin.

Shannon, C. E., 1948. A mathematical theory of communication. Bell System Technical Journal 27 (July 1928), 379–423.

Simon, H. A., 1962. The architecture of complexity. Proceedings Of The American Philosophical Society 106 (6), 467–482.

Slotine, J.-J. E., Li, W., 1991. Applied nonlinear control. Vol. 199. Prentice Hall New Jersey.

Smuts, J. C., 1926. Holism and evolution. MacMillan.

Sorensen, J. D., Christensen, H. H., 2006. Danish requirements for robustness of structures: background and implementation. Structural engineering international 16 (2), 172–177.

Sornette, D., 2004. Critical phenomena in natural sciences: chaos, fractals, selforganization, and disorder: concepts and tools. Springer.

Starossek, U., 2007a. Disproportionate collapse: a pragmatic approach. Proceedings of the ICE-Structures and Buildings 160 (6), 317–325.

Starossek, U., 2007b. Typology of progressive collapse. Engineering Structures 29 (9), 2302–2307.

Starossek, U., Haberland, M., 2010. Disproportionate collapse: terminology and procedures. Journal of Performance of Constructed Facilities 24 (6), 519–528.

Starossek, U., Haberland, M., 2011. Approaches to measures of structural robustness. Structure and Infrastructure Engineering 7 (7), 625–631.

Starossek, U., Haberland, M., 2012. Robustness of structures. International Journal of Lifecycle Performance Engineering 1 (1), 3–21.

Starossek, U., Wolff, M., 2005. Design of collapse-resistant structures. In: JCSS and IABSE workshop on robustness of structures, building research establishment, Garston, Watford, UK.

Starr, C., 1969. Social benefit versus technological risk. what is our society willing to pay for safety? Science.

Stelling, J., Sauer, U., Szallasi, Z., Doyle III, F. J., Doyle, J., 2004. Robustness of cellular functions. Cell 118 (6), 675–685.

Taleb, N. N., 2007a. The Black Swan: The Impact of the Highly Improbable. Random House Trade Paperbacks.

Taleb, N. N., 2007b. On Robustness and Fragility, Deeper Philosophical and Empirical Reflections. Les Belles Lettres.

Taleb, N. N., 2009. Errors, robustness, and the fourth quadrant. International Journal of Forecasting 25 (4), 744–759.

Taleb, N. N., 2011. A map and simple heuristic to detect fragility, antifragility, and model error. NYU Poly.

Taleb, N. N., 2012. Antifragile: things that gain from disorder. Random House LLC.

Taleb, N. N., Douady, R., 2013. Mathematical definition, mapping, and detection of (anti) fragility. Quantitative Finance 13 (11), 1677–1689.

Tanner, P., 2008. Development of risk acceptance criteria for the design of steel structures. In: EUROSTEEL Conference,. pp. 791–796.

Tempo, R., Blanchini, F., 1996. Robustness analysis with real parametric uncertainty. The Control Handbook, 495–505.

Trbojevic, V. M., 2005. Risk criteria in eu. Risk 10, 5.

Val, U. V., Lectufn, S., Isrljel, T., Israel, H., Val, E. G., 2006. Robustness of frame structures. Structural Engineering International.

Van Der Hofstad, R., 2009. Random graphs and complex networks. Tech. rep., Eindhoven University of Technology.

Van Nimwegen, E., Crutchfield, J. P., Huynen, M., 1999. Neutral evolution of mutational robustness. Proceedings of the National Academy of Sciences 96 (17), 9716–9720.

Venkatasubramanian, V., Li, Y., 2004. Analysis of 1996 western american electric blackouts. Bulk Power System Dynamics and Control-VI, Cortina d'Ampezzo, Italy.

Vrijling, J. K., Van Hengel, W., Houben, R. J., 1998. Acceptable risk as a basis for design. Reliability Engineering & System Safety 59 (1), 141–150.

Vrouwenvelder, T., 2008. Treatment of risk and reliability in the eurocodes. Proceedings of the ICE-Structures and Buildings 161 (4), 209–214.

Wang, X., Hu, N., Fukunaga, H., Yao, Z. H., 2001. Structural damage identification using static test data and changes in frequencies. Engineering Structures 23 (6), 610–621.

Watts, D. J., 2004. Six degrees: The science of a connected age. WW Norton & Company, New York.

Watts, D. J., Strogatz, S. H., 1998. Collective dynamics of 'small-world' networks. Nature 393 (6684), 440–442.

Wen, Y. K., Ellingwood, B. R., Bracci, J. M., 2004. Vulnerability function framework for consequence-based engineering. Mid-America Earthquake Center.

Wheater, S. M., McCue, D. L., 1992. Configuring distributed applications using object decomposition in an atomic action environment. In: International Workshop onConfigurable Distributed Systems. pp. 33–44.

Wiberg, N. E., 1970. System analysis in structural mechanics. Ph.D. thesis, Chalmer Tekniska Hogskola, Goteborg.

Winther, R. G., 2001. Varieties of modules: kinds, levels, origins, and behaviors. Journal of Experimental Zoology 291 (2), 116–129.

Wisner, B., Gaillard, J. C., Kelman, I., 2012. The Routledge handbook of harzards and distaster risk reduction, 1st Edition. Routledge, New York.

Wood, J. G., 2005. Paris airport terminal collapse: lessons for the future. Structural Engineer 83 (5).

Yao, J. T. P., Kozin, F., Wen, Y. K., Yang, J. N., Schueller, G. I., Ditlevsen, O., 1986. Stochastic fatigue, fracture and damage analysis. Structural Safety 3 (3-4), 231–267.

Young, P. C., 2002. Advances in real–time flood forecasting. Philosophical Transactions of the Royal Society of London. Series A: Mathematical, Physical and Engineering Sciences 360 (1796), 1433–1450.

Notations

List of symbols of Part I

A	Set of oriented edges of a digraph
$A(G)$	Adjacency matrix of a graph/digraph
$B(G)$	Incidence matrix of a graph
C, $C(\cdot)$	Global clustering coefficient
C_i	Clustering coefficient of node i
$C(S_k)$	Consequences of indirect behaviour S_k
$D(G)$	Incidence matrix of a digraph
D_j	Direct local damages
G, G'	Graph
E, $E(G)$	Set of edges of a graph
$E_{r,k}$	Energy in energy-based measure of robustness
$F(\cdot)$	Function of variable(s) $\cdot$
H_i	Hazard
I	Index of robustness
K^n	Complete graph of order n
$L(\cdot)$	Path length
$N_G(v)$, $N(v)$	Neighbourhood of vertex v
N_D	Number of direct (local) damages
N_H	Number of hazards
N_S	Number of indirect behaviours
P	Path in a graph
$Q(G)$	Laplacian of a graph/digraph
R	Risk
	Structural cluster
R_d	Damage-based metric for robustness
R_e	Energy-based metric for robustness
R_s	Stiffness matrix-based metric for robustness
RI	Redundancy Index
$S_\star$	Limit state in the model by Bos
S_k	Indirect behaviour
T	Traveling time in railroad network
	Period of vibration metric
T_d	Damage tolerance
U	Strain energy
V, $V(G)$	Set of vertices/nodes of a graph

V	Vulnerability
Z	Structural cluster
c	Number of connected components
d	Damage variable
$d\left(v\right)$	Degree of vertex v
d_G	Average degree of G
$d_G\left(x,y\right)$	Distance between vertex x and vertex y
e	Edge of a graph
f	Fraction of removed nodes
	Generic factor
$k_{\cdot\star}$	Component $(\cdot,\star)$ of the stiffness matrix
i,j,k,l	Counters
m	Arbitrary number
n	Number of vertices
	Number of glass layers in the model by Bos
	Matrix dimension
$\Pr\left(\star\right)$	Probability linked to event $\star$
p_{ER}	Erdös-Rényi random graph probability
p_f	Failure probability
p_{lim}	Acceptable limit probability
p_r	Reliability probability
p_t	Target probability
r	System state
t	Time
v	Vertex/node of a graph
x,y,z	Variables
$\mathbf{B}$	Incidence matrix of a graph
$\mathbf{D}$	Incidence matrix of a digraph
$\mathbf{K}$	Stiffness matrix
$\mathbf{M}$	Mass matrix
$\mathbf{Q}$	Laplacian of a graph/digraph
$\mathbf{f}$	External forces vector
$\mathbf{s}$	Displacement vector
$\mathcal{A}$	Set of actions acting on a structure
$\mathcal{A}^i$	Actions acting on the i-th member of a structure
$\mathcal{C}$	Capacity of the members of a structure
$\mathcal{C}^i$	Capacity on the i-th member of a structure

$\mathcal{R}$	Structural reliability
$\mathcal{S}_.$	Railway station in railroad network
$\mathcal{W}$	Cluster well-formedness
Δ_G	Maximum degree of G
$\Delta(G)$	Vertices degree matrix of G
Γ_f^i	Consequence factor
Φ^i	Resistance factor for member i
Φ	Stored energy metric
α	Function parameters
δ_G	Minimum degree of G
δ_S	Distance metric
γ_j	Load combination factor for action j
$\kappa(\cdot)$	Condition number of matrix $\cdot$
κ	Matrix conditioning number metric
$\lambda_i(\cdot)$, λ_i	i-th eigenvalue of matrix $\cdot$
ϕ	Graph diameter
ϱ	Number of broken glasses in the model by Bos
τ	Matrix trace metric
ξ	Arbitrary number
ζ	Matrix determinant metric
MCC	Member Consequence Class

List of symbols of Part II

A	Cross-section area
B, $B_\star$	Capacity bounds
C	Cut in a structure
E	Young's Modulus
$E(\cdot)$	Expected value of $\cdot$
F	Generic force, or force system)
$F_.$, $F_{.,\star}$	Force
H, H_i	Horizontal force
J	Cross-section inertia
K	Skewness
L	Distance between the columns
M	Generic bending moment
N	Axial force

Q	Total force
S	Constant in Shannon's Entropy
U	Strain energy
$\tilde{V}$	Set of vertices/nodes of a graph
V, V_i	Vertical force
	Shear
W, $W_\cdot$, $W_{\cdot,\star}$	Work of deformation
$W_{\mathcal{S}}$	Work of deformation in a fundamental structure
W_{in}	Work of deformation in a statically indeterminate structure
X, $X_\cdot$, $X_{\cdot,\star}$	Internal redundant force
$\hat{a}, \hat{b}, \hat{c}$	Stiffness matrix element
b	Cross-section length
$\tilde{c}$	Kolmogrov complexity constant
d, $d_\cdot$, $\dot{d}$	Damage variable
e	Number of elements
f	Functional
h	Interstory drift
$k_\cdot$, $k_{\cdot,\star}$	Stiffness matrix component
i, j, k, l, w	Counters
n	Cardinality of a set of elements
	Number of nodes in a structure
p	Probability
p_{xx}	xx-th percentile
s	Number of fundamental structures
$\tilde{s}$	Machine output
u	Horizontal displacement
v	Vertical displacement
$\tilde{v}$	Vertex of a graph
$\mathbf{B}$	Incidence matrix of a graph
$\mathbf{K}$	Stiffness matrix
$\mathbf{Q}$	Laplacian of a graph
$\mathbf{d}$, $\mathbf{d}_\cdot$	Displacement field (vector)
$\mathbf{f}$, $\mathbf{f}_\cdot$	Load field (vector)
$\mathcal{C}$	Cyclomatic Number
$\mathcal{H}$	Classical Entropy
$\mathcal{H}_f$	Functional Entropy
$\mathcal{K}$	Kolmogrov complexity

$\mathcal{S}$,$\mathcal{S}_i$	Fundamental structure
Γ	Degree of static indeterminacy of a structure
Φ	Generator in an Evolution Strategy
β, $\beta_{\cdot}$	Beam importance factor
δ, $\delta_{\cdot}$, $\delta_{\cdot,\star}$	General displacement
ε	Strain
$\kappa\left(\cdot\right)$	Machine algorithm to produce the output $\cdot$
$\lambda_i\left(\cdot\right)$, λ_i	i-th eigenvalue of matrix $\cdot$
μ	Mean value
ν_i	Final damage ratio
φ	Rotational displacement
ϖ	Minimum of damage variable
ψ, $\psi_{\cdot}$	Performance factor
$\rho_{\cdot,\star}$	Discriminant parameter
σ	Stress
	Variance
ξ	Load scaling factor
ζ	Shape factor
SCI	Structural Complexity Index
NSCI	Normalised Structural Complexity Index